

For Reference

NOT TO BE TAKEN FROM THIS ROOM

Ex libris
UNIVERSITATIS
ALBERTAENSIS





Digitized by the Internet Archive
in 2020 with funding from
University of Alberta Libraries

<https://archive.org/details/Ekwenchi1980>

T H E U N I V E R S I T Y O F A L B E R T A

RELEASE FORM

NAME OF AUTHOR.....Mbanefo Mbonu EKWENCHI.....
TITLE OF THESIS.....Hydrogen Atom Reactions with.....
.....Organosulfur Compounds.....
.....
DEGREE FOR WHICH THESIS WAS PRESENTED.....Ph.D.....
YEAR THIS DEGREE GRANTED.....1980.....

Permission is hereby granted to THE UNIVERSITY
OF ALBERTA LIBRARY to reproduce single copies of
this thesis and to lend or sell such copies for private,
scholarly or scientific research purposes only.

The author reserves other publication rights,
and neither the thesis nor extensive extracts from it
may be printed or otherwise reproduced without the
author's written permission.

DATED...September 4...

THE UNIVERSITY OF ALBERTA
HYDROGEN ATOM REACTIONS WITH ORGANOSULFUR COMPOUNDS

by



MBANEFO MBONU EKWENCHI

A THESIS
SUBMITTED TO THE FACULTY OF GRADUATE STUDIES AND RESEARCH
IN PARTIAL FULFILMENT OF THE REQUIREMENTS FOR THE DEGREE
OF DOCTOR OF PHILOSOPHY

IN

CHEMISTRY

DEPARTMENT OF CHEMISTRY

EDMONTON, ALBERTA

FALL 1980

THE UNIVERSITY OF ALBERTA
FACULTY OF GRADUATE STUDIES AND RESEARCH

The undersigned certify that they have read, and recommend to the Faculty of Graduate Studies and Research, for acceptance, a thesis entitled HYDROGEN ATOM REACTIONS WITH ORGANOSULFUR COMPOUNDS submitted by MBANEFO MBONU EKWENCHI in partial fulfilment of the requirements for the degree of Doctor of Philosophy in Physical Chemistry.

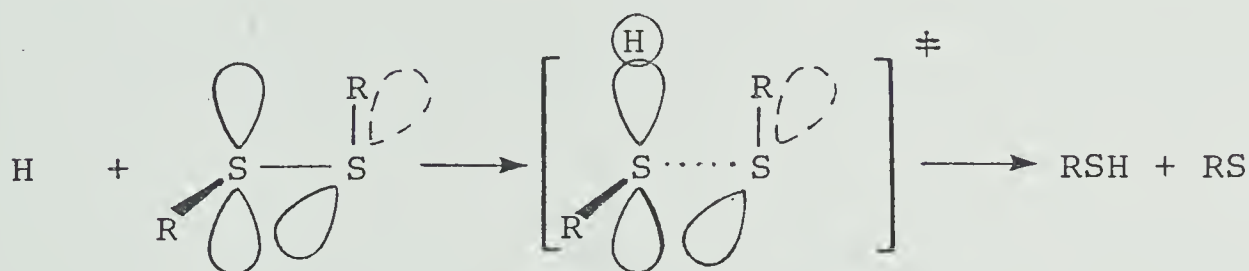
Dated September 4, 1980



To my wife, Uzo

ABSTRACT

The reactions of hydrogen atoms, generated by the $\text{Hg}(^3\text{P}_1)$ photosensitization of H_2 , with dimethyldisulfide, diethyldisulfide, ethylmethyldisulfide, bis(trifluoromethyl)disulfide and diethylsulfide, have been investigated in detail. With the exception of the fluorinated disulfide from which no retrievable products could be detected, the sole primary products are the corresponding thiols, formed in quantum yields ranging from 2.1 to 2.32 at room temperature. From the effects of exposure time, substrate pressure, light intensity, temperature and added gases, it is concluded that the sole primary reaction is attack by the H atom on the non-bonding orbitals of sulfur, e.g.,



For the $\text{H} + \text{CF}_3\text{SSCF}_3$ reaction polymerization is the observable reaction but experiments carried out in the presence of ethylene conclusively demonstrated that CF_3S radicals were present. It is believed that the expected primary product, CF_3SH , reacts with the substrate CF_3SSCF_3 to form some unidentified product(s).

Secondary reactions of the thiyl radicals generated in the primary step consist of combination and disproportionation, metathetical displacement, i.e., $RS + RSSR' \rightarrow RSSR + R'S$, and, for the case of C_2H_5S radicals, abstraction from the substrate: $C_2H_5S + C_2H_5SSC_2H_5 \rightarrow C_2H_5SH + C_2H_4SSC_2H_5$. The latter reaction is relatively efficient, the estimated activation energy being only $3.6 \text{ kcal mol}^{-1}$.

C_2H_5 radicals were shown to abstract hydrogen from $C_2H_5SC_2H_5$ and the relatively low activation energy for this reaction, $\sim 6.9 \text{ kcal mol}^{-1}$, as compared to abstraction from alkanes, points to a low methylenic C-H bond strength in this molecule.

The $H + CH_3SSC_2H_5$ system is complex owing to the occurrence of a chain sequence involving metathetical reactions of C_2H_5S and CH_3S radicals. The quantum yields of the symmetrical disulfides thus produced are initially very high, ~ 92 , and decrease with increasing exposure time to a steady state value. Computer modeling of a reaction sequence consisting of fifteen elementary steps adequately reproduces the experimentally observed trends.

Rate parameters for the $H + CH_3SSCH_3$, $C_2H_5SSC_2H_5$ and $C_2H_5SC_2H_5$ reactions were determined in competition with the $H + C_2H_4$ reaction and, for the $H + CF_3SSCF_3$ case, in competition with the $H + \triangle_S$ reaction. The activation energies are all low ranging from 0.1 to 4.5 kcal mol^{-1} in this sequence, and were shown to be directly

related to the overall exothermicities of the primary reaction.

On this basis, the activation energy for the $\text{H} + \text{CH}_3\text{SSC}_2\text{H}_5$ reaction is estimated to be $0.9 \leq E_a \leq 1.4$ kcal mol⁻¹. The A factors are in the 10^{12} - 10^{13} range and the experimental entropies of activation can be reproduced theoretically on the basis of a rigid transition state featuring H atom attack on the sulfur 3p orbitals.

ACKNOWLEDGMENTS

The author wishes to express his sincere appreciation and gratitude to Professor O. P. Strausz for his supervision, guidance, support and encouragement throughout the course of this study.

My special thanks go to the members of the Photochemistry group, particularly to Dr. I. Safarik whose help was invaluable in the interpretation of the results, Dr. T. Yokota for many interesting and helpful discussions, Mr. A. Clement, Drs. F.C. James, R.K. Gosavi, M. Torres, H. Murai, and J.W. Bottenheim for instructional assistance. I am especially grateful to Mr. A. Jodhan for his encouragement and invaluable technical assistance.

The author wishes to thank Dr. E. M. Lown for careful reading and assistance with the preparation of the manuscript and Mrs. Jacki Jorgensen for her conscientious efforts in typing this thesis.

The invaluable assistance of the entire technical and administrative staff of the Chemistry Department is also appreciated.

The author wishes to express his profound gratitude to his wife, Uzo, whose devotion and unceasing cooperation have made this work possible.

I am grateful to Professor C. O. Okafor for kindling my interest in academic research and to Dr. M. O. Eze for

continued interest and encouragement during the course of this study.

Finally, the financial assistance of the University of Alberta and the Federal Scholarship Board, Nigeria is gratefully acknowledged.

TABLE OF CONTENTS

	<u>PAGE</u>
ABSTRACT.....	v
ACKNOWLEDGMENTS.....	viii
LIST OF TABLES.....	xiv
LIST OF FIGURES.....	xvii
CHAPTER I: INTRODUCTION.....	1
1. Physical and Chemical Properties of Sulfides and Disulfides.....	2
(a) Disulfides	2
(i) Molecular Parameters of Disulfides.....	2
(ii) Structural Conformations of Disulfides.....	4
(iii) Spectral Properties of Disulfides.....	4
(iv) Reactions of Disulfides.....	5
(b) Sulfides	7
(i) Molecular Parameters of Sulfides.....	7
(ii) Structural Conformations of Sulfides...	7
(iii) Spectral Properties of Sulfides.....	9
(iv) Reactions of Sulfides.....	9
2. Atomic and Radical Reactions with Sulfides and Disulfides.....	12
(a) H Atom Reactions.....	12
(b) O(³ P) Atom Reactions.....	17
(i) With Sulfides.....	17

(ii) With Disulfides.....	20
(c) Reactions of S(³ P) Atoms.....	20
(d) Reactions of Alkyl Radicals.....	21
(i) With Sulfides.....	21
(ii) With Disulfides.....	26
(e) Reactions of Phenyl Radicals.....	26
(f) Reactions of Hydroxyl Radicals.....	27
3. Thiyl Radicals.....	29
(a) Generation, identification and physical properties.....	29
(b) Reactions of Thiyl Radicals.....	33
(i) Disproportionation-Combination.....	34
(ii) Abstraction.....	35
(iii) Addition Reactions.....	36
(iv) Metathetical Reactions.....	38
4. Transition State Theory for Bimolecular Reactions.....	39
5. Computer Modeling of Chemical Reactions.....	42
6. Aim of the Present Investigation.....	44
CHAPTER II: EXPERIMENTAL.....	47
1. High Vacuum System.....	47
2. Photolytic Assembly.....	49
3. Light Sources and Actinometry.....	51
4. Materials.....	52
5. The Analytical System.....	55
6. Operational Procedure.....	58

CHAPTER III: THE REACTION OF HYDROGEN ATOMS WITH	
DIMETHYLDISULFIDE.....	61
A. Results.....	61
1. Effects of time, CH_3SSCH_3 concentration and	
temperature on $\phi(\text{CH}_3\text{SH})$	61
2. Experiments in the presence of ethylene.....	63
B. Discussion	66
CHAPTER IV: THE REACTION OF HYDROGEN ATOMS WITH	
DIETHYLDISULFIDE.....	77
A. Results.....	77
1. Effects of time, $\text{C}_2\text{H}_5\text{SSC}_2\text{H}_5$ concentration and	
temperature on $\phi(\text{C}_2\text{H}_5\text{SH})$	77
2. Effect of added ethylene.....	79
B. Discussion.....	83
CHAPTER V: THE REACTION OF HYDROGEN ATOMS WITH	
ETHYLMETHYLDISULFIDE.....	100
A. Results.....	100
1. Products of the reaction.....	100
2. Effects of exposure time, pressure and	
temperature.....	100
B. Discussion.....	105
CHAPTER VI: THE REACTION OF HYDROGEN ATOMS WITH	
BIS(TRIFLUOROMETHYL)DISULFIDE.....	113
A. Results.....	113

1. Products of the reaction.....	113
2. Effect of added thiirane.....	115
B. Discussion.....	117
CHAPTER VII: THE REACTION OF HYDROGEN ATOMS WITH	
DIETHYLSULFIDE.....	127
A. Results.....	127
1. Effects of exposure time and $C_2H_5SC_2H_5$	
concentration.....	128
2. Effect of temperature.....	128
3. Effect of added ethylene.....	132
B. Discussion.....	132
CHAPTER VIII: SUMMARY AND CONCLUSIONS.....	
	151
BIBLIOGRAPHY.....	165
APPENDIX	177
A. Competitive Quenching Corrections.....	177
B. Mass Spectral Data.....	180
C. Kinetic Treatment of the $H/C_2H_4/C_2H_5SSC_2H_5$	
System.....	182

LIST OF TABLES

<u>TABLE</u>		<u>PAGE</u>
I	Some Reactions of Disulfides and Sulfides	8
II	Thermodynamic Properties of Some Organosulfur Compounds and Radicals	11
III	Arrhenius Parameters for Some Atom Transfer Reactions	23
IV	Generation and Spectral Characteristics of Some Thiyl Radicals	30
V	Sources of Materials Used and Purification Procedures	53
VI	Gas Chromatograph Retention Data and Operating Conditions	56
VII	Effect of Exposure time on $\phi(\text{CH}_3\text{SH})$	62
VIII	Effect of $\text{P}(\text{CH}_3\text{SSCH}_3)$ on $\phi(\text{CH}_3\text{SH})$	64
IX	Effect of Temperature on $\phi(\text{CH}_3\text{SH})$	65
X	Effect of C_2H_4 Pressure and Temperature on $\phi(\text{CH}_3\text{SH})$	67
XI	Slopes and Intercepts of the Plots in Figure 3	73
XII	Effect of Exposure time on $\phi(\text{C}_2\text{H}_5\text{SH})$	78
XIII	Effect of $\text{P}(\text{C}_2\text{H}_5\text{SSC}_2\text{H}_5)$ on $\phi(\text{C}_2\text{H}_5\text{SH})$	80
XIV	Effect of Temperature on $\phi(\text{C}_2\text{H}_5\text{SH})$	81
XV	Effect of C_2H_4 Pressure and Temperature on $\phi(\text{C}_2\text{H}_5\text{SH})$	82

XVI	Effect of Temperature on $\phi(2a)$, $\phi(2b)$, and $\phi(3)$	86
XVII	Effect of C_2H_4 Pressure and Temperature on $\phi(C_2H_5SH)$	92
XVIII	Slopes and Intercepts of the Plots in Figure 6	95
XIX	Time Dependence of the Quantum Yields of the Reaction Products	101
XX	Rate Constants ($cm^3 mol^{-1} s^{-1}$) Used in the Simulation	109
XXI	Effect of Exposure time on $\phi(C_2H_4)$ and $\phi(H_2S)$ from the $H + C_2H_4S$ Reaction	116
XXII	Effect of Temperature and C_2H_4S Pressure on γ	118
XXIII	Slopes and Intercepts of the Plots in Figure 11	123
XXIV	Effect of Exposure time on $\phi(C_2H_5SH)$	129
XXV	Effect of $P(C_2H_5SC_2H_5)$ on the Product Quantum Yields	130
XXVI	Effect of Temperature and Substrate Pressure on the Yields of Products	131.
XXVII	Effect of C_2H_4 Pressure and Temperature on $\phi(C_2H_5SH)$	133
XXVIII	Effect of Temperature and Substrate Pressure on the Quantum Yields of Products	136
XXIX	Effect of Temperature on $R_{C_2H_6}/R_{C_4H_{10}}^{1/2}$	140
XXX	Activation Energies for Methylene Hydrogen Abstraction by C_2H_5 Radicals.	142

XXXI	Heats of Reaction and Activation Energies for Some Metathetical Reactions Involving C_2H_5 Radicals	144
XXXII	Slopes and Intercepts of the Plots in Figure 14	148
XXXIII	Arrhenius Parameters and Heats of Reaction for H Atom Reactions With Organosulfur Compounds	157
XXXIV	Rate Constants for Atom or Radical Attack on the Sulfur Atom of Sulfides and Disulfides	162
XXXV	Arrhenius Parameters for Atom or Radical Reactions with Sulfides and Disulfides	163

LIST OF FIGURES

FIGURE		PAGE
1.	The high vacuum system	48
2.	The photolytic assembly	50
3.	$\phi(\text{CH}_3\text{SH})^{-1}$ <i>versus</i> $\text{P}[\text{C}_2\text{H}_4]/\text{P}[\text{CH}_3\text{SSCH}_3]$ at 25, 60, 85, 120 and 155°C. $\text{P}(\text{H}_2) = 580 \pm 10$ Torr; $\text{P}(\text{C}_2\text{H}_4) + \text{P}(\text{CH}_3\text{SSCH}_3) = 10\text{-}20$ Torr; photolysis time, 45 minutes.	72
4.	Arrhenius plot of k_9/k_1 <i>versus</i> $1/T$.	75
5.	Arrhenius plot of $\phi(3)/\{(2-\phi(3))/2\}^{1/2}[\text{C}_2\text{H}_5\text{SSC}_2\text{H}_5]$ <i>versus</i> $1/T$.	87
6.	$\frac{1}{\phi(1)+\phi(3)}$ <i>versus</i> $\text{P}[\text{C}_2\text{H}_4]/\text{P}[\text{C}_2\text{H}_5\text{SSC}_2\text{H}_5]$ at 25, 60, 80, 120 and 145°C. $\text{P}(\text{H}_2) = 580 \pm 10$ Torr; photolysis time, 45 minutes.	94
7.	Arrhenius plot of k_5/k_1 <i>versus</i> $1/T$.	96
8.	Average quantum yields for CH_3SSCH_3 and $\text{C}_2\text{H}_5\text{SSC}_2\text{H}_5$ formation as a function of irradiation time.	103
9.	Dependence of $\phi(\text{CH}_3\text{SH})/\phi(\text{C}_2\text{H}_5\text{SH})$ on irradiation time.	104
10.	Dependence of $\phi(\text{CH}_3\text{SSCH}_3)$ on irradiation time Curve A: instantaneous quantum yield calculated from the amount of CH_3SSCH_3 formed in one second; Curve B: average quantum yield, calculated from the integrated amount of CH_3SSCH_3 ;	

0:	experimental data.	111
11.	γ^{-1} <i>versus</i> $P[\text{CF}_3\text{SSCF}_3]/[\text{C}_2\text{H}_4\text{S}]$ at 25, 62, 84, 124 and 152°C. $P(\text{H}_2) = 580 \pm 10$ Torr; photolysis time, 45 minutes.	122
12.	Arrhenius plot of k_3/k_4 <i>versus</i> $1/T$.	125
13.	Arrhenius plot of $R_2/R_4^{1/2}$ <i>versus</i> $1/T$.	141
14.	$\phi(\text{C}_2\text{H}_5\text{SH})^{-1}$ <i>versus</i> $P[\text{C}_2\text{H}_4]/P[\text{C}_2\text{H}_5\text{SC}_2\text{H}_5]$ at 25, 96, 132, 170 and 188°C.	146
15.	Arrhenius plot of k_{12}/k_1 <i>versus</i> $1/T$.	149
16.	Plot of an empirical relationship for activation energies: $E_a = 0.9\Delta H + 19.36$ for the reaction series $\text{H} + \text{CH}_3\text{SSCH}_3$, $\text{C}_2\text{H}_5\text{SSC}_2\text{H}_5$, CH_3SCH_3 and $\text{C}_2\text{H}_5\text{SC}_2\text{H}_5$.	159

CHAPTER I

INTRODUCTION

Knowledge concerning the mechanism of the reactions of atoms and radicals with the sulfur moiety of alkyl disulfides and sulfides has many practical implications. For example, it might aid in interpreting some of the complex kinetic behaviour of certain biological systems since disulfide and sulfide bridges occur frequently in the structures of many proteins and enzymes; these are primarily responsible for maintaining the tertiary structure of many proteins.^{1,2} The sulfur atoms in these compounds are very susceptible to radical attack, and radiation damage to enzymes and other protein material could occur *via* attack on the disulfide moiety. Studies on hydrogen atom reactions with disulfides and sulfides are also of particular significance to the petroleum industry,³⁻⁵ where hydrodesulfurization constitutes a major process in the upgrading of crudes. In particular, the sulfur content of Alberta oil sand bitumens is unusually high, of the order of ~5%, and this creates serious problems in catalyst poisoning and removal of volatile sulfur-containing components from the effluent gases. Another area of practical importance is the polymer industry, where disulfides have been shown to be effective polymerization initiators.^{6,7}

Before reviewing recent developments in atomic and radical reactions with disulfides and sulfides, let us turn our attention to the physical and chemical properties of sulfides and disulfides.

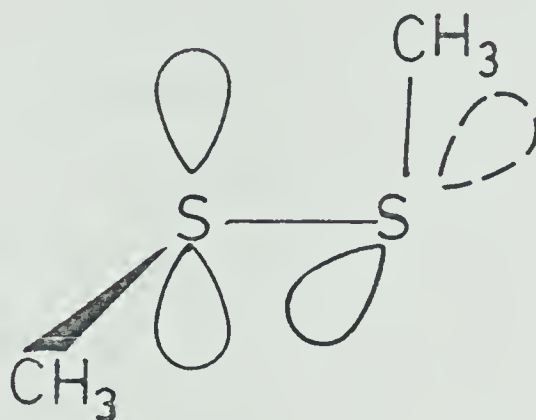
1. Physical and Chemical Properties of Disulfides and Sulfides

(a) Disulfides

(i) Molecular Parameters of Disulfides

The S-S bond in disulfides is appreciably stronger ($\sim 67-74 \text{ kcal mol}^{-1}$) than the O-O bond in peroxides ($\sim 40-45 \text{ kcal mol}^{-1}$) and this accounts, in part, for the greater relative stability of disulfides, RSSR, compared to ROOR compounds. The covalent radius of the sulfur atom is also appreciably larger than that of the oxygen or carbon atom; the bond lengths⁸ are, C-C 1.53 \AA , C-O 1.45 \AA , and C-S 1.82 \AA . Similarly, disulfide bond lengths ($d(\text{S-S}) \sim 2.0-2.1 \text{ \AA}$) are about $0.5-0.6 \text{ \AA}$ greater than those of C-O or C-C bonds. Hence steric accessibility of the S-S moiety to reagent attack should be quite favourable, and this is indeed observed experimentally.⁹ Furthermore, sulfur can accommodate more than eight outer valence electrons *via* valence shell expansion involving d orbitals; however, the possible consequences with regard to the reactivity of disulfides is not well established.

Organic disulfides, RSSR, have, in general, a geometry corresponding to that of CH_3SSCH_3 . It has been shown by electron diffraction¹⁰ and microwave spectroscopy¹¹ that CH_3SSCH_3 has the structure shown below:



The molecular orbitals filled by the valence electrons in C-S-S-C skeleton are constructed mainly from the atomic orbitals, $3s$, $3p_x$, $3p_y$, $3p_z$, and sp^3 orbital of C atom. Various MO calculations consistently predict the two highest occupied molecular orbitals to be of lone-pair character formed largely by out-of-plane $3p$ atomic orbitals on each sulfur, i.e., $n(p \text{ type})$.^{12,15} Due to the appreciable size of these orbitals in the S-S moiety, the pairs of the non-bonded electrons on the adjacent atoms are considered to repel one another so that in order to minimize this repulsion, the CH_3 groups of CH_3SSCH_3 assume a dihedral angle $\sim 90^\circ$. The molecular parameters found for CH_3SSCH_3 ¹² are as follows: $d(\text{S-S}) = 2.03 \text{ \AA}$, $d(\text{C-S}) = 1.81 \text{ \AA}$, $d(\text{C-H}) = 1.10 \text{ \AA}$, $\alpha(\text{CSS}) = 103^\circ$, and $\tau(\text{dihedral angle}) = 84^\circ$. In general, alkyl disulfides have $d(\text{S-S})$, α and τ values which are dependent on the nature of R. The barrier to

rotation around the S-S bond has been claimed to vary from $2.7 \text{ kcal mol}^{-1}$ (H_2S_2) to $14.2 \text{ kcal mol}^{-1}$ (S_2Cl_2),¹³ the values for CH_3SSCH_3 and $\text{C}_2\text{H}_5\text{SSC}_2\text{H}_5$ being 9.5 and 13.2 kcal mol^{-1} respectively.¹⁴

(ii) Structural Conformations of Disulfides

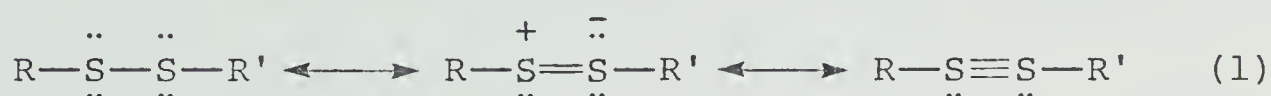
Considerable attention has been devoted recently to the structures and conformational preferences of simple alkyl disulfides.^{15,16} CH_3SSCH_3 has been assumed to exist only in one conformation, the gauche conformer. However, results from a gas phase electron diffraction study¹⁵ indicate that $\text{CH}_3\text{SSC}_2\text{H}_5$ exists as a mixture of at least two conformations. From Raman spectral studies¹⁶ on $\text{CH}_3\text{SSC}_2\text{H}_5$ and $\text{C}_2\text{H}_5\text{SSC}_2\text{H}_5$, the variation in the positions and intensities of the fundamentals in the spectra of these compounds as a function of temperature from ~ 77 to 320°K are claimed to be consistent with the presence of three rotational isomers, differing in their conformations about their C-S bonds. In $\text{C}_2\text{H}_5\text{SSC}_2\text{H}_5$, the gauche-gauche conformation is apparently the most stable of the three rotamers in the gas phase.

(iii) Spectral Properties of Disulfides

The UV spectra of most aliphatic disulfides show a rather broad maximum at $\sim 250 \text{ nm}$ which is associated with an electronic transition from the non-bonding n orbital (p type) to the antibonding σ^* orbitals. The absorption

maximum was shown to be displaced to progressively shorter wavelengths in the series $(\text{CH}_3)_2\text{S}_2$ ($\lambda_{\text{max}} = 254.5 \text{ nm}$), $(\text{C}_2\text{H}_5)_2\text{S}_2$ ($\lambda_{\text{max}} = 251.5 \text{ nm}$) and $(i\text{-C}_3\text{H}_7)_2\text{S}_2$ ($\lambda_{\text{max}} = 245.0 \text{ nm}$).¹⁷ MO calculations on various disulfide-bond containing molecules have shown that, in general, the further the dihedral angle from 90° , the more red shifted the lowest energy transition.¹⁷

In the PE spectra of organic disulfides¹⁸ a splitting of the first band is observed, corresponding to ionization from one of the $3p_\pi$ orbitals. These two molecular orbitals thus formed are always the highest occupied orbitals in the molecule. Since the first band in the spectrum of RSR is always unsplit, the cause of the splitting in RSSR species has been attributed to p_π - p_π interactions whereby the 3d orbitals of the sulfur atom give rise to pd_π bonds:¹⁹



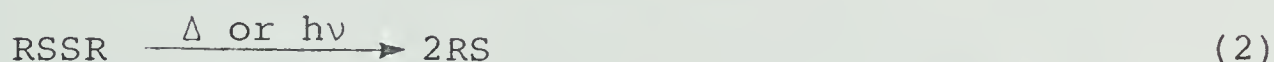
(2 forms)

(iv) Reactions of Disulfides

The chemistry of disulfides has been extensively investigated,²⁰ with the main emphasis on redox reactions, bimolecular reactions and thermal exchange reactions.

Simple disulfides can be reduced easily and completely to thiols.²¹ Oxidation of disulfides leads ultimately to sulfonic acids, and several of the intermediates, namely, sulfenic and sulfinic acids or thiosulfinates, thiosulfonates, sulfinylsulfones and α -disulfones, frequently can be isolated.²²

Homolytic scission of disulfides readily takes place in thermolysis, photolysis, and also in electrochemical and other reactions²³ and can be unimolecular, arising from S-S cleavage,



or bimolecular, for example as a result of thiyl radical attack:



The resulting chain is long enough that this system has found practical application in the synthesis of unsymmetrical disulfides,²⁴ e.g.,



C-S cleavage is relatively unimportant in thermolysis and photolysis.²⁵

Disulfides also undergo heterolytic scission of the S-S bond in the presence of nucleophiles or electrophiles and these reactions are now fairly well understood.^{6,7}

Some of the more important reactions of disulfides are summarized in Table I.

(b) Sulfides

(i) Molecular Parameters of Sulfides

C-S bonds ($70\text{--}72\text{ kcal mol}^{-1}$) are weaker than C-O bonds ($79\text{--}80\text{ kcal mol}^{-1}$) and for both cases the bond strengths are little affected by simple alkyl groups. C-S and C-O bond lengths for simple alkyl sulfides and ethers are generally close to 1.82 \AA (C-S) and 1.41 \AA (C-O).²⁶ The corresponding bond angles, $\angle\text{C-S-C}$ and $\angle\text{C-O-C}$, are around 105° and 112° respectively. In general, substitution of oxygen by sulfur leads to much longer bond lengths and somewhat smaller bond angles.

(ii) Spectral Properties

The spectra of simple dialkyl sulfides show strong bands in the region $200\text{--}215\text{ nm}$ and a weak continuum having a maximum near 230 nm . The former bands are thought to be due to a $\sigma\text{--}\sigma^*$ transition in the C-S bond and the latter to an $n_p\text{--}\sigma^*$ transition involving the unshared electrons of sulfur.²⁶ MO calculations predict that the lowest energy transition in sulfides should be largely $4s_S$ in character while the next three degenerate transitions should be primarily $3d_S$. The calculated transition energies were in good agreement with experimentally observed values.²⁷

TABLE I

Some Reactions of Disulfides and Sulfides

Type of Reaction	Disulfides	Sulfides
1. Photolytic or thermal S-S or C-S scission	$\text{RSSR} \xrightarrow{h\nu \text{ or } \Delta} 2\text{RS}^\bullet$	$\text{RSR} \xrightarrow{h\nu \text{ or } \Delta} \text{RS} + \text{R}$
2. Catalytic scission of the S-S bond	$\text{Fe}^{2+} + \text{RSSR} \rightarrow \text{RS}^\bullet + \text{RS}^\bullet + \text{Fe}^{3+}$	
3. Electrophilic Reaction	$\text{RSSR} + \text{H}^+ \rightarrow \text{RSH} + \text{RS}^+$	
4. Nucleophilic Reaction	$\text{RSSR} + 2\text{NaH} \xrightarrow{\text{aq}} 2\text{RSH} + 2\text{NaOH}$	
5. Oxidation	$\text{RSSR} \xrightarrow{[\text{O}]} \text{RSSR} \xrightarrow{\text{O}} \text{RSSR} \text{ etc.}$	$\text{RSR} \xrightarrow{[\text{O}]} \text{RSSR} \xrightarrow{\text{O}} \text{RSSR} \text{ etc.}$
6. Reduction	$\text{RSSR} \xrightarrow{[\text{H}]} 2\text{RSH}$	$\text{RSR} \xrightarrow{[\text{H}]} \text{RSH} + \text{RH}$
7. Disproportionation	$\text{R}^1\text{SSR}^1 + \text{R}^2\text{SSR}^2 \rightarrow 2\text{R}^1\text{SSR}^2$	
8. Metathetical Displacement Reactions	$\text{R}^1 + \text{RSSR} \rightarrow \text{RSR}^1 + \text{SR}$	$\text{R}^1 + \text{RSR} \rightarrow \text{RSR}^1 + \text{R}$
9. Hydrogen Abstraction	$\text{RS} + \text{RSSR} \rightarrow \text{RSH} + \text{RSSR}(-\text{H})$	$\text{R}^1 + \text{RSR} \rightarrow \text{R}^1\text{H} + \text{RSR}(-\text{H})$

(iii) Structural Conformations of Sulfides

The molecular vibrations of alkyl sulfides have been extensively studied.²⁸ CH_3SCH_3 has a C_{2v} molecular symmetry while Scott *et al.* postulated three possible conformations, C_{2v} (TT), C_1 (TG) and C_2 (GG) for $\text{C}_2\text{H}_5\text{SC}_2\text{H}_5$. Only two conformers however, C_{2v} and C_1 , appear to be stable since the C_2 conformation was not observed in the spectrum.^{28b}

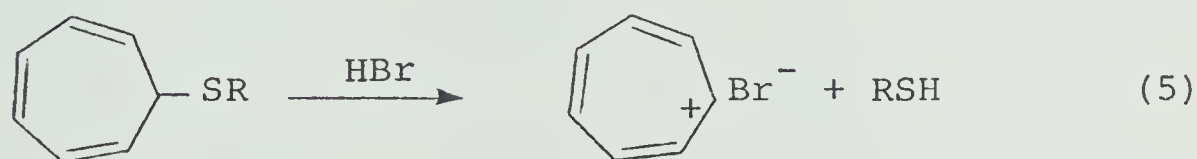
MO calculations on organic sulfides suggest that the contribution of 3d orbitals to the charge distribution is important, but that to the stable conformation and rotational barrier is very small. The shape and energy of the lowest unoccupied molecular orbital are particularly sensitive to the participation of 3d orbitals.²⁹

(iv) Reactions of Sulfides

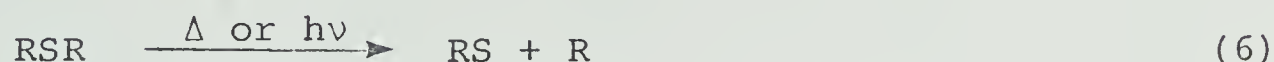
It is well known that the nucleophilicity of the lone pairs of electrons of the sulfur atom is larger than that of oxygen. However, the basicity of the sulfur atom is smaller than that of oxygen. Consequently, sulfur compounds exhibit chemical properties different from those of their oxygen counterparts. In most reactions involving sulfides, it is commonly assumed that the site of attack must be at the sulfur atom. There are several reasons for this;³⁰ (1) sulfur is more electropositive and polarizable than carbon; (2) the electronegativity of

the sulfur atom is much less than that of oxygen; and
 (3) sulfur can utilise its 3d orbitals in chemical bonding.

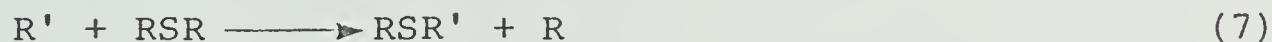
Reactions of sulfides may be divided into (1) those taking place directly on the sulfur atom, (2) those occurring at another part of the molecule, and (3) those occurring by C-S cleavage. The sulfur atom in aliphatic sulfides is generally stable towards nucleophilic reagents but an electrophilic reagent promotes C-S cleavage, for example,³¹



Cleavage of the C-S bond of sulfides is also known to occur in thermal and photochemical reactions,



and the free radicals thus generated react with the sulfides exclusively by metathetical radical displacement.



The most common reactions of sulfides are summarized in Table I.

Some thermodynamic properties of sulfides and disulfides are summarized in Table II, along with those of other species pertinent to this study.

TABLE II

Thermodynamic Properties of Some Organosulfur Compounds and Radicals

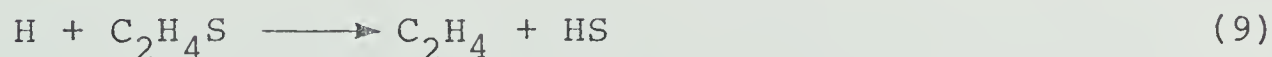
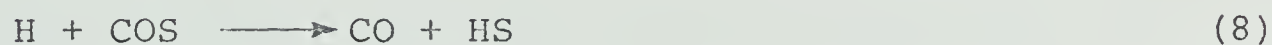
Species	ΔH_f (kcal mol ⁻¹)	Ref.	Thermochemical bond strength (kcal mol ⁻¹)	Ref.
<u>D(S-S)</u>				
HSSH			65	32c
CH ₃ SSCH ₃	-5.71	32a	67	32c
C ₂ H ₅ SSC ₂ H ₅	-17.4	32a	69	32c
<u>D(S-H)</u>				
CH ₃ SH	-5.46	32a	88	32c
C ₂ H ₅ SH	-11.03	32a	88.5	32c
<u>D(C-S)</u>				
CH ₃ SCH ₃	-8.98	32a	70	32c
C ₂ H ₅ SC ₂ H ₅	-19.77	32a	71	32c
CH ₃ S	30.5	32a		
C ₂ H ₅ S	26.0	32a		
CH ₃	30.5	32b		
C ₂ H ₅	25.7	32b		
H	52.1	32b		

2. Atomic and Radical Reactions with Sulfides and Disulfides.

(a) H Atom Reactions With Sulfides

For kinetic studies in the gas phase, the most commonly employed sources of hydrogen atoms are microwave discharge of H_2 ,³³ $\text{Hg } ({}^3\text{P}_1)$ sensitized decomposition of H_2 ,³⁴ and the photolysis of H_2S .³⁵ In the latter case H atoms are initially produced with a substantial amount of excess kinetic energy and consequently high pressures of a moderator gas are required for thermalization. A less commonly used but viable source of H atoms is the photolysis of alkanethiols.³⁶

With COS ³⁷ and thiirane³⁸ efficient desulfurization was shown to take place,

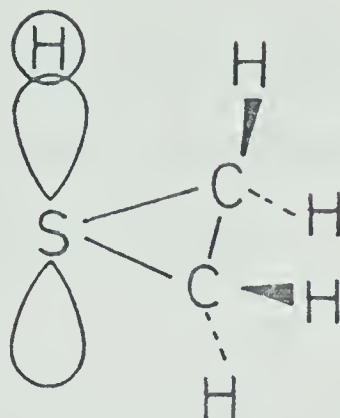


and the corresponding rate constants, derived from competitive experiments, are

$$k_8 = (9.1 \pm 1.2) \times 10^{12} \exp[(-3900 \pm 370)/RT] \text{ cm}^3 \text{ mol}^{-1} \text{ s}^{-1}$$

$$k_9 = (5.7 \pm 0.7) \times 10^{13} \exp[(-1944 \pm 175)/RT] \text{ cm}^3 \text{ mol}^{-1} \text{ s}^{-1}$$

On the basis of absolute rate theory calculations it was concluded that the initial interaction involves the non-bonding 3p orbital of the S atom, e.g.,



It should be noted that the analogous hypothetical deoxygenation reaction with oxirane has not been observed; instead, hydrogen atoms react with oxirane exclusively by hydrogen abstraction,³⁹



and the rate constant is

$$k_{10} = (3.8 \pm 0.5) \times 10^{13} \exp[(-8500 \pm 200)/RT] \text{ cm}^3 \text{ mol}^{-1} \text{ s}^{-1}$$

H atoms react with CH_3SCH_3 to yield CH_3SH and CH_4 as major products.⁴⁰ From the effects of exposure time, concentrations, and added gases it was concluded that the only primary reaction of importance is:



i.e., here again, attack takes place exclusively at the sulfur atom. Relative to the $\text{H} + \text{H}_2\text{S}$ reaction, the rate parameters for step (11) were found to be:

$$k_{11} = (1.71 \pm 0.26) \times 10^{13} \exp[-(2612 \pm 88)/RT] \text{ cm}^3 \text{ mol}^{-1} \text{ s}^{-1}$$

It was also shown that the experimental entropy of activation, -24.6 e.u., could be reproduced theoretically if a symmetrical transition state,

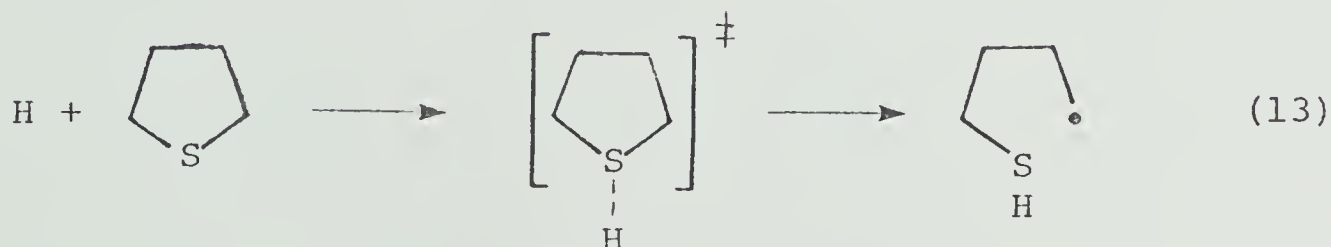


featuring H atom attack on sulfur was assumed. Since the source of H atoms in this study was the photolysis of H_2S , the overall mechanism is quite complex owing to the presence of HS radicals, e.g., it was shown that HS engages in a metathetical reaction with the substrate,



thereby initiating a short chain.

With thiolane, it is believed that the H atom adds to sulfur and the intermediate fragments *via* C-S cleavage:⁴¹

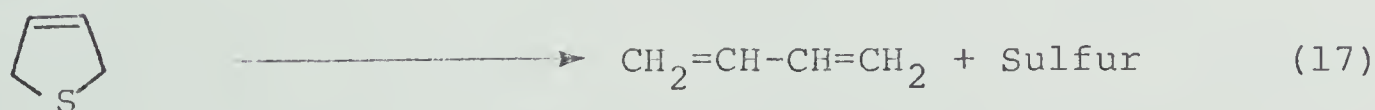
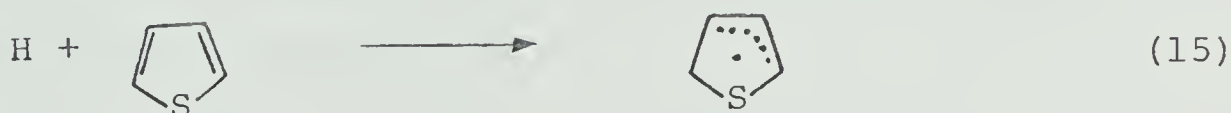


The resulting radical then combines with an H atom to form 1-butanethiol:



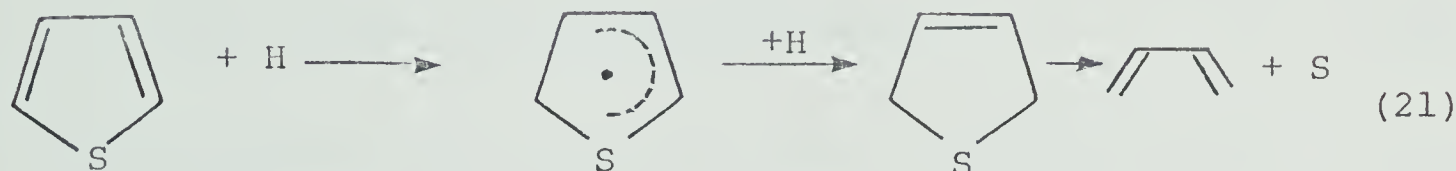
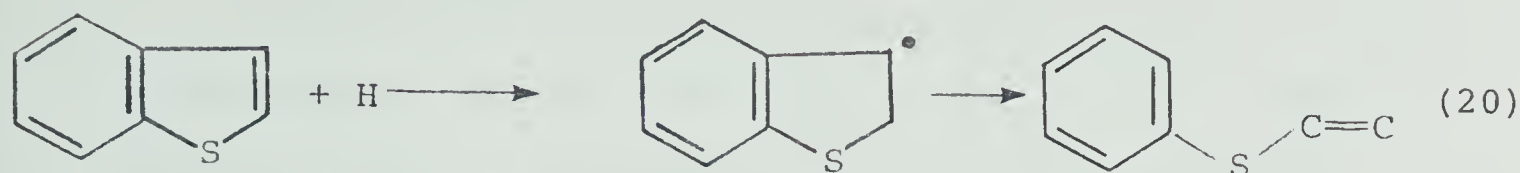
This system is in complete contrast to the $\text{H} + \text{C}_2\text{H}_4\text{S}$ reaction where sulfur abstraction is the only observed process; the reason for this was ascribed⁴¹ to differences in the stabilization of the products.

H atoms react with thiophene to yield 1,3-butadiene and elemental sulfur as major products.⁴² Several minor products were also detected, including H_2S and $\text{C}_1\text{-C}_4$ compounds. It was postulated that two H atoms add to the ring in succession, and that the resulting intermediate, 1,4-dihydrothiophene, decomposes to yield butadiene and sulfur:



The detection of H_2S as one of the minor reaction products

of thiophene, where H atoms attack the 2-position.



(b) $\text{O}(^3\text{P})$ Atom Reactions

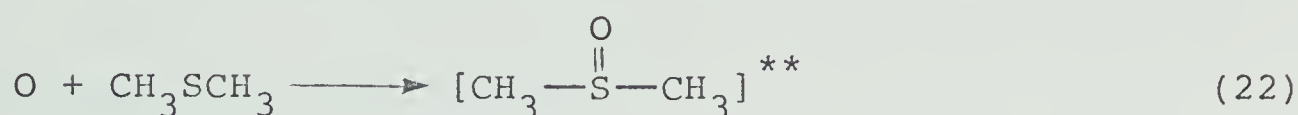
In contrast to the H + organosulfur systems, where the absence of H abstraction from the substrate had to be deduced from product analysis and kinetic considerations, the occurrence of H atom abstraction in O + organosulfur systems can be readily recognized. From the few studies reported to date however, no evidence has been reported to the effect that abstraction takes place and the results overwhelmingly point to S atom attack.

(i) With Sulfides

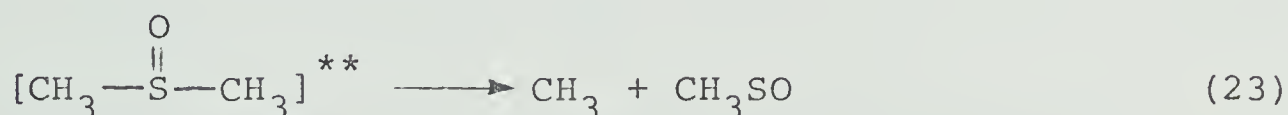
In gas phase kinetic studies, the most frequently employed sources of oxygen (^3P) atoms are electrical and microwave discharge of O_2 ,^{44,45} photolysis ($\lambda > 130 \text{ nm}$) of O_2 ,⁴⁶ and the Hg ($^3\text{P}_1$) sensitized decomposition of

N_2O .⁴⁷

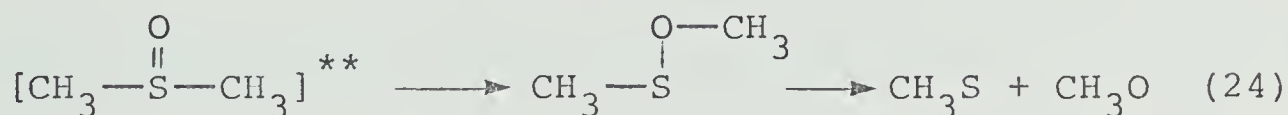
O atoms also appear to attack the S atom of CH_3SCH_3 and the major products are CH_4 and CH_3SO .^{45,48} The excited adduct, postulated to be dimethylsulfoxide, contains about $85\text{--}88 \text{ kcal mol}^{-1}$ excess internal energy.



This energy is about 23 kcal mol^{-1} in excess of that required for unimolecular decomposition *via* S- CH_3 bond cleavage and therefore the excited adduct decomposes rapidly to CH_3 and CH_3SO :



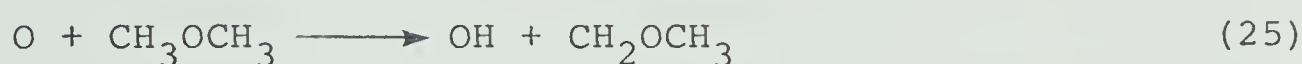
The minor products observed in this system, namely CH_3S and CH_3O , are probably formed as a result of rearrangement of the excited adduct followed by fragmentation, e.g.,



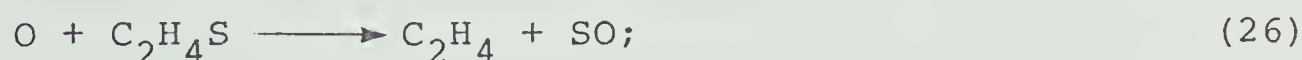
It was estimated however that rearrangement constitutes less than 1% of the decomposition. The rate constant for reaction (22) determined by the flash photolysis-resonance fluorescence method,⁴⁸ is:

$$k_{22} = (8.6 \pm 0.4) \times 10^{12} \exp[(727 \pm 31)/RT] \text{ cm}^3 \text{ mol}^{-1} \text{ s}^{-1}$$

and exhibited a negative temperature dependence. Thus the primary process in the $O + CH_3SCH_3$ system is completely analogous to that of the $H + CH_3SCH_3$ reaction, i.e., the attacking site is the S atom of the substrate. This result is however in complete contrast to the $O + CH_3OCH_3$ reaction where it is believed that the initial reaction is hydrogen atom abstraction,⁴⁹



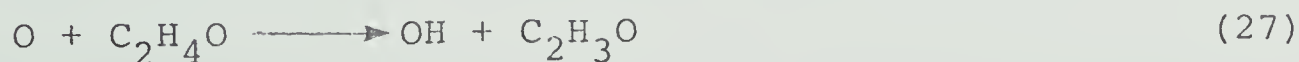
With thiirane⁴⁸ efficient desulfurization takes place,



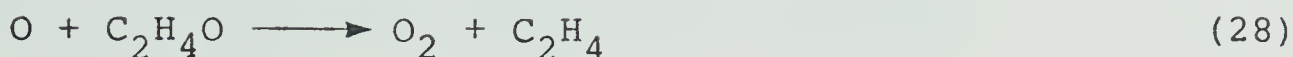
in complete analogy with the H and S atom reactions (*vide infra*) with this substrate. The rate constant for reaction (26), determined by the flash photolysis-resonance fluorescence method is

$$k_{26} = (8.1 \pm 0.5) \times 10^{12} \exp[-(35 \pm 40)/RT] \text{ cm}^3 \text{ mol}^{-1} \text{ s}^{-1}$$

With oxirane H atom abstraction is the only observable reaction⁵⁰



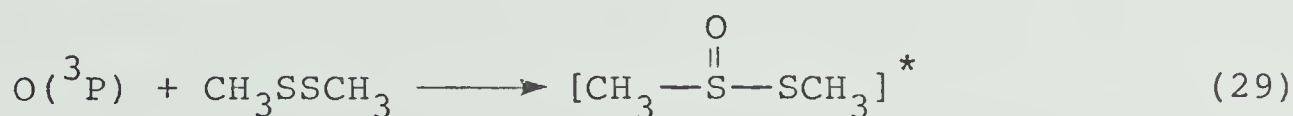
in spite of the fact that the direct formation of $O_2 + C_2H_4$ is energetically more favourable.



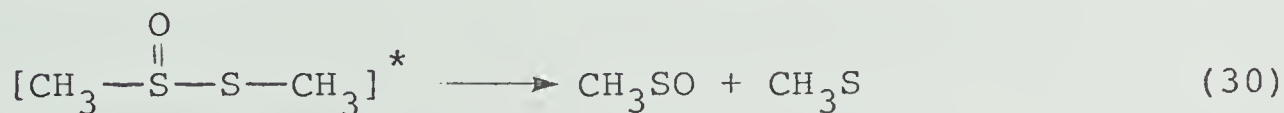
Bond energy-bond order calculations predict a prohibitively high activation energy for step (28), perhaps as a consequence of the somewhat lower exothermicity and the higher value of the higher value of the excitation energy of the $^1\text{D}_2$ state of the oxygen than sulfur atom.

(ii) With Disulfides

The gas phase reaction of oxygen atoms with dimethyl-disulfide has been studied recently.⁴⁸ Although no stable products could be isolated, competitive experiments in the presence of CH_3SH showed that reaction does take place, as evidenced in the drastically reduced yields of CH_4 , CH_3SO and CH_3SOH from the $\text{O} + \text{CH}_3\text{SH}$ reaction.⁵¹ By analogy with the $\text{O} + \text{CH}_3\text{SCH}_3$ reaction and on the basis of kinetic considerations it was proposed that O atoms attack the S atom of the disulfide forming a vibrationally excited adduct,

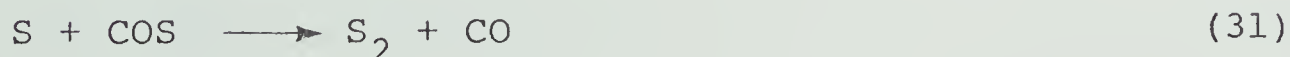


which subsequently decomposes *via* S-S cleavage:



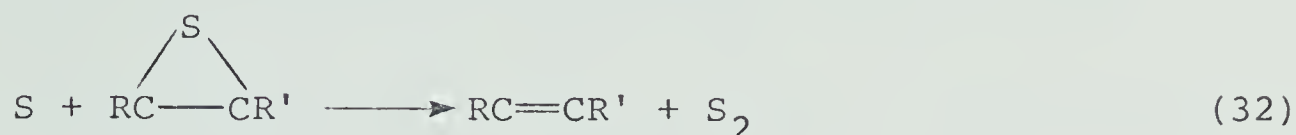
(c) Reactions of Ground State $\text{S}(^3\text{P})$ Atoms with Sulfides

S atoms have been shown to desulfurize COS ,⁴⁵



$$k_{31} = 7.2 \times 10^{11} \text{ cm}^3 \text{ mol}^{-1} \text{ s}^{-1}, \text{ at } 25^\circ\text{C}$$

and thiiranes⁵² *via* a single step, concerted process:



The absolute rate constants, measured by the flash photolysis-kinetic spectroscopic technique,⁵² at 25°C, are:

$$\text{R} = \text{R}' = \text{H}, k = 1.4 \times 10^{13} \text{ cm}^3 \text{ mol}^{-1} \text{ s}^{-1}$$

$$\text{R} = \text{CH}_3, \text{R}' = \text{H}, k = 2.7 \times 10^{13} \text{ cm}^3 \text{ mol}^{-1} \text{ s}^{-1}$$

$$\text{R} = \text{R}' = \text{CH}_3, k = 4.0 \times 10^{13} \text{ cm}^3 \text{ mol}^{-1} \text{ s}^{-1}$$

It has also been shown that $E_a = 0$ for the $\text{S} + \text{C}_2\text{H}_4\text{S}$ reaction.⁵³

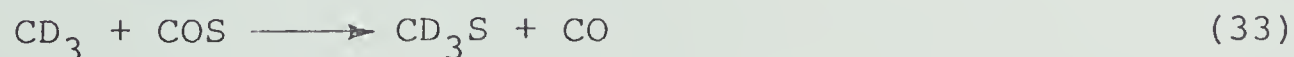
To date, the reactions of S atoms with alkyl sulfides and disulfides have not been reported.

(d) Reactions of Alkyl Radicals with Sulfides and Disulfides

Very few studies concerning radical reactions with organosulfur molecules have been reported to date.

(i) With Sulfides

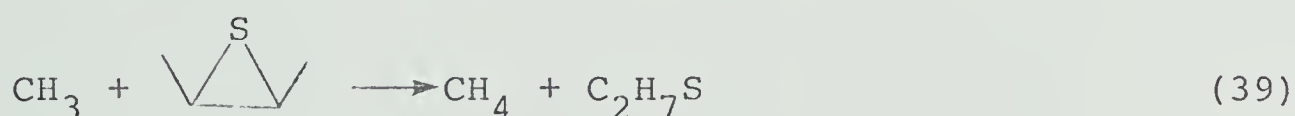
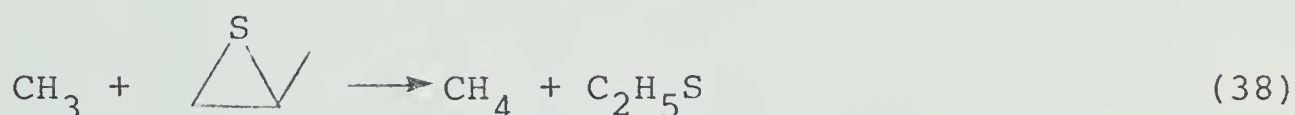
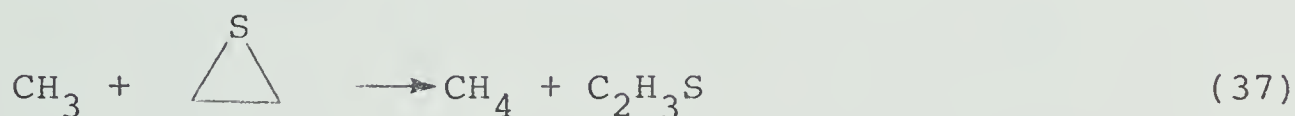
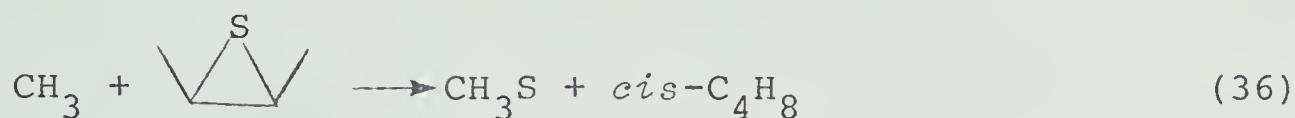
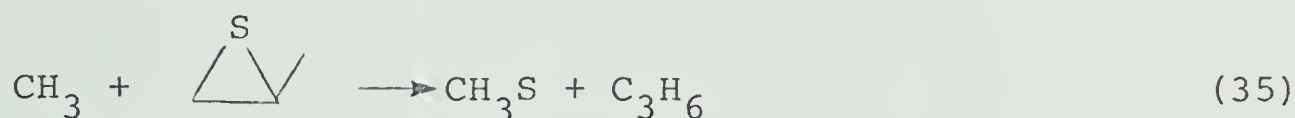
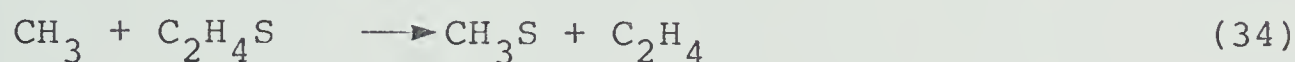
With COS, desulfurization by CD_3 radicals takes place,⁵⁴



and the rate constant, determined in competition with the $2\text{CH}_3 \rightarrow \text{C}_2\text{H}_6$ reaction is:

$$k_{33} = 3.8 \times 10^{11} \exp[-(11350)/RT] \text{ cm}^3 \text{ mol}^{-1} \text{ s}^{-1}$$




Methyl radicals react with thiirane, methylthiirane and *cis*-1,2-dimethylthiirane^{54,55} *via* concerted desulfurization and, to a lesser extent, hydrogen abstraction:



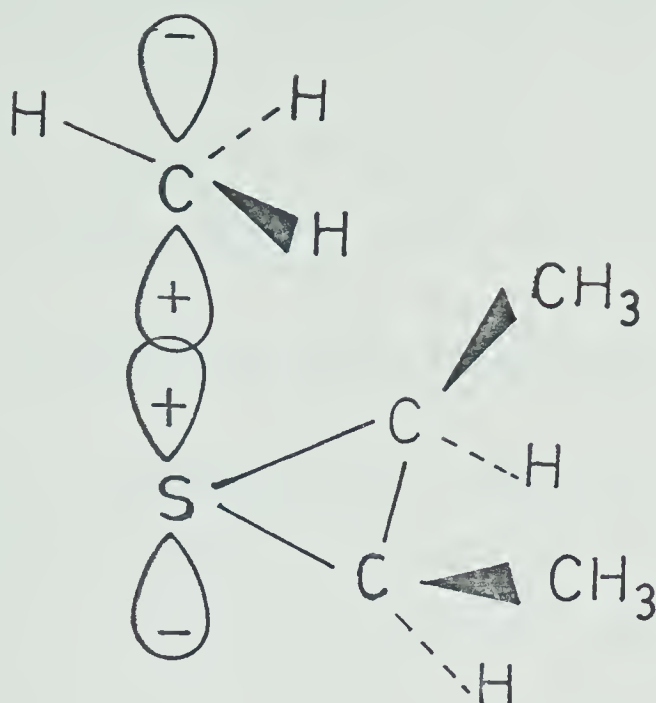
The corresponding Arrhenius parameters derived from kinetic analysis of the data are listed in Table III. Strausz and coworkers⁵⁴ suggested that the initial interaction involves the π orbital of the CH_3 radical and the non-bonding 3p orbital of the S atom:

TABLE III

Arrhenius Parameters for Some Atom Transfer Reactions

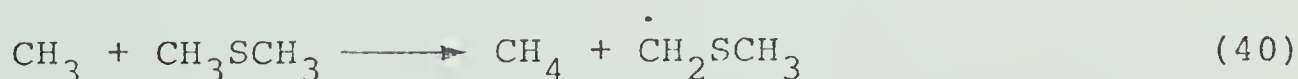
Compound	CH ₃			
	S-abstraction		H-abstraction	
	log A ^a	E _a ^b	log A ^a	E _a ^b
	11.35 ± 0.51 ^c	7.4 ± 0.9 ^c	11.34 ± 0.60 ^c	9.54 ± 1.00 ^c
	11.33 ± 0.92 ^d	7.5 ± 1.7 ^d	11.00 ± 0.48 ^d	8.26 ± 0.87 ^d
	12.31 ± 2.57 ^d	6.8 ± 3.9 ^d	11.03 ± 1.5 ^d	7.00 ± 2.41 ^d
COS	11.58 ± 0.25 ^c	11.4 ± 0.4 ^c		

^acm mol⁻¹ s⁻¹; ^bkcal mol⁻¹; ^cRef. 54; ^dRef. 55.



These results are in marked contrast to the $\text{CH}_3 + \text{epoxide}$ systems,⁵⁶ where hydrogen abstraction is the only observable process in spite of the fact that the enthalpy changes for deoxygenation and desulfurization are not different. As noted above, however, BEBO calculations⁵⁶ predict a prohibitively high activation energy for deoxygenation by atoms and radicals. Moreover, the non-bonding 3p orbital of S is more nucleophilic than the corresponding 2p orbital of O and sulfur has a higher aptitude for valence shell expansion; consequently, the activation energy for desulfurization is lowered.

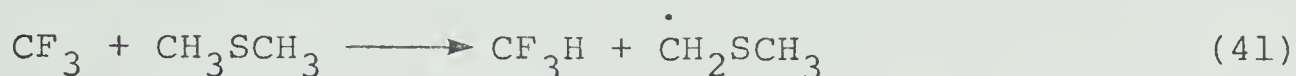
Methyl radicals produced from the photolysis of CH_3SCH_3 react with dimethylsulfide to yield methane *via* hydrogen abstraction:⁵⁷



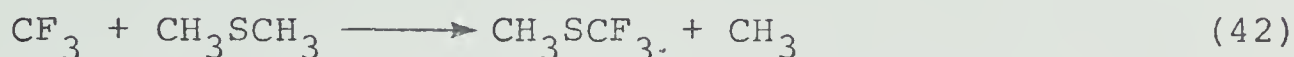
The activation energy for reaction (40) was reported by Rao and Knight^{57a} to be 9.30 ± 0.50 kcal mol⁻¹ and the rate constant, determined by Arthur and Lee^{57b}, in competition with the $2\text{CH}_3 \rightarrow \text{C}_2\text{H}_6$ reaction, is:

$$k_{40} = (4.17 \pm 0.84) \times 10^{11} \exp[-(9166 \pm 162)/RT] \text{ cm}^3 \text{ mol}^{-1} \text{ s}^{-1}$$

Recently Arthur and Yeo⁵⁸ reported that trifluoromethyl radicals produced by the photolysis of hexafluoroacetone also react with CH_3SCH_3 *via* hydrogen abstraction:



Surprisingly, the metathetical CH_3 group displacement reaction,



was not detected. The rate constant for hydrogen abstraction by CF_3 radicals is:

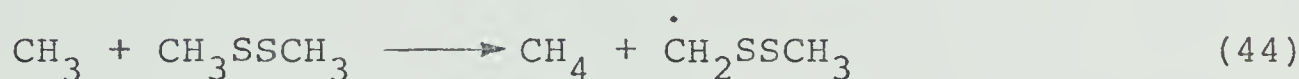
$$k_{42} = (4.76 \pm 1.00) \times 10^{11} \exp[-(6432 \pm 107)/RT] \text{ cm}^3 \text{ mol}^{-1} \text{ s}^{-1}$$

Comparing the reactivities of CH_3 and CF_3 radicals with regard to hydrogen abstraction from CH_3SCH_3 it is seen that at room temperature the rate of abstraction by CF_3 is 51 times higher than that by CH_3 and this difference is entirely due to the lower activation energy associated with the former reaction; this is in keeping with the general trend observed in the reactivities of CH_3 and CF_3

radicals with other compounds such as CH_3OCH_3 and CH_3COCH_3 .⁵⁷

(ii) With Disulfides

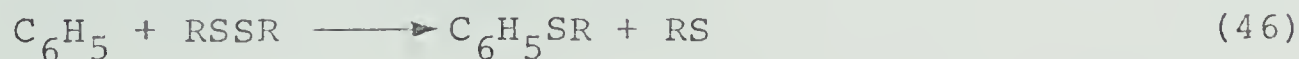
The photolysis of azomethane (at $253.7 \ll \lambda < 315 \text{ nm}$) in the presence of dimethyldisulfide at 100°C leads to the formation of CH_4 and CH_3SCH_3 . From this, together with kinetic analysis of the data, Suama and Takezaki⁵⁹ concluded that methyl radicals undergo hydrogen abstraction with the substrate as well as CH_3S group displacement,



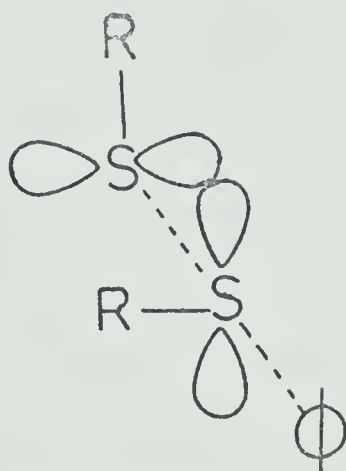
The relative rate constant ratio for reactions (43) and (44) is $k_{43}/k_{44} = 3.4$, and thus sulfur atom attack is again preferred over hydrogen abstraction.

(e) Reactions of phenyl radicals with disulfides

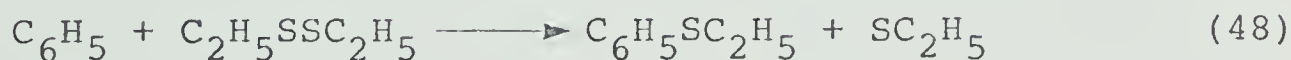
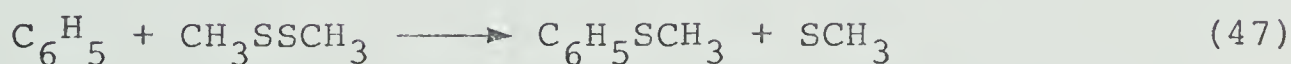
Pryor and Guard^{9a} studied the reactions of phenyl radicals, generated from phenylazotriphenylmethane, with aliphatic disulfides at 60° . Phenyl radicals undergo reactions analogous to those of alkyl radicals, i.e., hydrogen abstraction and thiyl radical displacement,



The relative importance of attack on the S atom of the disulfide decreased with increasing steric hindrance at the sulfur atom, as indicated by the 98% yield of $\text{C}_6\text{H}_5\text{SCH}_3$ *via* attack on CH_3SSCH_3 and the 49% yield of sulfide *via* attack on $(t\text{-C}_4\text{H}_9)_2\text{S}_2$. They proposed that the radical reaction involved a 3-atom-in-a-line Walden inversion type transition state



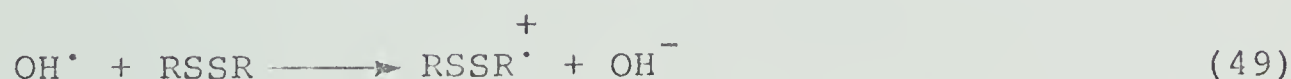
The relative rate constant ratio for reactions (47) and (48)



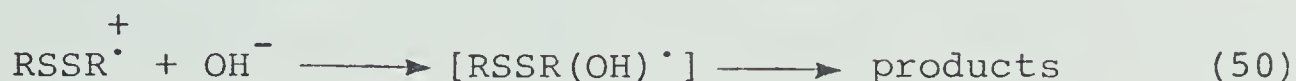
is $k_{47}/k_{48} = 1.78$.

(f) Reactions of Hydroxyl Radicals with Disulfides

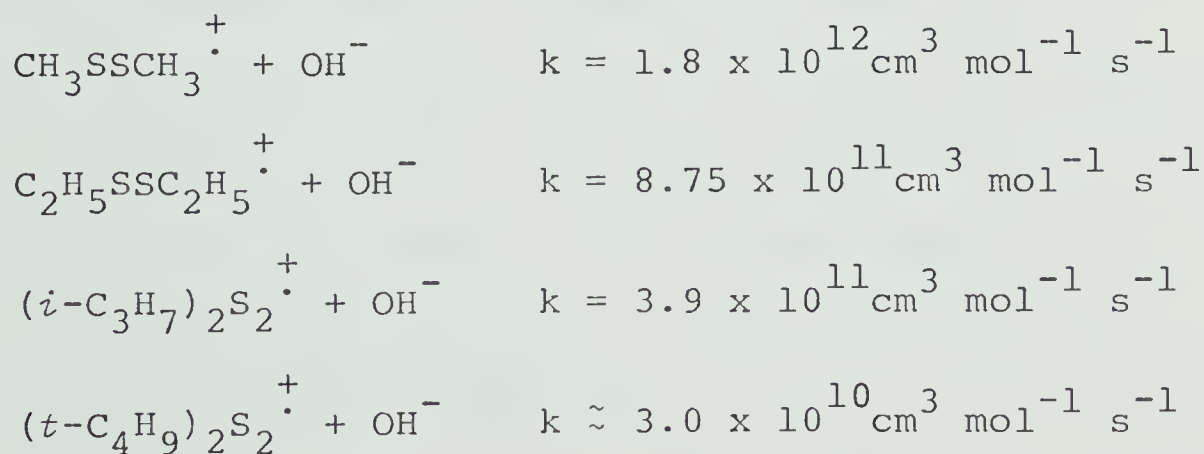
The interaction of hydroxyl radicals with simple aliphatic disulfides has been shown to lead to electron transfer,⁶⁰



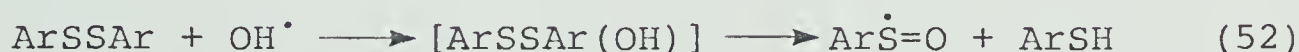
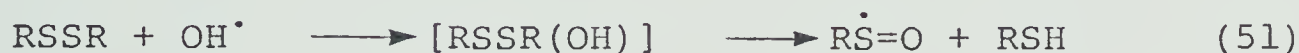
and the resulting radical cation decays by a diffusion-controlled bimolecular process:



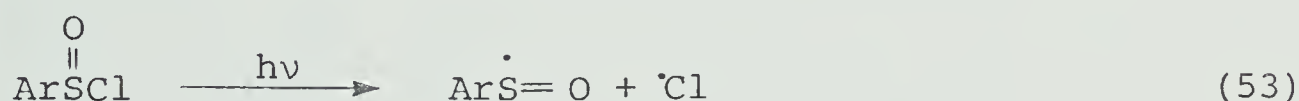
The rate constant for the neutralization of $\text{RSSR}^{\cdot+}$ by OH^- is controlled to a certain extent by the effective positive charge density at the sulfur bridge. Since the electron-donating properties of the substituents increase in the series $\text{CH}_3 < \text{C}_2\text{H}_5 < (\text{CH}_3)_2\text{CH} < (\text{CH}_3)_3\text{C}$, the net positive charge is expected to be highest for the $(\text{CH}_3)_2\text{S}_2^{\cdot+}$ and lowest for the $((\text{CH}_3)_3\text{C})_2\text{S}_2^{\cdot+}$ radical ions, and therefore the rate constants should follow that order. In addition, structural effects are considered to contribute to the observed changes in the rate constant for bimolecular decay since steric hindrance also increases, parallel to inductive effects. In agreement with these considerations the lowest value for the rate constant is found for the case of the $(t\text{-Bu})_2\text{S}_2^{\cdot+}$ radical ion. The observed rate constants are as follows:



When the reactions were monitored by esr spectroscopy new transient radical intermediates were observed, the signals of which were assigned to sulfinyl (ArSO or RSO) radicals.



A variety of these species have been detected and characterized. Further support for the assignment comes from the finding that radicals of the same type were detected during the low temperature photolysis of aromatic sulfinyl chlorides in diethyl ether.⁶¹



3. Thiyl Radicals.

(a) Generation, identification and physical properties

Thiyl radicals are commonly generated from the direct or mercury sensitized photolysis, or thermolysis, of thiols, sulfides and disulfides.⁶² In the solid phase, they are readily apparent from their characteristic blue and red colours, and several reports have appeared on their spectral characteristics. Some representative examples are listed in Table IV.


TABLE IV

Generation and Spectral Characteristics of Some Thiyl Radicals

Precursor	Method	Conditions	Thiyl Radical	λ_{max} , nm	Ref.
CH_3SH	photolysis ($\lambda = 254$ nm)	in cavities of a water clathrate lattice	CH_3S	310	65
$\text{C}_2\text{H}_5\text{SH}$	photolysis ($\lambda = 254$ nm)	in cavities of a water clathrate lattice	$\text{C}_2\text{H}_5\text{S}$	370	65
RSH	photolysis ($\lambda = 254$ nm)	rigid glass at 77°K	RS	~ 400	64a
RSSR	photolysis ($\lambda = 254$ nm)	neat matrix at 77°K	RS	~ 360	64a
CH_3SH CH_3SCH_3 CH_3SSCH_3	flash photolysis ($\lambda = 195$)	gas phase	$\left. \begin{array}{c} \text{CH}_3\text{S} \end{array} \right\}$	219	67

.....continued

TABLE IV (continued)

$\phi_3\text{CSH}$	photolysis ($\lambda=313$)	benzene matrix at 77°K	$\phi_3\text{CS}$	330	64b
CF_3SSCF_3	photolysis ($\lambda=254\text{ nm}$)	neat matrix at 77°K	CF_3S	-	63
	photolysis ($\lambda=254\text{ nm}$)	neat matrix at 77°K	$\text{CH}_2\text{CH}_2\text{CH}_2\text{S}$	-	63

The thermal stability of thiyl radicals is relatively high.⁶³⁻⁶⁶ CH_3S and $\text{C}_2\text{H}_5\text{S}$ decay at temperatures where rotation about the C-S bond in the lattice is still restricted. Apparently heavier thiyl radicals are able to rotate to some extent before decaying, e.g., (*t*-butyl)S has a single line spectrum at $\sim 130^\circ\text{K}$ and decays at temperatures greater than 150°K . Radicals adsorbed on Vycor glass showed higher thermal stability, with rapid decay commencing only above 200°K . The observed increased thermal stability of the adsorbed radical is expected since adsorption decreases the mobility of the radical. It is this enhanced stability of adsorbed radicals which accounts for the characteristic decay rate differences between matrix and Vycor glass photolyses. Adsorption seems to prevent cage recombination of the geminate thiyl radical pair in disulfide photolyses and thus increases the apparent rate of photolysis. In the photolysis of mercaptans, cage recombination is unimportant because of the ease by which H atoms escape the cage.

The ESR spectra of various alkylthiyl radicals,^{63,64} CF_3S , ϕS , $\phi_3\text{CS}$, $\cdot\text{CH}_2\text{CH}_2\text{CH}_2\text{S}\cdot$, and substituted ϕS have been obtained upon irradiation ($\lambda < 220\text{ nm}$) of either neat solid disulfide matrices or of disulfides adsorbed on Vycor glass at 77°K . Simple alkylthiyl radicals have three g-values (generally referred to as the characteristic "sulfur pattern") about 2.058, 2.025, and 2.001.

The spectrum of CF_3S radicals is unusual in that it exhibits only two principal g-values (2.030 and 2.004), suggesting that the radical has axial symmetry. Arylthiyl radicals exhibit esr spectra similar to those of alkylthiyl radicals and only differ in the hyperfine structure; however, in the absence of α -hydrogens which will couple with the electronic spin, three distinct anisotropic g values are obtained, indicating large spin-orbit coupling.

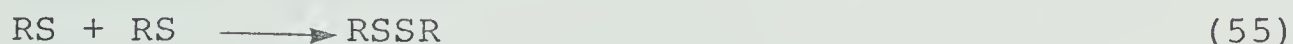
The unpaired spin is largely localized on the non-bonding orbital of the S atom. Para or electron-donating substituents stabilize ArS (presumably making ArS more like the stable species ArS^- , in contrast to the effect of electron withdrawing substituents which would make them more like the highly reactive species RS^+).⁶⁶ In solution or gas phase, alkylthiyl radicals clearly exist as neutral free radicals. The gas phase characteristic UV absorption band for CH_3S radicals has been reported by Callear *et al.* as being 218.5 nm.⁶⁷

(b) Reactions of Thiyl Radicals

Similarly to alkyl radicals, thiyl radicals undergo disproportionation, combination, abstraction, addition and metathetical reactions. Surprisingly, very little kinetic data are available but the results suggest that thiyl radicals are more reactive than alkyl radicals.

(i) Disproportionation-Combination

Thiyl radicals, e.g., produced in the photolysis or thermolysis of thiols, alkylsulfides and disulfides disproportionate and combine according to the following equations:



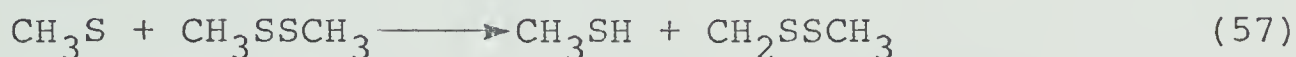
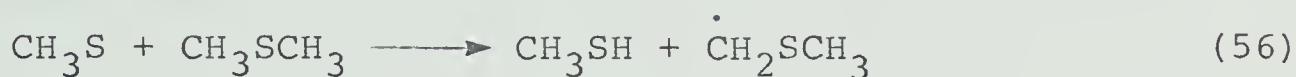
and the rate constant ratio k_d/k_c can be calculated from the relative yields of thiol and disulfides. For the cases of CH_3S and C_2H_5S values of $k_d/k_c \leq 0.05$ and 0.13 , respectively, have been derived from the photolysis of CH_3SCH_3 ^{57a} and Hg photosensitized decomposition of $C_2H_5SC_2H_5$.⁶⁸ The small values are another example in the growing body of evidence indicating that organosulfur compounds do not readily undergo transformations in which C-S bonds are converted to C=S, unlike the well established tendency of their oxygen analogs. This is a consequence of the relative exothermicities of the two processes. The generally smaller exothermicity of the $C-S \rightarrow C=S$ rearrangement results from the relatively small difference in the CS single and double bond strengths.

The rate constant for the combination of methylthiyl radical was determined in rotating sector experiments to be, $k = (2.5 \pm 0.7) \times 10^{13} \text{ cm}^3 \text{ mol}^{-1} \text{ s}^{-1}$.⁶⁹ This

value is, within experimental error, equal to the combination rate, $k = (2.43 \pm 0.24) \times 10^{13} \text{ cm}^3 \text{ mol}^{-1} \text{ s}^{-1}$ reported for CH_3 radicals.⁷⁰

(ii) Abstraction

CH_3S is a major product of the gas phase photolysis^{57,71} (and thermolysis⁷²) of CH_3SCH_3 and CH_3SSCH_3 , indicating that hydrogen abstraction takes place:



The measured activation energies for reactions (56) and (57) are $5.4 \text{ kcal mol}^{-1}$ and $5.1 \text{ kcal mol}^{-1}$.

From competitive experiments with 2-methylpentane,



the activation energy for step (58) was estimated to be $7.5 \text{ kcal mol}^{-1}$.^{57a}

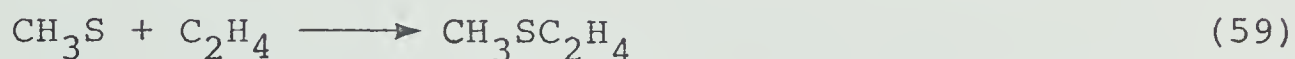
Thus two conclusions emerge:

1. Alkylthiyl radicals are more reactive than alkyl radicals for which abstraction reactions from alkanes commonly feature activation energies ranging from 9 to 12 kcal mol^{-1} .
2. Alkylthiyl radicals abstract much more efficiently from sulfides and disulfides than from alkanes. This

would seem to suggest that the adjacent C-H bond in sulfides and disulfides are even weaker than a typical tertiary C-H bond in alkanes.

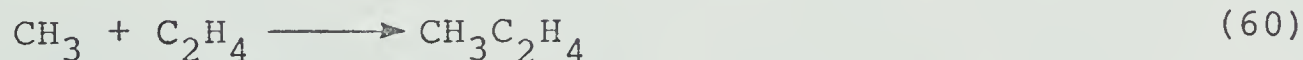
(iii) Addition

The addition reactions of thiyl radicals to alkenes have not been extensively studied.^{69,73} From the photolysis of CH_3SH ($\lambda = 254\text{--}265\text{ nm}$) in the presence of ethylene, the rate constant for



was determined to be $4.8 \times 10^8 \text{ cm}^3 \text{ mol}^{-1} \text{ s}^{-1}$.⁶⁹ The relative inefficiency of this reaction was also clearly demonstrated by Rao and Knight who showed that CH_3S and $\text{C}_2\text{H}_5\text{S}$ radicals produced in the photolysis of a mixture of 3 Torr dimethyldisulfide and 3 Torr diethyldisulfide could not be scavenged by 500 Torr C_2H_4 .

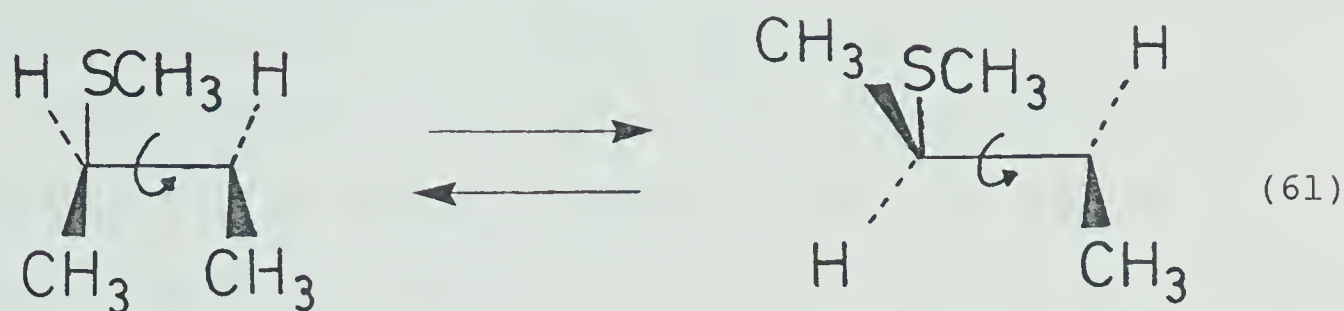
Comparison with methyl radical addition to ethylene however



for which $k_{60} = 7.4 \times 10^5 \text{ cm}^3 \text{ mol}^{-1} \text{ s}^{-1}$ ⁷⁴ again shows that CH_3S is a better electrophile than CH_3 .

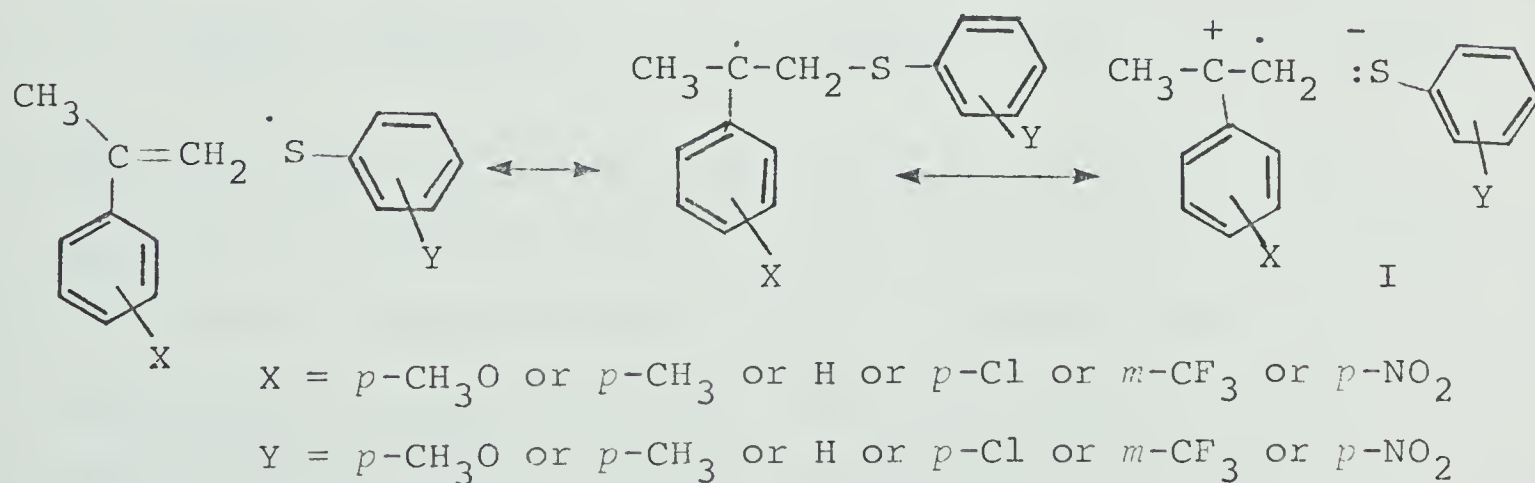
Walling and coworkers^{73a} have shown that for the particular case of $\text{CH}_3\text{S} + \text{cis-2-butene}$ reaction (59) is reversible. Thus substantial amounts of *trans*-2-butene

were detected, indicating that rotation takes place in the adduct:



Decomposition of the adduct into CH_3S and 2-butene was very fast compared to hydrogen abstraction from CH_3SH , by a factor of 80 for the *trans*-2-butene adduct and 20 for the *cis*-butene adduct at 60°C .

In experiments involving the addition of substituted phenylthiyl radicals to substituted α -methylstyrene, Geers *et al.*^{73b} suggested that the addition reactions in such systems might, in general, be controlled by ground state and transition state electronic effects:



The ground state effects arise from (i) the presence of a strong electron-withdrawing group in the aromatic

portion of the alkene which tends to minimize the electron density at the reactive double bond, and (ii) the electrophilic character of the phenylthiyl radicals.

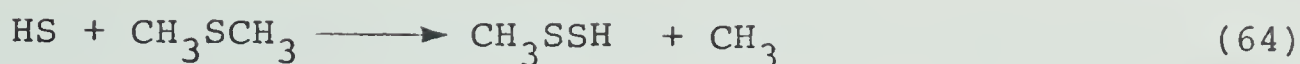
The transition state electronic effect comes from the fact that particular alkenes are able to assume a charge separated canonical structure I. Such a contributing form is most compatible when the anionic portion of the system is also electronically stabilized.

(iv) Metathetical Reactions

Metathetical reactions of thiyl radicals are of general occurrence in the photolysis and thermolysis of disulfides. To give one example, co-photolysis of CH_3SSCH_3 and $\text{C}_2\text{H}_5\text{SSC}_2\text{H}_5$ ⁷⁵ led to the formation of large amounts of $\text{CH}_3\text{SSC}_2\text{H}_5$, far exceeding the amount expected on the basis of $\text{CH}_3\text{S} + \text{C}_2\text{H}_5\text{S}$ combination:

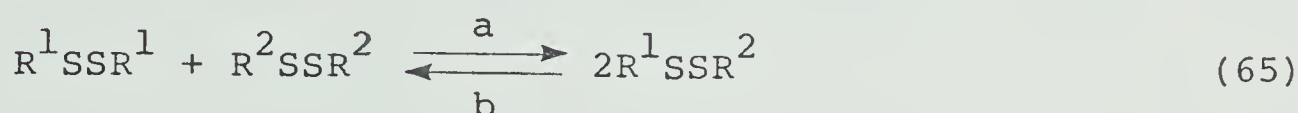


The chain thus initiated is sufficiently long that this system is frequently used for the synthesis of asymmetrical disulfides. Unfortunately, no rate constants have been reported for these reactions. Recently however it was shown that HS radicals undergo an analogous metathetical reaction with CH_3SCH_3 :



and the rate parameters were estimated to be $A \sim 10^9\text{--}10^{10} \text{ cm}^3 \text{ mol}^{-1} \text{ s}^{-1}$ and $E_a < 2.7 \text{ kcal mol}^{-1}$.⁴⁰

Disproportionation of dialkyldisulfides is found to be an equilibrium reaction and a number of studies have been reported by Haraldson *et al.* and Olander and Sunner.^{24,76} Haraldson and coworkers irradiated a number of pairs of symmetrical disulfides and from the asymmetrical disulfide yield



obtained the equilibrium constant,

$$K_{65} = k_{65a}/k_{65b} \quad (66)$$

at 25°C and 60°C. The statistically expected value for K_{65} is 4; experimentally, it was found to be ~5.5 for groups such as CH_3 , C_2H_5 , and $i\text{-C}_3\text{H}_7$ and was also temperature independent, i.e., $\Delta H_{65} = 0$. However, $K_{65} = 24$ for the mixture $(\text{C}_2\text{H}_5\text{S})_2\text{--}(t\text{-C}_4\text{H}_9\text{S})_2$, thus favoring $\text{C}_2\text{H}_5\text{S}t\text{-C}_4\text{H}_9$. This result was attributed to the presence of rigid conformations in the *t*-butyldisulfide molecule.

4. Transition State Theory for Bimolecular Reactions.

Transition state theory formulates the rate of any reaction in terms of a "transition" state - a molecular

complex having the proper configuration in space and a minimum energy for the reaction to occur - situated on top of the potential energy barrier along the reaction path. The nature of this potential energy barrier can be calculated as a function of the relative positions of the different nuclei or as a function of different atom positions. Collision theory relates the minimum energy necessary for the reactants to reach the top of the energy barrier and attain the configuration of the transition state - or the activated complex - to the energy of activation.

Transition state theory further assumes an equilibrium between reactants, e.g., A and B and the activated complex AB^\ddagger . The equilibrium constant K^\ddagger is then

$$K^\ddagger = \frac{[AB^\ddagger]}{[A][B]} \quad (67)$$

The bimolecular rate constant k_{AB} , which is the rate of passage of the complex over the potential energy barrier, can then be expressed as

$$k_{AB} = \left(\frac{kT}{h}\right) K_{AB}^\ddagger \quad (68)$$

where k is the Boltzmann constant, T the temperature and h , Planck's constant. Now since

$$-RT \ln K^\ddagger = \Delta H^\ddagger - T \Delta S^\ddagger \quad (69)$$

equation (69) can be expressed as

$$k_{AB} = \frac{kT}{h} e^{\Delta S_{AB}^{\ddagger}/R} e^{-\Delta H_{AB}^{\ddagger}/RT} \quad (70)$$

From the Arrhenius form of the rate constant,

$$k = A e^{-E/RT} \quad (71)$$

it is seen that

$$A = \left(\frac{ekT}{h}\right) e^{\Delta S_{AB}^{\ddagger}/R} \text{ and } E = \Delta H_{AB}^{\ddagger} + RT \quad (72)$$

For ground state molecules the standard entropies are either known or can be calculated from statistical mechanics with fairly good precision. Another, more rapid and nearly as accurate a method, developed by Benson,⁷⁷ is an empirical one based on additivities of molecular properties with the assumption that the activated complex is a rigid molecule. In this way, lower limits of ΔS^{\ddagger} are estimated. The latter method is extremely useful in that it can be applied for the calculation of the entropies of activated complexes. In such calculations the translational, rotational, symmetry and spin contributions to the entropy can be readily evaluated; the vibrational contributions are less straightforward and the usual method is to adjust the normal frequencies on the basis of those of analogous compounds. For reactions involving a light atom, such

as H or D, with a large polyatomic molecule, the transition state complex has approximately the same intrinsic entropy as the substrate and hence,

$$\Delta S^\ddagger = (S^\circ(\text{Substrate}) + 1.4) - (S^\circ(\text{Substrate}) + S^\circ(\text{H})) \quad (73)$$

where 1.4 is the spin correction. Symmetry corrections may also be necessary.

In this way, preexponential factors for reactions for which experimental data are not available can be calculated, usually with a fair degree of precision. Of perhaps more significance however is that valuable information can be brought to light on the activated complex.

5. Computer Modeling of Chemical Reactions.

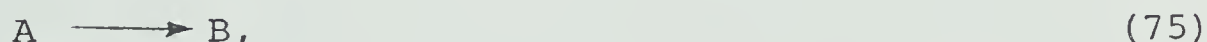
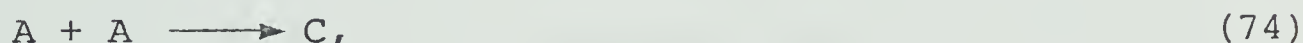
With the general availability of high performance digital computers, computer modeling of complex chemical reactions has become a powerful method in gas phase reaction kinetics for the interpretation of experimental data in terms of a detailed mechanism and the corresponding rate constants.

Computer modeling of chemical reactions consists of the construction of a model mechanism and the subsequent numerical integration of its representative set of coupled simultaneous ordinary differential equations.⁷⁸ The single independent variable is time, the dependent

variables are the concentrations of all chemical species that change during the course of the reaction.

The model mechanism consists of a sequence of elementary reactions and a set of the corresponding rate constants. It is varied (some elementary reactions are deleted or new ones are added, the values of unknown or uncertain rate constants are adjusted) until satisfactory agreement between the observed and calculated time dependence of the concentrations is achieved.

In chemical kinetics the rate equations can be directly deduced from the mechanism and they provide explicit algebraic expressions for the time derivatives of all species concentrations, as shown in the following simple example



$$\frac{d[A]}{dt} = -2k_{74}[A]^2 - k_{75}[A], \quad (76)$$

$$\frac{d[B]}{dt} = k_{75}[A], \quad (77)$$

$$\text{and } \frac{d[C]}{dt} = k_{74}[A]^2. \quad (78)$$

Complex reaction mechanisms usually consist of numerous elementary reactions having a wide range in rates, especially when transient intermediates at very

low concentrations are created and consumed rapidly. This characteristic results in a so-called "stiff" set of differential equations, the solution of which requires extremely short integration steps and hence very long computation times using conventional methods.

For the numerical integration, usually an algorithm developed by C.W. Gear,⁷⁹ or one based on its subsequent development, is used. The program applies a multistep, predictor-corrector method, and successfully overcomes the difficulty presented by the "stiffness" of the differential equations. It also continuously adjusts the time increments in order to reduce the computational times.

Computer modeling of complex chemical reactions has been found to be a very useful method, both for testing of the compatibility of a suggested mechanism with the experimental data, and for the derivation of values for unknown rate constants of elementary reactions. In more recent years it has become a powerful method for the simulation of the ongoing chemistry of polluted atmospheres.⁸⁰

6. Aim of the Present Investigation.

As seen from the above discussion the results available to date strongly suggest that atom and radical attack on alkylsulfides and disulfides takes place

mainly, in some cases exclusively, at the nonbonding 3p orbital of sulfur. Kinetic data however are sparse and, for the particular case of H atoms, have only been determined for the H + COS, C₂H₄S, and CH₃SCH₃ systems. The reactions of H atoms with disulfides have not been investigated at all.

It was therefore decided to initiate a kinetic-mechanistic study of the gas phase reactions of H atoms with low molecular weight disulfides with the aim of elucidating the nature of the primary processes and to establish the overall mechanism by means of product analysis, together with the effects of exposure time, concentration and temperature on the product quantum yields. Next, rate coefficients for the primary reaction would be established in competition with the H + C₂H₄ reaction, for which the rate parameters are well known. From the measured activation energies and preexponential factors, it was anticipated that some correlation with the exothermicities of the reactions could be established, and, more importantly, that knowledge concerning the nature of the activated complex could be deduced. As a corollary to these studies, some aspects of the chemical reactivity of simple alkylthiyl radicals can be brought to light.

The following disulfides were selected for study:

- (a) dimethyldisulfide, the simplest in the series. It was anticipated that the overall mechanism would be relatively uncomplicated since few radicals can be produced, and hence kinetic-mechanistic interpretation of the results would be fairly straightforward;
- (b) diethyldisulfide, in order to see whether increasing alkyl substitution would have any effect on the nature of the primary process;
- (c) ethylmethyldisulfide, where the possibility of competing primary processes can be investigated;
- (d) bis(trifluoromethyl)disulfide, to study the possible effects of strongly electron-withdrawing substituents on the nature and rate of the primary reaction.

Finally, the $\text{H} + \text{diethylsulfide}$ reaction was investigated in order to determine whether the metathetical alkyl displacement reaction previously established for the $\text{H} + \text{dimethylsulfide}$ reaction is common to alkylsulfides.

CHAPTER II

EXPERIMENTAL

1. High Vacuum System.

A conventional high vacuum system (Figure 1), consisting of pumps, two distillation units (one for purification of substrates, the other for separation of products), a photolytic assembly, gas storage bulbs, Töepler pump-gas buret and metering units, has been used throughout. The system was pumped down to 10^{-6} Torr by means of a two stage mercury diffusion pump backed by a Welch Duoseal mechanical pump. Delmar float and Helium tested Hoke valves, and Delmar Teflon plug stopcocks were used throughout the system in order to minimize loss of the sulfur-containing products during gas transfers. Absolute pressures were measured with either a Mcleod gauge, a constant volume mercury manometer, a Barocel electronic manometer, Model 1174 Type 570A-10T, or an MKS Baratron pressure meter, serial 19854, Type 170M-6B, associated with a high temperature pressure head having a 100 torr pressure range, serial 19853, Type 315BHS-100. Pirani tubes (Consolidated Vacuum Corporation Catalogue No. GP-001), conveniently located in the system, were used to monitor gas transfers. The Mcleod gauge was used to calibrate the Pirani Vacuum gauges (Type G-140C). The distillation trains consisted of several U- and multi-coil traps, and a solid nitrogen

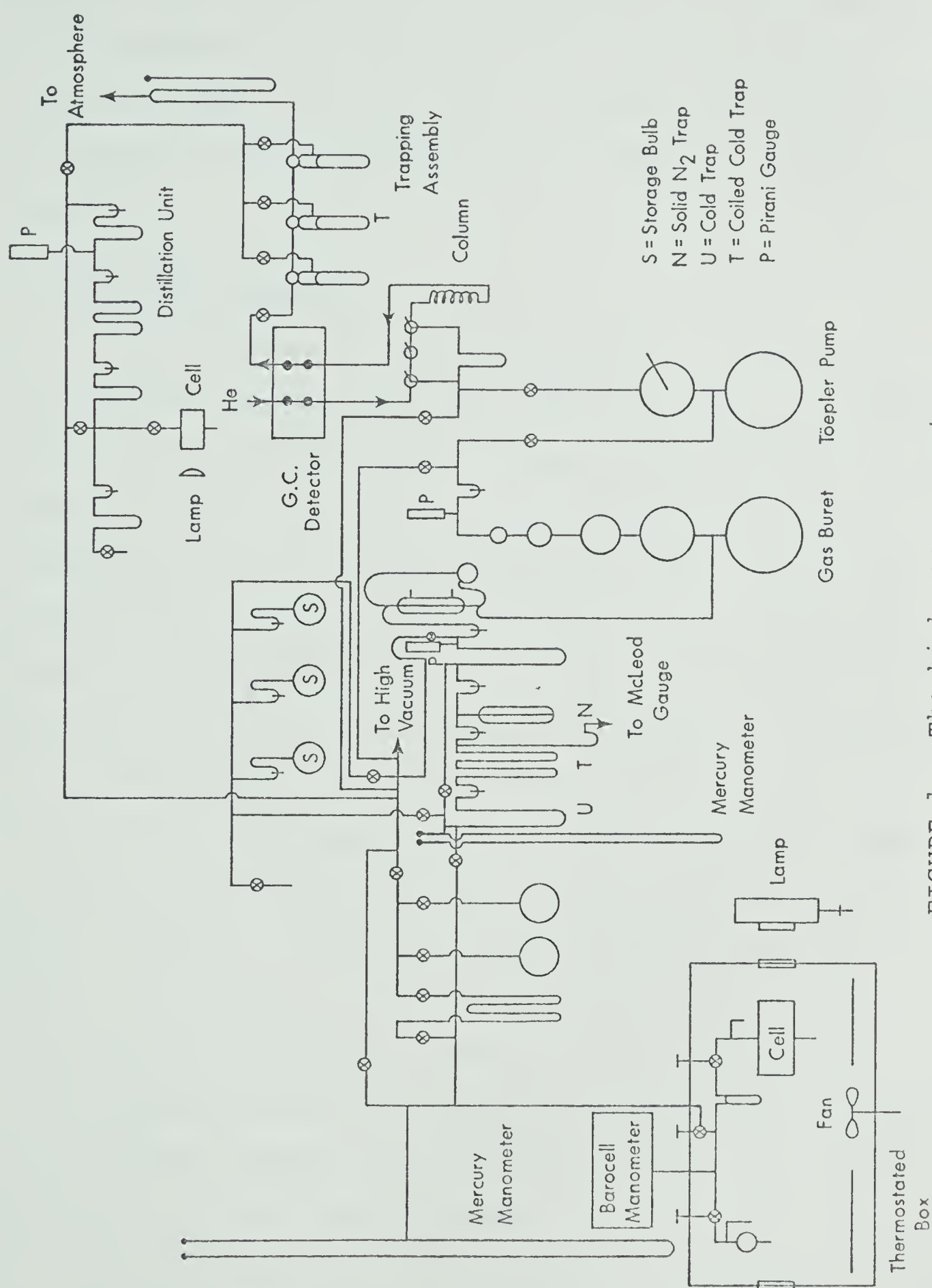


FIGURE 1. The high vacuum system.

trap interconnected by mercury float and Hoke valves. Samples were introduced to the attached gas chromatograph from the Töepler pump and gas buret into the trapping assembly. The latter was used in conjunction with the gas chromatograph for preparative purification or product separation.

2. Photolytic Assembly.

The photolytic assembly, illustrated in Figure 2, was specially designed for the study of H atom reactions with low vapor pressure disulfides. The cylindrical quartz reaction cell (5 x 10 cm), of volume 200 cm³, including the cold finger and the dead space between the cell and the shutoff valve, was enclosed in an aluminum block furnace insulated by a 2 cm thickness of glass wool and equipped with iron-constantan thermocouples connected to a readout dial. The furnace faces had aluminum brackets in which quartz filters could be inserted. The furnace was heated electrically to temperatures in the range 25-199°C, by two 10 cm pencil heaters placed in axial holes, each located at the furnace face, in the two halves of the aluminum block furnace. Temperatures ($\pm 1^\circ\text{C}$) were monitored by standard iron-constantan thermocouples and a thermometer placed in an axial hole located at the face of the block furnace.

The whole assembly, consisting of a U-trap, a storage bulb, Hoke valves, a calibrated volume, and the

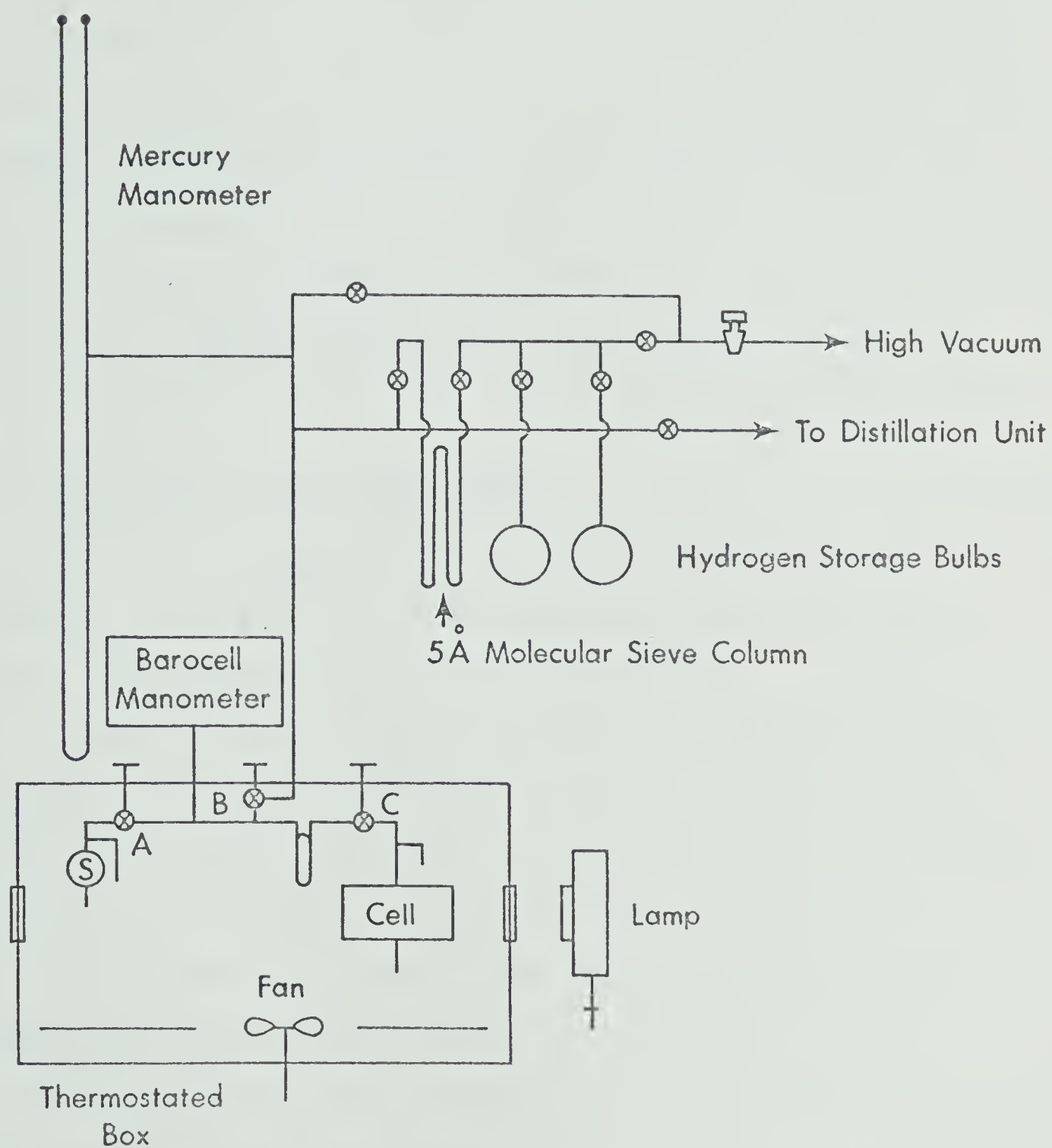


FIGURE 2. The photolytic assembly.

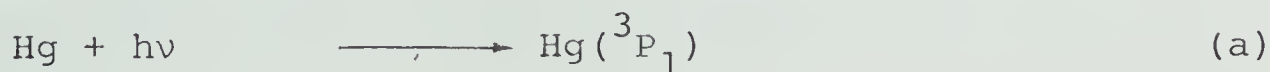
cell enclosed in an aluminum block furnace, was in a thermostated box (100 x 70 x 50 cm), constructed of asbestos, 15 mm thick. The box was heated electrically to constant temperatures in the range 25-65°C, by a spiral heater located at the bottom of the box. The thermostated housing served to maintain the substrate in the gaseous state during transfer to the reaction cell, and was also found to lead to more quantitative product transfer from the reaction cell to the analytical system. To ensure uniform temperature ($\pm 1^\circ\text{C}$) inside the box the air was circulated by a fan, driven by an induction motor.

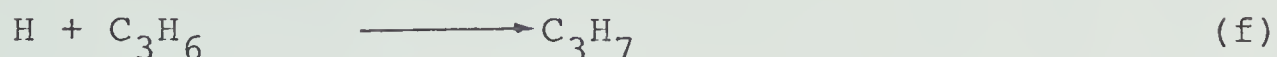
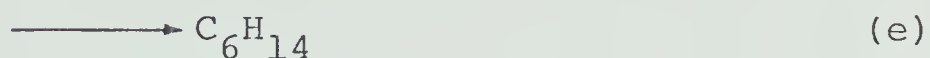
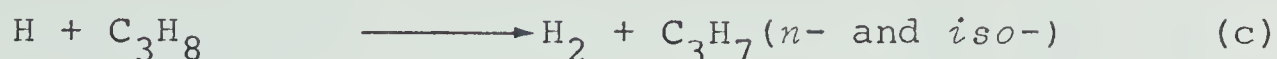
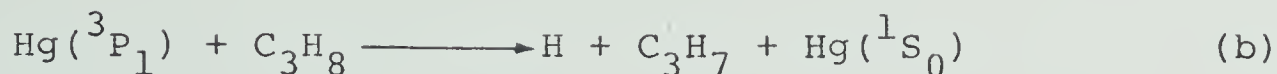
3. Light Sources and Actinometry.

For the H atom reactions, the light source was a Hanovia low pressure Hg resonance lamp equipped with a 253.7 nm Baird Atomic interference filter.

For photolytic synthetic purposes, a Hanovia medium pressure Hg lamp, Model 30620, was used without a filter. This lamp and the photolytic assembly for the preparative purposes are located at the top section of Figure 1.

The light intensity of the low pressure Hg resonance lamp was determined by propane actinometry.⁸¹ Under conditions of low lamp intensities the only elementary processes of importance are the following:





Back⁸² has shown that $\phi(\text{H}_2)$, the quantum yield of hydrogen production, decreases with irradiation time until the concentration of C_3H_6 reaches a steady state, after which $\phi(\text{H}_2) = 0.581$ at 27°C and remains constant. In the present experiments, about 600 torr propane was irradiated repeatedly until the rate of hydrogen production became constant and this value was used to calculate the lamp intensity. The lamp intensity was kept as low as possible, of the order of $0.014 \text{ einstein min}^{-1}$, in order to minimize radical-radical reactions and to ensure a low concentration of H atoms.

4. Materials.

All materials used in this study were of research grade and were routinely purified by distillation *in vacuo*. Table V lists the sources and methods of purification of the various compounds used. The purities of all the distillates collected were further checked by gc.

TABLE V

Sources of Materials Used and Purification Procedures

Material	Source	Grade and Purity	Purification
Hydrogen	Airco	Research grade >99.9%	distilled through at 5 Å molecular sieve column
Ethylene	Phillips	Research grade >99.5%	distilled at -160°C
Hydrogen Sulfide	Matheson	Research grade	distilled at -160°C
Propane	Phillips	Research grade >99.5%	distilled at -130°C
n-Butane	Phillips	Research grade	distilled at -130°C
Methanethiol	Matheson	Research grade	distilled at -130°C
Ethanethiol	Matheson	Research grade	distilled at -130°C
Dimethyldisulfide	Eastman	Research grade	gc 4 ft tricresyl- phosphate at 25°C
Diethyldisulfide	Eastman	Research grade	gc 4 ft tricresyl- phosphate at 110°C
Ethylmethyldisulfide	Prepared (<i>vide infra</i>)	Contained mixtures of CH ₃ SSCH ₃ and C ₂ H ₅ SSC ₂ H ₅	gc 4 ft tricresyl- phosphate at 25°C

....continued

TABLE V (continued)

Ethylmethanethiol	Baker	Research grade >99.5%	gc 10 ft tricresyl- phosphate at 25°C
Diethanethiol	Baker	Research grade	gc 10 ft tricresyl- phosphate at 25°C
Bis(trifluoromethyl)- disulfide	Peninsular Chemical Research	Technical (~80%)	distilled at -130°C
Thiirane	Peninsular Chemical Research	Technical (~80%)	distilled at -130°C

Ethylmethyldisulfide was prepared from the photolysis of equimolar amounts of dimethyldisulfide and diethyldisulfide. It was purified by gc using a 4 ft 10% tricresylphosphate on Chromosorb W column operated at room temperature using helium as carrier gas at a flow rate of $110 \text{ cm}^3 \text{ min}^{-1}$ (retention time, 41 min). The purified disulfide was always stored *in vacuo* at -196°C .

5. The Analytical System.

The analytical system used, illustrated in Figure 1, consisted of a calibrated gas burette connected directly to the injection loop of a gas chromatograph. The detector was a Gow-Mac Model TRIIB, which was powered by a Gow-Mac power supply Model 9999-C operated at 110°C . The unit was operated at 200 mA, and the results were read out on a Sargent recorder, Model S-72180, operated at a chart speed of one inch per minute. Helium, dried and purified by passage through a 5 \AA molecular sieve column, was used as carrier gas, at flow rates determined by an open-end oil manometer which was calibrated against a soap bubble flowmeter. The types of gc columns used, the operating conditions and retention times of the various compounds encountered in this study are summarized in Table VI.

The gc effluent could be passed through a series of coiled cold traps in which desired compounds could be

TABLE VI

Gas Chromatograph Retention Data and Operating Conditions

Column	Length, ft	Temperature, °C	Flow Rate, cm ³ min ⁻¹	Compounds analyzed	Retention time, min.
Tricresylphosphate	4	25	100	CH ₃ SH	1.50
				C ₂ H ₅ SH	1.85
				CH ₃ SSCH ₃	18.6
				C ₂ H ₅ SSCH ₃	45.0
				C ₂ H ₅ SSC ₂ H ₅	67.0
	10	25-110°C	25	CH ₃ SH	5.5
				C ₂ H ₅ SCH ₃	8.0
				C ₂ H ₅ SH	5.0
				C ₂ H ₅ SC ₂ H ₅	8.0
				n-C ₄ H ₁₀	3.65
				C ₂ H ₅ C(CH ₃)HSC ₂ H ₅	32.0
				C ₂ H ₅ SC(Me)HC(Me)-	
				HSC ₂ H ₅	94.0
Porapak N	8	59	40	C ₂ H ₄	9.0
				C ₂ H ₆	10.3
				H ₂ S	14.0

.....continued

TABLE VI (continued)

Porapak Q	5	60	60	CF ₃ SCF ₃	12.0
				CF ₃ SSCF ₃	24.0
Molecular Sieve	10	25	60	CH ₄	4.5

isolated for further analysis and identification.

Provisions were also made to bypass the detector for the cases of unstable compounds.

Product identification was made initially on the basis of comparison of the gc retention times with those of authentic samples and then subsequently confirmed by mass spectrometric analysis. The detector response was calibrated from authentic samples and checked periodically for reproducibility. Peak areas were measured with an Otto planimeter.

6. Operational Procedure.

The reaction cell and the thermostated box were heated overnight to the desired reaction temperature and 65°C, respectively. The lamp was allowed to equilibrate at least 30 minutes prior to irradiation. Control experiments were made at each temperature in order to check whether thermal decomposition of the substrate was involved. All experiments were carried out in the gas phase.

The substrate was expanded from the storage bulb to the reaction cell and then the Hoke valves A and B, shown in Figure II, were shut off. Its pressure was measured by the Barocel electronic manometer and then the Hoke valve C was shut off. The substrate (≤ 30 torr) was condensed in the cold finger of the photolytic cell

by using liquid nitrogen contained in a small Dewar flask introduced into the thermostated box through a window. Excess substrate was pumped out by opening the Hoke valve B to the high vacuum.

Approximately 580 ± 10 torr hydrogen was then admitted into the reaction cell. The hydrogen pressure was measured with a mercury manometer and then the Hoke valve C was shut off. Excess hydrogen was transferred to the storage section by condensing it in a 5\AA molecular sieve column kept at -196°C , then expanding it into two hydrogen storage bulbs.

The reaction mixtures were equilibrated for 30 minutes before irradiation. After photolysis, the hydrogen was pumped out very slowly through a series of cold traps, five at -196°C and one at -210°C , keeping the pressure reading on the Barocel electronic manometer in the range 1-2 torr. The remaining fraction, consisting of substrate and products, was analyzed by gc on the 10 ft tricresylphosphate column.

For experiments carried out in the presence of ethylene the substrate was condensed in the reaction cell and the Hoke valves A and C were shut off. Ethylene was admitted into a calibrated volume, and then Hoke valve B was shut off. The ethylene pressure (≤ 30 torr) was measured by the Barocel electronic manometer. The Hoke valve C was then opened and the measured amount of

ethylene was condensed into the cold finger of the photolytic cell. The remaining procedures were similar to those described above, except that after pumping out the hydrogen, ethylene was distilled from the reaction mixture at -160°C prior to analysis of the remaining fraction.

In the experiments with diethylsulfide, the fraction volatile at -160°C , consisting of C_2H_4 and C_2H_6 , was analyzed on an 8 ft porapak N column, while the fraction volatile at -130°C was analyzed on a 10 ft tricresylphosphate column. In order to ascertain whether methane was formed in the reaction the hydrogen fraction was condensed on a 3 \AA molecular sieve column. The column was then heated to 100°C and the fraction volatile at this temperature was analyzed on a 10 ft 3 \AA molecular sieve column.

It was found that 24 hours were required for quantitative transfer of the products from the reaction cell to the gc injection port.

CHAPTER III

THE REACTIONS OF HYDROGEN ATOMS WITH DIMETHYLDISULFIDE

Results

The mercury photosensitization of H_2 in the presence of CH_3SSCH_3 led to the formation of only one retrievable product, CH_3SH . Polymer formation on the cell window was quite extensive, hence actinometric measurements were performed before and after each experiment and the average value was taken as the absorbed light intensity. The extent of quenching of the excited mercury atoms by CH_3SSCH_3 or C_2H_4 at the highest concentrations used was estimated to be less than 5%; see appendix A for the calculation. Control experiments made at each temperature indicated that CH_3SSCH_3 was thermally stable in the temperature range 25-155°C.

1. Effects of time, CH_3SSCH_3 concentration and temperature on $\phi(CH_3SH)$.

In the first set of experiments, the quantum yield of CH_3SH was determined at 60°C as a function of exposure time at a constant CH_3SSCH_3 pressure of 10.06 Torr. The results, listed in Table VII, show that the quantum yield of CH_3SH was approximately 2.1 and invariant with exposure time up to 60 minutes, hence CH_3SH must be formed in a primary process.

TABLE VII

Effect of Exposure time on $\phi(\text{CH}_3\text{SH})^a$

Time, min.	CH ₃ SH		$\phi(\text{CH}_3\text{SH})$	$I_a(\text{ave.})$ ($\mu\text{einstein min}^{-1}) \times 10^2$
	Yield(μmoles)	Rate($\mu\text{moles min}^{-1}) \times 10^2$		
15	0.470±0.002	3.13±0.01	2.13±0.01(3) ^b	1.47
30	0.950±0.006	3.17±0.02	2.09±0.01(2)	1.52
45	1.526±0.009	3.39±0.02	2.12±0.01(3)	1.60
60	1.680±0.006	2.80±0.01	2.12±0.01(2)	1.32
Ave 2.11±0.02 ^c				

^aT = 58-60°C; P(H₂) = 580±10 Torr; P(CH₃SSCH₃) = 10.06±0.02 Torr

^bnumber of experiments

^cstandard error

Next, $\phi(\text{CH}_3\text{SH})$ was determined as a function of CH_3SSCH_3 pressure. The results (Table VIII) show that $\phi(\text{CH}_3\text{SH})$ is also independent of CH_3SSCH_3 pressure in the range 2-20 Torr, indicating that scavenging of H atoms by CH_3SSCH_3 is complete.

The results in Tables VII and VIII show that $\phi(\text{CH}_3\text{SH})$ was also invariant with lamp intensity in the range 0.011 - 0.016 $\mu\text{einstein min}^{-1}$. This result constitutes additional evidence to the effect that most, if not all, of the CH_3SH is formed in a primary process.

The effect of temperature on $\phi(\text{CH}_3\text{SH})$ for a mixture of 580 Torr hydrogen and 5 Torr CH_3SSCH_3 was examined over the range 25-120°C. The results, listed in Table IX, show that increasing the temperature has no effect on the quantum yield of CH_3SH , and it can therefore be concluded that side reactions such as thermolysis and/or secondary decomposition of CH_3SH do not take place within the temperature range examined.

2. Experiments in the presence of ethylene.

In the presence of C_2H_4 several additional reaction products were formed, three of which were identified as $n\text{-C}_4\text{H}_{10}$, C_2H_6 , and $\text{CH}_3\text{SC}_2\text{H}_5$; polymer formation was greatly reduced. Ethane, which was identified as a product, could not be separated from the large amounts of ethylene and was, therefore, not determined

TABLE VIII

Effect of P(CH₃SSCH₃) on ϕ(CH₃SH)^a

P(CH ₃ SSCH ₃), Torr	I _a (ave.), (μeinstein min ⁻¹)x10 ²	CH ₃ SH yield(μmoles) Rate(μmole min ⁻¹)x10 ²	ϕ(CH ₃ SH)
2.00	1.52	1.427±0.009	3.17±0.02
10.06	1.60	1.526±0.009	3.39±0.02
20.00	1.23	1.142±0.004	2.54±0.01
			2.09±0.01(2) ^b
			2.12±0.01(3)
			2.07±0.01(2)

^aT = 58-60°C; P(H₂) = 580±10 Torr; exposure time = 45 min.

^bnumber of experiments

TABLE IX

Effect of Temperature on $\phi(\text{CH}_3\text{SH})^a$

Temperature, °C	I_a (ave.) ($\mu\text{einstein min}^{-1}$) $\times 10^2$	CH_3SH		$\phi(\text{CH}_3\text{SH})$
		Yield(μmoles)	Rate($\mu\text{mole min}^{-1}$) $\times 10^2$	
25	1.14	1.191 \pm 0.005	2.38 \pm 0.01	2.09 \pm 0.01(2) ^b
60	1.60	1.526 \pm 0.009	3.39 \pm 0.02	2.12 \pm 0.01(2)
85	1.63	1.542 \pm 0.009	3.43 \pm 0.02	2.10 \pm 0.01(2)
120	1.38	1.274 \pm 0.005	2.83 \pm 0.01	2.05 \pm 0.01(2)

^a $P(\text{H}_2)$ = 580 \pm 10 Torr; Photolysis time = 45 min.; $P(\text{CH}_3\text{SSCH}_3)$ = 5.00 \pm 0.02 Torr

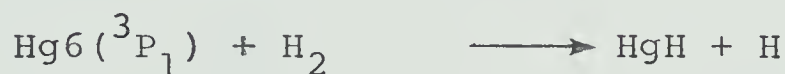
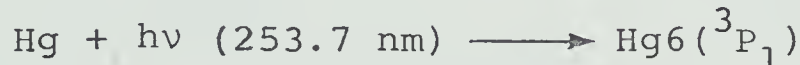
^bnumber of experiments

quantitatively. Product quantum yields for a mixture of 580 Torr H_2 and 5 Torr CH_3SSCH_3 in the presence of increasing amounts of ethylene at five different temperatures are given in Table X where it is seen that $\phi(\text{CH}_3\text{SH})$ decreases with increasing pressure of ethylene, owing to the competitive scavenging of H atoms by C_2H_4 ,



Discussion

At the relative $\text{H}_2/\text{CH}_3\text{SSCH}_3$ and $\text{H}_2/\text{CH}_3\text{SSCH}_3/\text{C}_2\text{H}_4$ concentrations used in this work it is estimated that >95% of the excited mercury atoms are quenched by H_2 :



Although $\phi(\text{HgH}) = 0.67^{83-85}$ the lifetime of HgH is so short that the overall kinetics are indistinguishable from those of H atoms, for which $\phi(\text{H}) = 2.0^{86}$

Since methanethiol is the only product of the reaction, and its invariance with exposure time indicates that it is a primary product, the following simple mechanism would seem to apply:

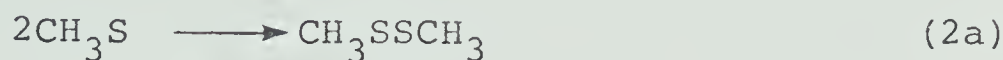
TABLE X

Effect of C₂H₄ Pressure and Temperature on $\phi(\text{CH}_3\text{SH})^a$

P(C ₂ H ₄), torr	[C ₂ H ₄]/ [CH ₃ SSCH ₃]	$\phi(\text{CH}_3\text{SH})$	1/ $\phi(\text{CH}_3\text{SH})$
<u>25°C</u>			
5.00	1.00	1.86	0.538
7.50	1.50	1.75	0.571
10.0	2.00	1.65	0.606
15.0	3.00	1.50	0.667
<u>60°C</u>			
5.00	1.00	1.76	0.568
10.00	2.00	1.53	0.654
12.50	2.50	1.42	0.704
15.00	3.00	1.34	0.746
<u>85°C</u>			
5.00	1.00	1.72	0.581
7.50	1.50	1.55	0.645
10.0	2.00	1.43	0.699
12.5	2.50	1.33	0.752
15.0	3.00	1.24	0.806
<u>120°C</u>			
5.00	1.00	1.63	0.614
10.0	2.00	1.33	0.752
12.5	2.50	1.21	0.826
15.0	3.00	1.12	0.893
<u>155°C</u>			
5.00	1.00	1.53	0.654
10.0	2.00	1.21	0.826
12.5	2.50	1.09	0.917
15.0	3.00	0.980	1.02

^aPhotolysis time = 45 min; $I_a = 1.27 \times 10^{-8}$ einstein min⁻¹

P(H₂) = 580±10 Torr; P(CH₃SSCH₃) = 5.00 Torr.

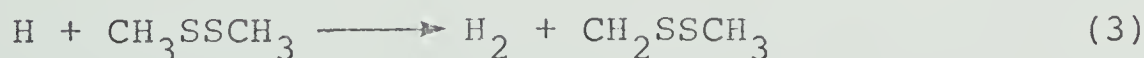


From this mechanism $\phi(\text{CH}_3\text{SH}) = \phi(1) + \phi(2b) = 2.1$ and $\phi(1)/2 = \phi(2a) + \phi(2b)$. The value of $\phi(2b)/\phi(2a)$ reported by Rao and Knight^{57a} is ~ 0.05 (Lossing and coworkers' value of 0.4^{87} is probably erroneous), from which $\phi(1)/2 = \phi(2b)/0.05 + \phi(2b) = 21\phi(2b)$. Therefore,

$$\phi(1) = 42\phi(2b), \quad \phi(2b) = 2.1/43 \sim 0.05$$

and $\phi(1) = 2.05$ or, within experimental error, 2.0. This means that scavenging of H atoms by dimethyldisulfide is complete and the only reaction consuming H atoms is reaction (1). Since $\phi(\text{CH}_3\text{SH})$ is approximately equal to 2.1 between 25 and 120°, it is concluded that k_{2b}/k_{2a} is temperature independent in this temperature range, i.e., E_{2b} is zero or negligibly small.

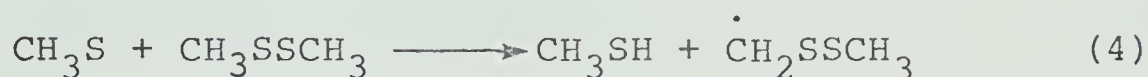
The absence of the radical combination products such as $\text{CH}_3\text{SCH}_2\text{SSCH}_3$ and $(\text{CH}_2\text{SSCH}_3)_2$ which are expected to be stable under the conditions employed, is evidence that the abstractive route to H_2 formation does not occur:



It was not possible to ascertain whether H_2 is one of the

reaction products, however, on the basis of the exothermicities of reaction (1) ($\sim -21.4 \text{ kcal mol}^{-1}$) and reaction (3) ($\sim -8 \text{ kcal mol}^{-1}$) it is very likely that the latter will be relatively slow compared to the former. Reaction (3) may, however become important at higher temperatures.

On the same basis, the occurrence of H abstraction by CH_3S ,

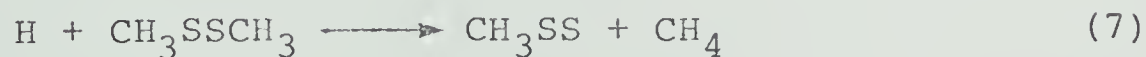


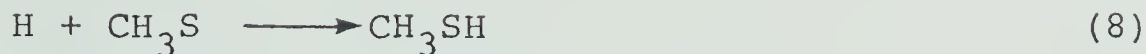
for which $\Delta H \sim 7 \text{ kcal mol}^{-1}$, does not appear to be important. Moreover, this reaction is expected to feature a substantial activation energy whereas $\phi(\text{CH}_3\text{SH})$ was observed to be independent of temperature up to 120°C .

The following metathetical primary processes can also be discounted since CH_4 , CH_3SCH_3 and H_2S were demonstrably absent:



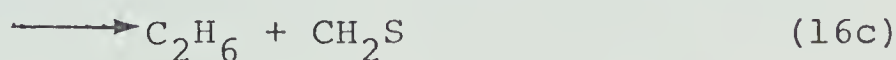
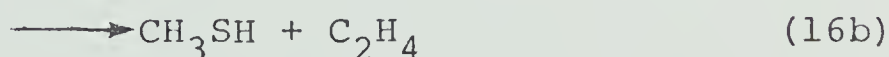
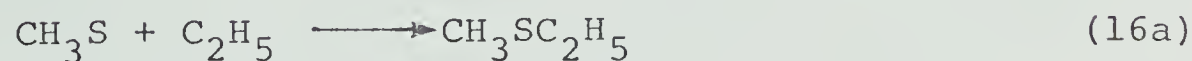
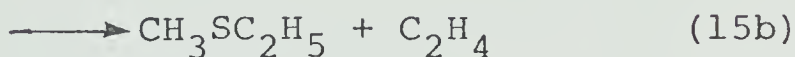
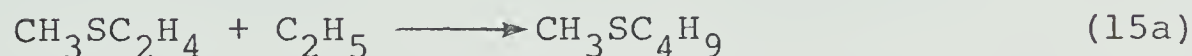
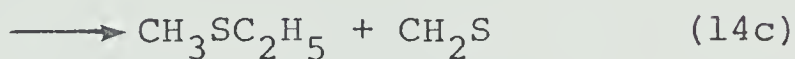
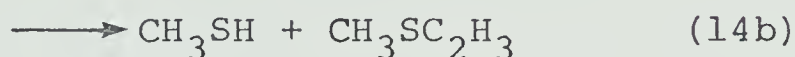
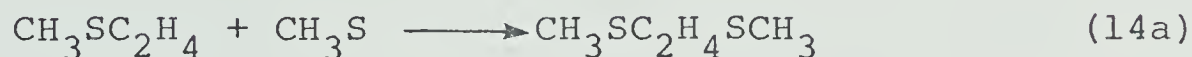
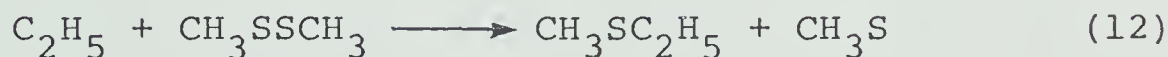
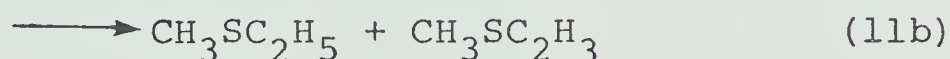
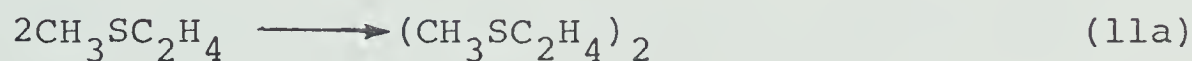
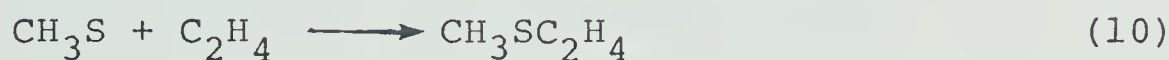
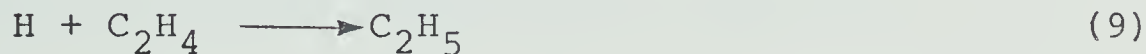
The detection of CH_3SSH as a product, if formed, is not possible because CH_3SSH is known^{40,88} to be very unstable and decomposes to CH_3SH and sulfur. Finally, the overall stoichiometric balance indicates that the following reactions,

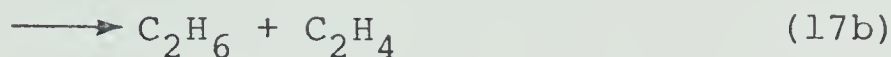
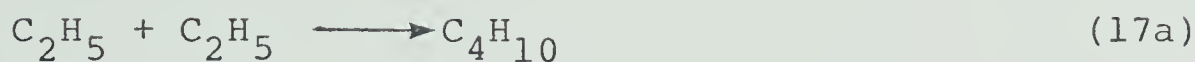




are of very minor importance.

In the presence of ethylene a complete hypothetical reaction sequence would consist of steps (1), (2) and (9)-(18)





The metathetical radical displacement reaction,



probably requires a considerable activation energy hence it was assumed to be unimportant in this system. Also, reactions (10), (11), (12), (13), (14) and (15) can be discounted since $\text{CH}_3\text{SCH}_2\text{H}_3$, $\text{CH}_3\text{SC}_2\text{H}_4\text{SCH}_3$, $\text{CH}_3\text{SC}_4\text{H}_9$, and $(\text{CH}_3\text{SC}_2\text{H}_4)_2$ were demonstrably absent. Finally, step (18) does not seem to be important since polymer formation was greatly suppressed in the presence of C_2H_4 . Steady state treatment of steps (1), (2), (9), (16) and (17) leads to the following rate expression:

$$\phi(\text{CH}_3\text{SH})^{-1} = \frac{1}{2(1+\alpha)} + \frac{1}{2(1+\alpha)} \frac{k_9[\text{C}_2\text{H}_4]}{k_1[\text{CH}_3\text{SSCH}_3]} \quad \text{I}$$

where $\alpha \approx \Sigma k_{\text{disproportionation}} / \Sigma k_{\text{combination}}$ of the CH_3S radical resulting in the formation of CH_3SH and in the disappearance of CH_3S by other reactions, respectively. Plots of equation I, illustrated in Figure 3, are indeed linear at the five temperatures studied and feature a common intercept. The least mean square slopes and intercepts are summarized in Table XI. The average value

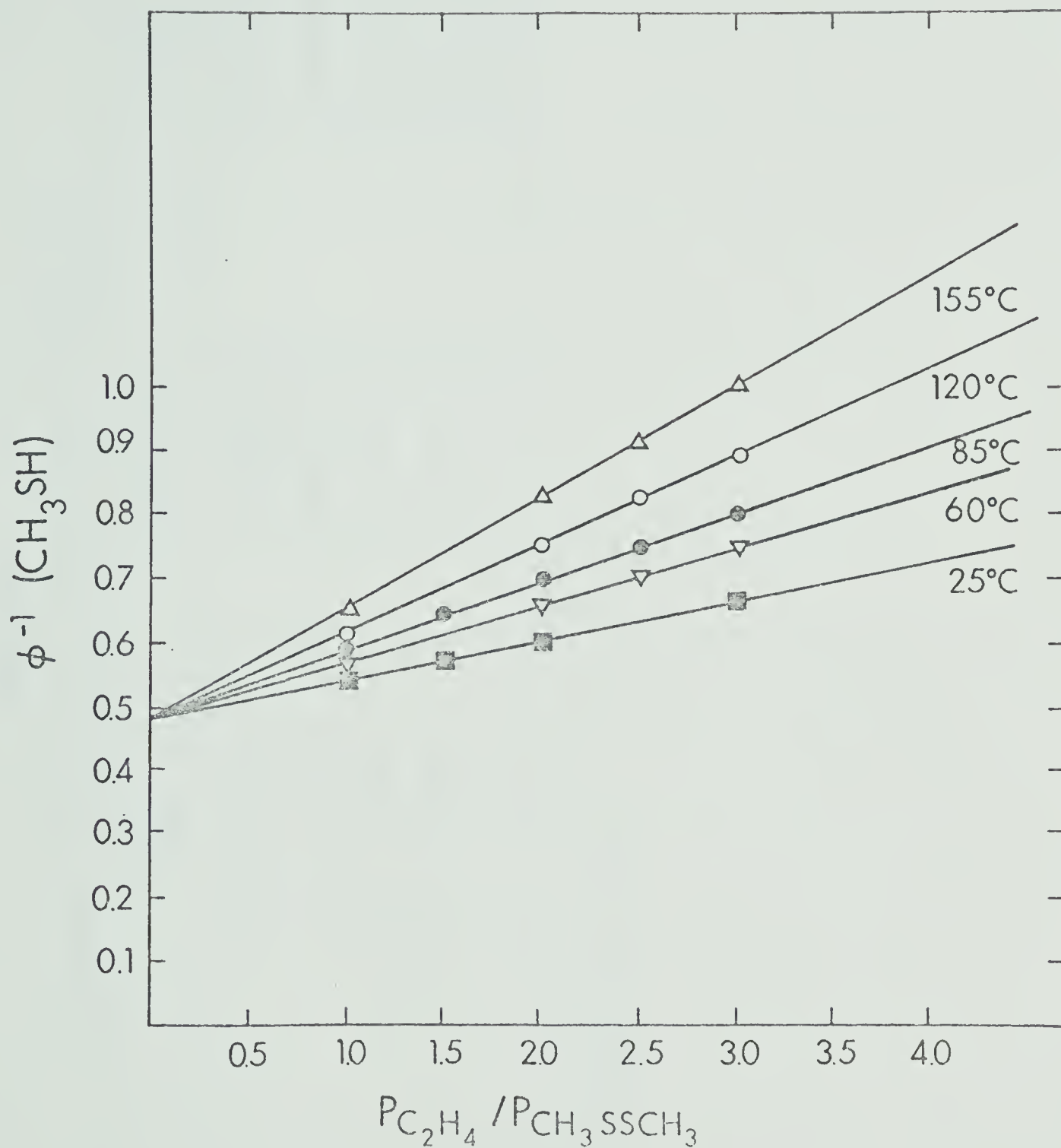


FIGURE 3. $\phi(\text{CH}_3\text{SH})^{-1}$ versus $P[\text{C}_2\text{H}_4]/P[\text{CH}_3\text{SSCH}_3]$ at 25, 60, 85, 120 and 155°C. $P(\text{H}_2) = 580 \pm 10$ Torr; $P(\text{C}_2\text{H}_4) + P(\text{CH}_3\text{SSCH}_3) = 10\text{-}20$ Torr; photolysis time, 45 minutes.

TABLE XI

Slopes and Intercepts of the Plots in Figure 3^a

T, °C	Slope	Intercept	k ₉ /k ₁
25	0.0645±0.0015	0.475±0.003	0.136±0.003
60	0.0897±0.0020	0.478±0.005	0.189±0.004
85	0.111 ±0.002	0.474±0.004	0.234±0.004
120	0.140 ±0.002	0.473±0.004	0.295±0.004
155	0.182 ±0.005	0.468±0.012	0.384±0.001

^aThe errors are standard deviations

of α is 0.059, in good agreement with the value of 0.05 reported in the literature.^{57a} The values of k_9/k_1 , also listed in Table XI, are plotted in the Arrhenius form in Figure 4, from which

$$\log(k_9/k_1) = (0.592 \pm 0.039) - (2000 \pm 64)/2.3RT$$

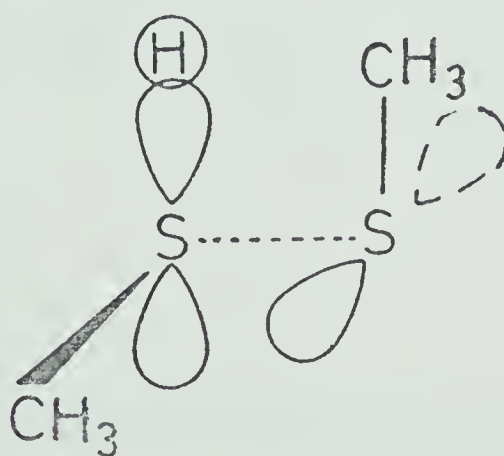
Taking the limiting high pressure rate parameters for step (9) as⁸⁹

$$k_9 = (2.2 \pm 0.4) \times 10^{13} \exp[-(2066 \pm 83)/RT] \text{ cm}^3 \text{ mol}^{-1} \text{ s}^{-1},$$

those for step (1) are

$$k_1 = (5.7 \pm 1.2) \times 10^{12} \exp[-(100 \pm 100)/RT] \text{ cm}^3 \text{ mol}^{-1} \text{ s}^{-1}.$$

The experimental entropy of activation, $\Delta S_{\text{exp}}^\ddagger = -26.2$ e.u. for the standard state of 1 atm., suggests a very rigid transition state for the $\text{H} + \text{CH}_3\text{SSCH}_3$ reaction. If one assumes an activated complex of the type



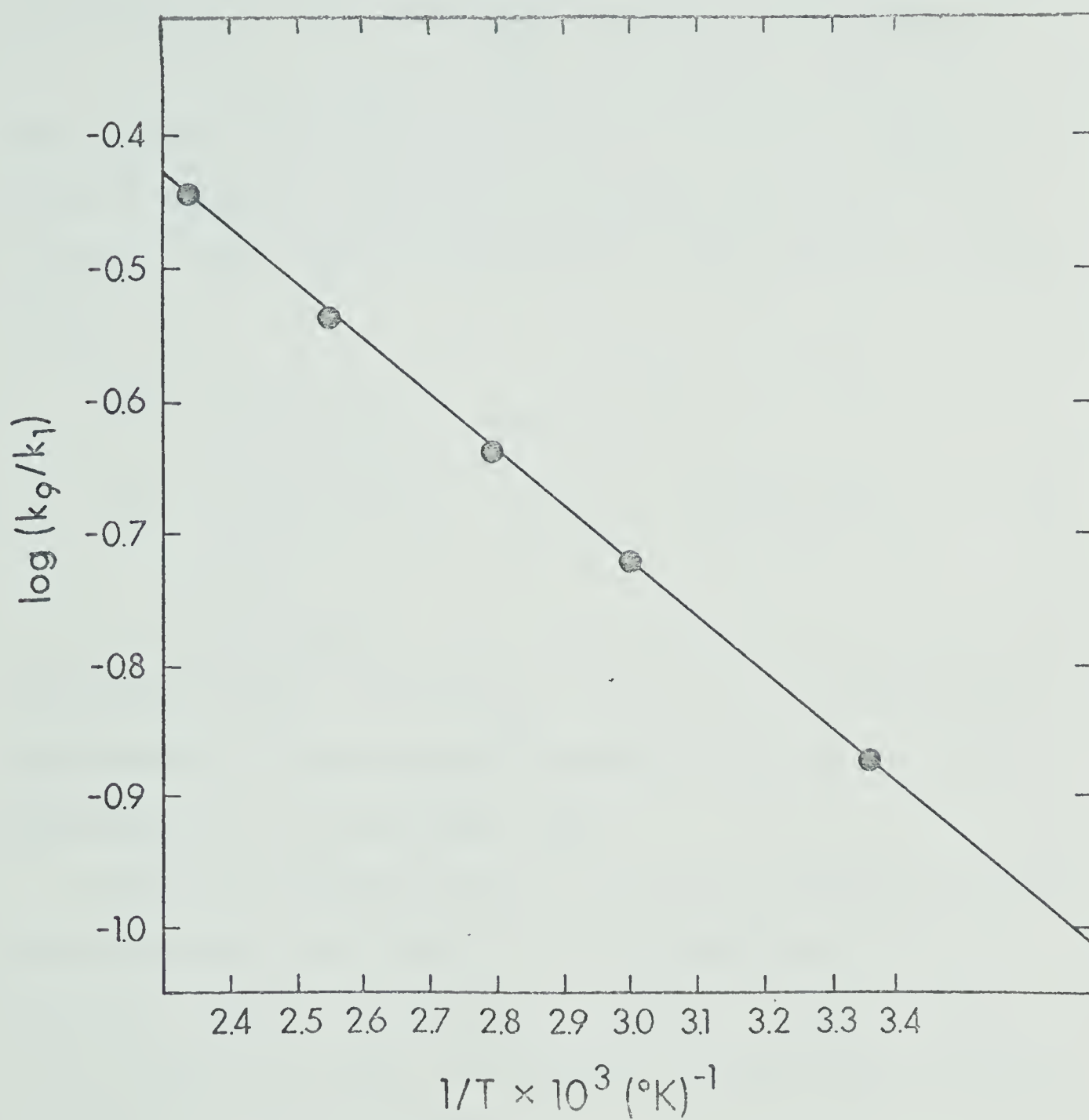


FIGURE 4. Arrhenius plot of k_9/k_1 versus $1/T$.

ΔS^\ddagger can be calculated by Benson's method⁷⁷ since the gas phase structural parameters of CH_3SSCH_3 have been reported.^{12,16} The standard entropy of the activated complex, $(\text{H}\cdot\text{CH}_3\text{SSCH}_3)^\ddagger$, will then only require a correction of $R \ln 2 = 1.4$ e.u. from the spin contribution since the contribution from the other factors, such as moments of inertia change, vibrational entropy consisting of contribution from each of the internal vibrations are small. Thus,

$$S^\ddagger = S^\circ(\text{CH}_3\text{SSCH}_3) + 1.4 \text{ e.u.}$$

$$\begin{aligned} \Delta S^\ddagger &= S^\circ(\text{CH}_3\text{SSCH}_3) + 1.4 \text{ e.u.} - S^\circ(\text{CH}_3\text{SSCH}_3) - S^\circ(\text{H}) \\ &= -26.0 \text{ e.u.} \end{aligned}$$

The good agreement with $\Delta S_{\text{exp}}^\ddagger = -26.2$ e.u. suggests that the geometry of the assumed transition state is a good approximation to the actual case.

From the present results, it is not possible to draw any conclusion with regard to the intermediacy of the transient complex $(\text{H}\cdot\text{CH}_3\text{SSCH}_3)$; however, to date, there is no indication that such complexes could have a finite lifetime in the gas phase.

CHAPTER IV

THE REACTIONS OF HYDROGEN ATOMS WITH DIETHYLDISULFIDE

Results

The mercury photosensitized decomposition of H_2 in the presence of $C_2H_5SSC_2H_5$ yields C_2H_5SH as the sole retrievable reaction product. Substantial amounts of polymer were formed at long exposure times. The extent of quenching of the excited mercury atoms by $C_2H_5SSC_2H_5$ was estimated to be less than 5%. Control experiments made at each temperature showed that $C_2H_5SSC_2H_5$ was thermally stable in the range 25-145°C.

1. Effects of time, $C_2H_5SSC_2H_5$ concentration and temperature on $\phi(C_2H_5SH)$.

The quantum yield of ethanethiol formed from the mercury sensitization of 580 Torr H_2 in the presence of 5.0 Torr $C_2H_5SSC_2H_5$ was determined at 60°C as a function of exposure time. The results are listed in Table XII. The quantum yield of ethanethiol at 60°C was 2.47 and independent of exposure time up to 70 minutes at constant $C_2H_5SSC_2H_5$ pressure, hence C_2H_5SH must be formed in the primary process.

In the next series of experiments $\phi(C_2H_5SH)$ was determined as a function of diethyldisulfide pressure.

TABLE XII

Effect of Exposure Time on $\phi(\text{C}_2\text{H}_5\text{SH})^a$

Time min.	$\text{C}_2\text{H}_5\text{SH}$		$\phi(\text{C}_2\text{H}_5\text{SH})$
	Yield(μmoles)	Rate($\mu\text{moles min}^{-1}$) $\times 10^2$	
15	0.4465	2.98	2.40 (1) ^b
30	0.9040 \pm 0.003	3.01 \pm 0.01	2.43 \pm 0.01(2)
45	1.379 \pm 0.009	3.06 \pm 0.02	2.47 \pm 0.02(2)
60	1.850 \pm 0.006	3.08 \pm 0.01	2.48 \pm 0.01(2)
65	1.983 \pm 0.007	3.05 \pm 0.01	2.46 \pm 0.02(2)
75	2.115 \pm 0.007	3.02 \pm 0.01	2.44 \pm 0.01(2)
			Ave 2.46 \pm 0.02 ^c

^aT = 60-62°C; P(H₂) = 580 \pm 10 Torr; P(C₂H₅SSC₂H₅) = 5.00 \pm 0.02 Torr;

I_a(ave.) (ueinstein min⁻¹) $\times 10^2$ = 1.24

^bnumber of experiments

The results, listed in Table XIII, show that $\phi(\text{C}_2\text{H}_5\text{SH})$ is also independent of $\text{C}_2\text{H}_5\text{SSC}_2\text{H}_5$ pressure in the range 2-15 Torr, suggesting that scavenging of H atoms by $\text{C}_2\text{H}_5\text{SSC}_2\text{H}_5$ is complete.

5.00 Torr diethyldisulfide were allowed to react with H atoms for 45 minutes at temperatures ranging from 25°C to 145°C. The results, shown in Table XIV, show that $\phi(\text{C}_2\text{H}_5\text{SH})$ is somewhat dependent on temperature, ranging from 2.32 at 25° to 2.84 at 145°C.

2. Effects of added ethylene.

In the presence of ethylene several additional reaction products were formed, three of which were identified as C_2H_6 , $n\text{-C}_4\text{H}_{10}$ and $\text{C}_2\text{H}_5\text{SC}_2\text{H}_5$. One possible reaction product, ethylvinylsulfide, was demonstrably absent. Polymer formation was greatly suppressed. Product quantum yields from the mercury photosensitization of a mixture of 580 Torr H_2 and 5.0 Torr $\text{C}_2\text{H}_5\text{SSC}_2\text{H}_5$ in the presence of increasing amounts of ethylene at five different temperatures are given in Table XV where it is seen that $\phi(\text{C}_2\text{H}_5\text{SH})$ decreases with increasing pressure of C_2H_4 , owing to the competitive scavenging of H atoms by C_2H_4 ,



TABLE XIII

Effect of P(C₂H₅SSC₂H₅) on ϕ(C₂H₅SH)^a

P(C ₂ H ₅ SSC ₂ H ₅), Torr	C ₂ H ₅ SH		ϕ(C ₂ H ₅ SH)
	Yield(μmoles)	Rate(μmoles min ⁻¹)x10 ²	
2.00	1.379±0.009	3.06±0.02	2.47±0.01(2) ^b
5.00	1.379±0.009	3.06±0.02	2.47±0.01(2)
15.00	1.373±0.005	3.05±0.01	2.46±0.01(2)

^aT = 60-62°C; P(H₂) = 580±10 Torr; Exposure time = 45 min.

I_a(ave.) (μeinstein min⁻¹)x10² = 1.24

^bnumber of experiments

TABLE XIV

Effect of Temperature on $\phi(\text{C}_2\text{H}_5\text{SH})^a$

Temperature °C	C ₂ H ₅ SH		$\phi(\text{C}_2\text{H}_5\text{SH})$
	Yield(μmoles)	Rate(μmoles min ⁻¹)x10 ²	
25	1.293±0.005	2.87±0.01	2.32±0.01(2) ^b
60	1.379	3.06	2.47
80	1.440	3.20	2.58
120	1.507	3.35	2.70
145	1.586±0.009	3.52±0.02	2.84±0.02(2)

^aP(H₂) = 580±10 Torr; Photolysis time = 45 min.; P(C₂H₅SSC₂H₅) = 5.00±0.02 Torr;

I_a(ave.) (μeinstein min⁻¹)x10² = 1.24

^bnumber of experiments

TABLE XV

Effect of C₂H₄ Pressure and Temperature on ϕ (C₂H₅SH)^a

P(C ₂ H ₄) Torr	[C ₂ H ₄]/ [C ₂ H ₅ SSC ₂ H ₅]	ϕ_{Total} (C ₂ H ₅ SH)
<u>25°C</u>		
0.00	0.00	2.32
5.00	1.00	1.84
10.00	2.00	1.49
15.00	3.00	1.31
<u>60°C</u>		
0.00	0.00	2.47
5.00	1.00	1.94
10.00	2.00	1.59
15.00	3.00	1.34
<u>80°C</u>		
0.00	0.00	2.58
5.00	1.00	1.99
10.00	2.00	1.61
15.00	3.00	1.37
<u>120°C</u>		
0.00	0.00	2.70
5.00	1.00	2.09
10.00	2.00	1.69
15.00	3.00	1.43
<u>145°C</u>		
0.00	0.00	2.84
5.00	1.00	2.17
10.00	2.00	1.79
15.00	3.00	1.49

^aPhotolysis time = 45 min; I_a = 1.24 x 10⁻⁸ einstein min⁻¹

P(H₂) = 580 ± 10 Torr; P(C₂H₅SSC₂H₅) = 5.00 Torr

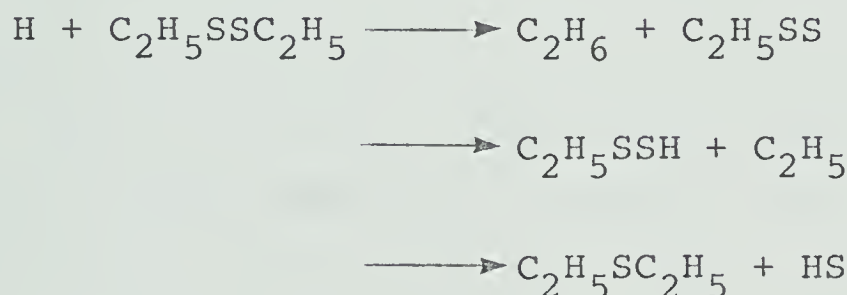
Discussion

Under the experimental conditions employed it is estimated that >95% of the $\text{Hg}(^3\text{P}_1)$ atoms are quenched by H_2 and the overall process⁸⁶ is



for which $\phi(\text{H}) = 2.0$.

The absence of products such as C_2H_4 , C_2H_6 , C_4H_{10} , $\text{C}_2\text{H}_5\text{SC}_2\text{H}_5$ and H_2S can be taken as evidence that the following hypothetical primary processes do not occur:



The possibility of hydrogen abstraction taking place in parallel and in competition with $\text{C}_2\text{H}_5\text{S}$ displacement,

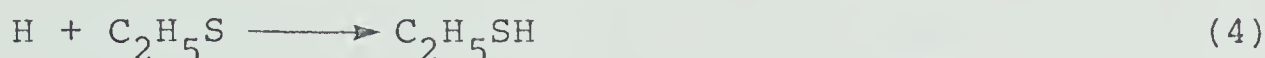
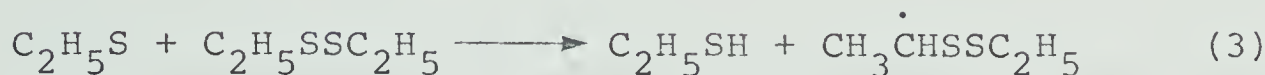
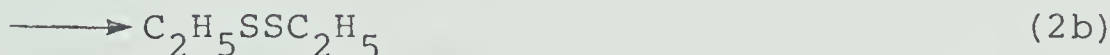
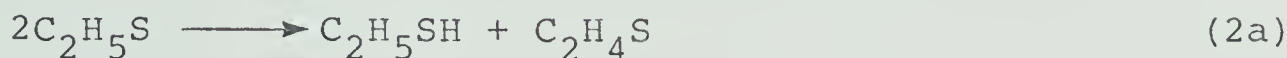


cannot be discounted at this time, but kinetic considerations (*vide infra*) suggest that this reaction is unimportant within the temperature range examined.

Hence, and also by analogy with $\text{H} + \text{CH}_3\text{SSCH}_3$ reaction, the sole primary process of significance is postulated to be:



The following secondary reactions may then take place:



However, at the low light intensities used in the present investigation, step (4) is unlikely to be important.

$\phi(\text{C}_2\text{H}_5\text{SH})$ varies between 2.32 at 25° and 2.84 at 145°C.

This may be due to the temperature dependence of step (2a), or that of the abstractive route to thiol formation, reaction (3). Now it has been shown (Chapter III) that k_d/k_c for CH_3S radicals is temperature independent: it is therefore reasonable to assume that the same is true for $\text{C}_2\text{H}_5\text{S}$ and that the temperature dependence of $\phi(\text{C}_2\text{H}_5\text{SH})$ is due to that of step (3). Note that the expected radical combination products arising from the $\text{CH}_3\dot{\text{C}}\text{HSSC}_2\text{H}_5$ radical formed in step (3) were not detected. Either this radical is not stable and polymerizes, or the products were lost during transfer. In any case, it will be shown that inclusion of step (3) in the overall mechanism leads to reasonable kinetic-mechanistic conclusions.

Thus, assuming that C_2H_5SH is formed exclusively *via* steps (1), (2a) and (3), then at $25^\circ C$ where $\phi(C_2H_5SH) = 2.32$, the following steady state equations apply:

$$\phi(C_2H_5S) = 2\phi(2a) + 2\phi(2b) + \phi(3) = 2 \quad I$$

$$\phi(1) + \phi(2a) + \phi(3) = 2.32 \quad II$$

Given that scavenging of H atoms by $C_2H_5SSC_2H_5$ is complete, $\phi(1) = 2$ and $\phi(2a) + \phi(3) = 0.32$. From Knight and Smith's value of $k_{2a}/k_{2b} = 0.13$,⁶⁸ equation I becomes

$$\phi(C_2H_5S) = 0.13\phi(2b) + 2\phi(2b) + 0.32 = 2 \quad III$$

$\phi(2a)$, $\phi(2b)$ and $\phi(3)$ were calculated from equation III and are listed in Table XVI at the five temperatures examined.

Further steady state treatment of steps (2a), (2b) and (3) leads to the following rate equation:

$$\frac{k_3}{(k_{2a} + k_{2b})^{1/2}} = \frac{\phi(3)}{\left(\frac{2 - \phi(3)}{2}\right)^{1/2} [C_2H_5SSC_2H_5]} \quad IV$$

The Arrhenius plot of $\phi(3)/\left(\{(2 - \phi(3))/2\}^{1/2} [C_2H_5SSC_2H_5]\right)$ (these values are also listed in Table XVI), Figure 5, is linear over the temperature range examined, in agreement with the above mechanism, and the slope yields

$(E_{2a} + E_{2b})/2 - E_3 = -3.61 \pm 0.09 \text{ kcal mol}^{-1}$. If $E_{2a} \sim 0$, as was shown to be the case for CH_3S radicals, and since E_{2b} is zero or negligibly small, then this value corresponds

TABLE XVI

Effect of Temperature on $\phi(2a)$, $\phi(2b)$, and $\phi(3)$

Temperature, °C	$\phi(C_2H_5SH)$	$\phi(2a)$	$\phi(2b)$	$\phi(3)$	$\frac{\phi(3)}{(\frac{2-\phi(3)}{2})^{1/2}} [C_2H_5SSC_2H_5]^a$
25	2.32	0.103	0.79	0.22	8.55×10^2
60	2.47	0.094	0.72	0.38	1.73×10^3
80	2.58	0.087	0.67	0.49	2.50×10^3
120	2.70	0.079	0.61	0.62	3.67×10^3
145	2.84	0.070	0.54	0.77	5.12×10^3

^a $[C_2H_5SSC_2H_5] = 5.0/(62.361T)$

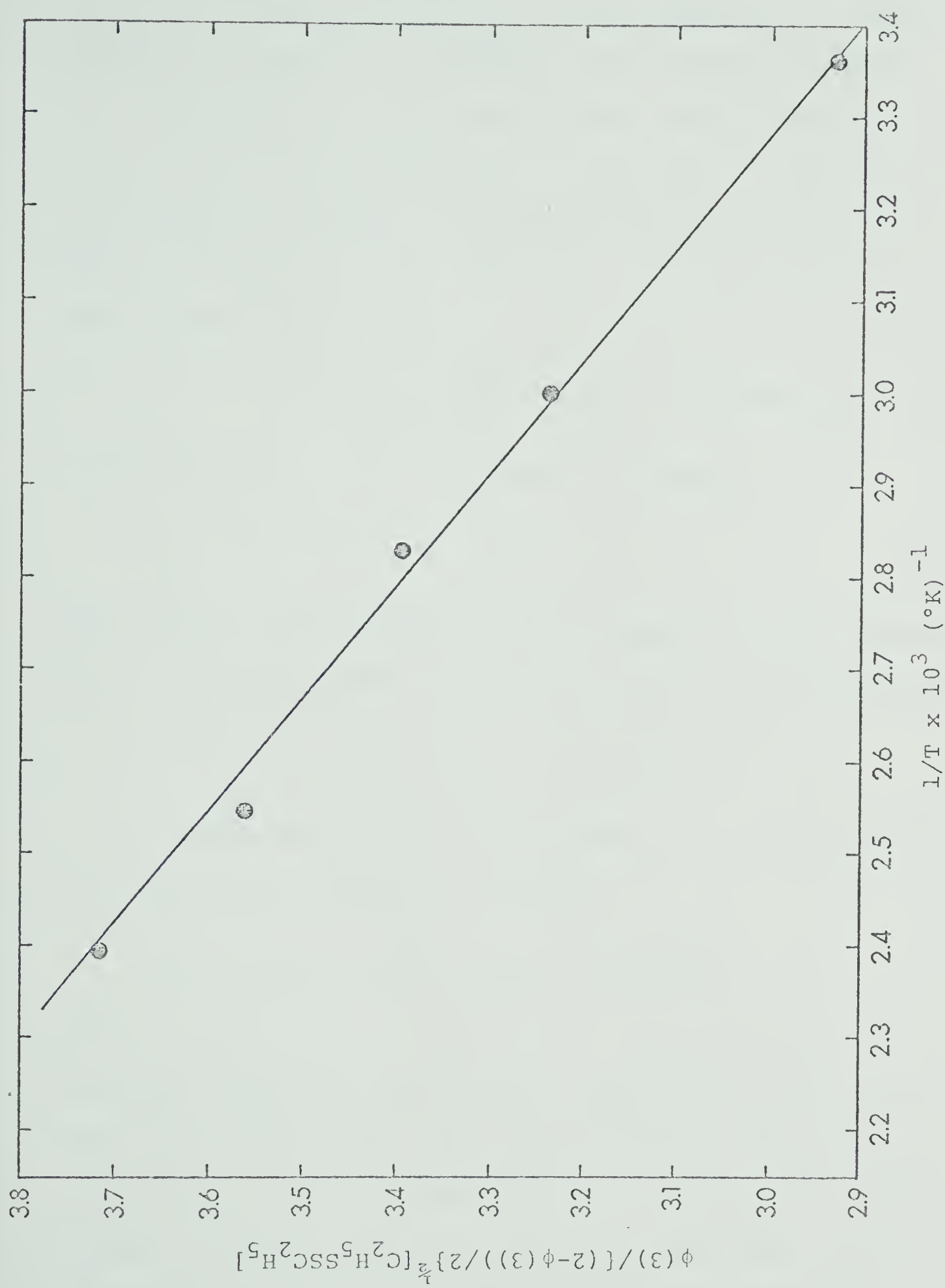
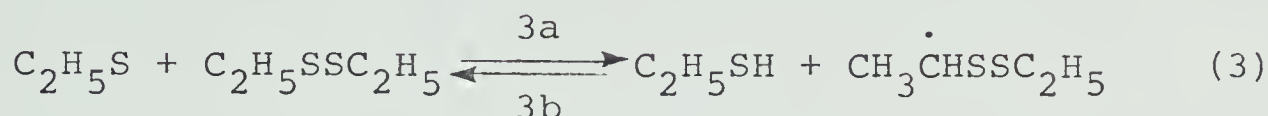


FIGURE 5. Arrhenius plot of $\phi(3)/\{(2-\phi(3))/2\}^{1/2} [C_2H_5SSC_2H_5]$

to $E_3 = 3.61 \pm 0.09 \text{ kcal mol}^{-1}$. The methylenic C-H bond dissociation energy in $\text{C}_2\text{H}_5\text{SSC}_2\text{H}_5$ has not been reported but a reasonable estimate can be made. Thus, because of the adjacent sulfur atom which is expected to stabilize the resulting radical, it is assumed that $D(\text{methylenic-C-H})$ is close to the *tert* C-H value, 90-91 kcal mol^{-1} . Then ΔH for reaction (3a)



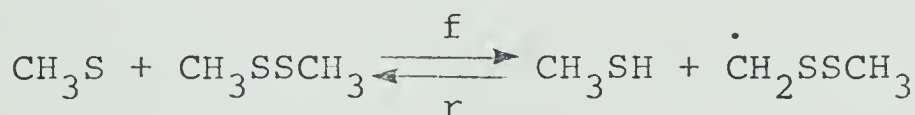
is approximately $1.5\text{-}2.5 \text{ kcal mol}^{-1}$ and hence

$$E_{3b} = 1.6 \pm 0.5 \text{ kcal mol}^{-1}$$

This estimate is the right order of magnitude when compared to the values reported for some radical + thiol reactions,^{57b}



In comparison, $D(\text{C-H})$ for CH_3SSCH_3 is $\sim 95 \text{ kcal mol}^{-1}$, and ΔH for the abstraction reaction



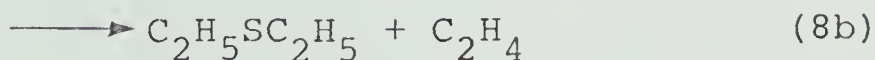
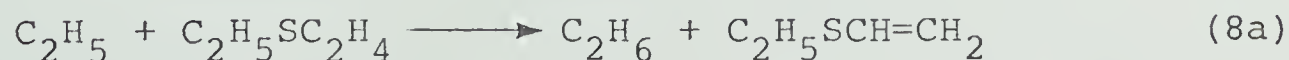
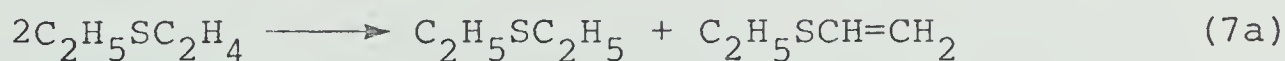
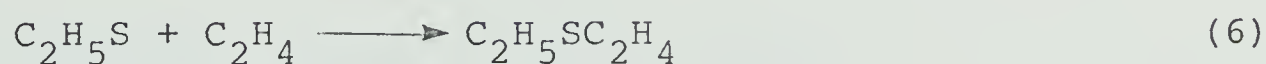
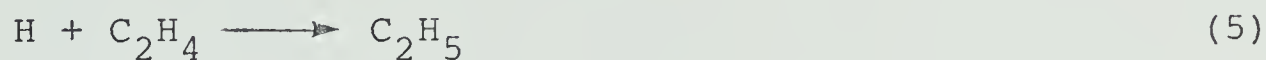
will be approximately 7 kcal mol^{-1} . Assuming that the activation energy for the reverse reaction is similar to that for reaction (3b), then the activation energy for the above reaction is approximately $8.6 \text{ kcal mol}^{-1}$. This estimate is quite reasonable since hydrogen abstraction from primary C-H bonds by radicals generally features a

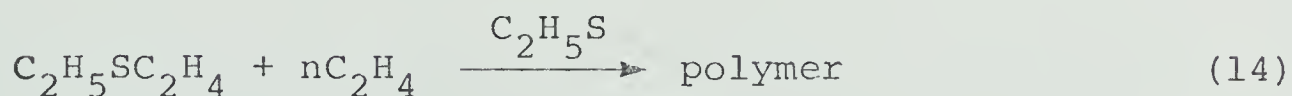
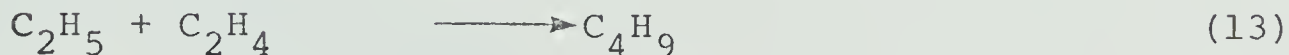
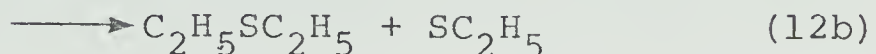
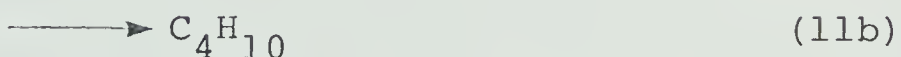
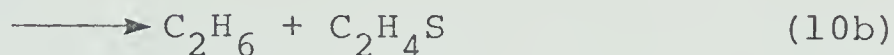
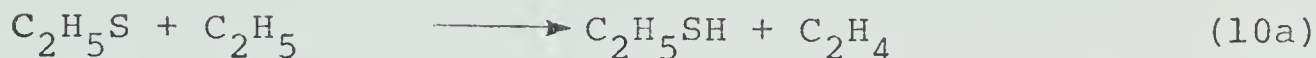
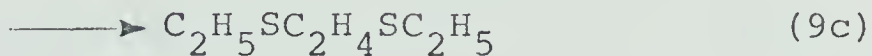
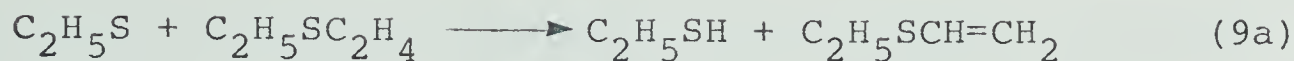
relatively high activation energy, in the range 9-12 kcal mol⁻¹.⁹⁰

Recalling that k_d/k_c for $\text{CH}_3\text{S} = 0.05$, the substantially higher value for $\text{C}_2\text{H}_5\text{S}$, 0.13, suggests that the activation energy for the disproportionation of $\text{C}_2\text{H}_5\text{S}$ is lower than that for CH_3S radicals. This may be due to an enhanced stability of the $\text{C}=\text{S}$ bond upon ethyl substitution or, more likely, to the lower bond dissociation energy of the

$\text{CH}_3\overset{\text{S}}{\underset{|}{\text{CH}}}-\text{H}$ than the $\text{H}_2\overset{\text{S}}{\underset{|}{\text{C}}}-\text{H}$ bond. In any case, comparison with $k_d/k_c = 9.3$ and 12.0 for CH_3O and $\text{C}_2\text{H}_5\text{O}$ radicals,⁹¹ respectively, clearly shows that $\text{C}-\text{S}$ bonds are not readily converted to $\text{C}=\text{S}$ bonds.

In the presence of ethylene a complete reaction sequence would consist of steps (1)-(3) and (5)-(14)





Although not all of the products formed could be identified in this system, a careful search failed to reveal the presence of $\text{C}_2\text{H}_5\text{SCH}=\text{CH}_2$, $\text{C}_2\text{H}_5\text{SC}_4\text{H}_9$ and $\text{C}_2\text{H}_5\text{SC}_2\text{H}_4\text{SC}_2\text{H}_5$ which would have been formed had steps (7a), (8a), (8c), (9a) and (9c) taken place. The meta-thetical reaction (12b), postulated by analogy with the $\text{CH}_3 + \text{CH}_3\text{SSCH}_3$ reaction,⁵⁹ is probably relatively

inefficient and can be neglected in the kinetic treatment. Addition of C_2H_5 to C_2H_4 is a relatively slow process ($k = 7.5 \times 10^8 \text{ cm}^3 \text{ mol}^{-1} \text{ s}^{-1}$ at 25°C ⁹²) compared with other radical-radical reactions taking place in the system and moreover, butene, the expected disproportionation product of C_4H_9 radicals,



was demonstrably absent.

If the suppressing effect of added C_2H_4 on the quantum yield of C_2H_5SH is denoted by f , it can be shown (cf Appendix C) that, assuming the steady state concentration of thiyl radicals to vary linearly with that of hydrogen atoms, f is proportional to the reactive C_2H_4 concentration:

$$f = 1 + \frac{k_5 [C_2H_4]}{k_1 [C_2H_5SSC_2H_5]} \quad V$$

For each C_2H_4 concentration at the various temperatures used in this study f was determined by iteration such that the following relationship was obeyed:

$$\frac{\phi^\circ(1)}{f} + \frac{\phi^\circ(2a)}{f^2} + \frac{\phi^\circ(3)}{f} = \phi(C_2H_5SH)_{\text{total}} \quad VI$$

where ϕ° and ϕ are the quantum yields in the absence and presence of C_2H_4 , respectively. The quantum yields for steps (1), (2a) and (3) calculated in this way are listed in Table XVII.

TABLE XVII

Effect of C₂H₄ Pressure and Temperature on $\phi(\text{C}_2\text{H}_5\text{SH})^a$

P(C ₂ H ₄) Torr	[C ₂ H ₄]/ [C ₂ H ₅ SSC ₂ H ₅]	ϕ(C ₂ H ₅ SH)				
		ϕ(1)	ϕ(2a)	ϕ(3)	ϕ(1)+ϕ(3)	$\frac{1}{\phi(1)+\phi(3)}$
25°C						
0.00	0.00	2.00	0.100	0.220	2.10	0.476
5.00	1.00	1.60	0.064	0.176	1.664	0.600
10.00	2.00	1.33	0.044	0.147	1.374	0.728
15.00	3.00	1.14	0.032	0.126	1.172	0.853
60°C						
0.00	0.00	2.00	0.090	0.38	2.09	0.478
5.00	1.00	1.58	0.056	0.30	1.64	0.610
10.00	2.00	1.31	0.038	0.25	1.348	0.742
15.00	3.00	1.12	0.028	0.21	1.148	0.871
80°C						
0.00	0.00	2.00	0.090	0.49	2.09	0.478
5.00	1.00	1.56	0.055	0.38	1.61	0.619
10.00	2.00	1.28	0.037	0.31	1.317	0.759
15.00	3.00	1.08	0.027	0.26	1.107	0.903
120°C						
0.00	0.00	2.00	0.08	0.62	2.08	0.481
5.00	1.00	1.55	0.048	0.48	1.598	0.626
10.00	2.00	1.265	0.032	0.39	1.297	0.771
15.00	3.00	1.08	0.023	0.33	1.103	0.907
145°C						
0.00	0.00	2.00	0.07	0.77	2.07	0.483
5.00	1.00	1.54	0.041	0.59	1.581	0.632
10.00	2.00	1.25	0.027	0.48	1.277	0.783
15.00	3.00	1.05	0.019	0.40	1.069	0.935

^aPhotolysis time = 45 min; $I_a = 1.24 \times 10^{-8}$ einstein min⁻¹

P(H₂) = 580 ± 10 Torr; P(C₂H₅SSC₂H₅) = 5.00 Torr.

From Equation VI it follows that

$$\begin{aligned}\phi(1) + \phi(2a) &= \phi^{\circ}(1)/f + \phi^{\circ}(2a)/f^2 \\ &= \frac{1}{f} \left(2.0 + \frac{\phi^{\circ}(2a)}{f} \right)\end{aligned}$$

Substituting f from Equation V and rearranging gives:

$$1/(\phi(1) + \phi(2a)) = \frac{1}{(2+\beta)} + \frac{1}{(2+\beta)} \frac{k_5 [C_2H_4]}{[C_2H_5SSC_2H_5]} \quad VII$$

where $\beta = \phi^{\circ}(2a)/f$. Although β is somewhat dependent on the ratio $[C_2H_4]/[C_2H_5SSC_2H_5]$, plots of Equation VII, illustrated in Figure 6, are linear at the five temperatures studied and, within experimental error, feature a common intercept of 0.48. The least mean square slopes and intercepts are summarized in Table XVIII. The average values of β and f are 0.08 and 1.5 respectively and therefore $\phi^{\circ}(2a) = 0.12$, in reasonably good agreement with the value of 0.103 derived from the unscavenged system, Table XVI. These results indicate that the assumption whereby C_2H_5S radical disappear mainly *via* abstraction, disproportionation and combination reactions is probably correct. The values of k_5/k_1 listed in Table XVIII are plotted in the Arrhenius form in Figure 7, from which

$$\log(k_5/k_1) = (-0.332 \pm 0.023) - (356 \pm 37)/2.3RT$$

Taking the limiting high pressure rate parameters for step (5) as,⁸⁹

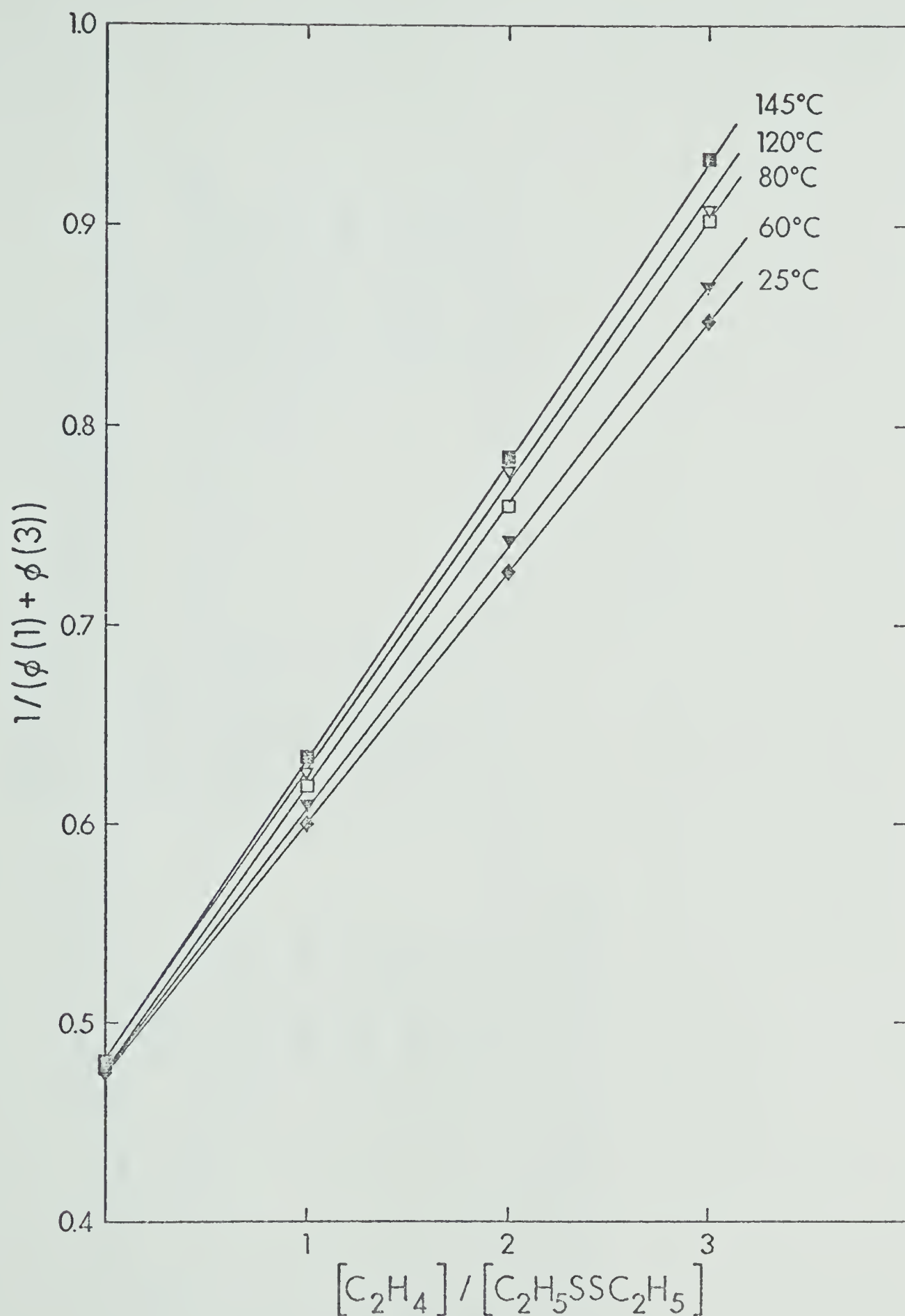


FIGURE 6. $\frac{1}{\phi(1) + \phi(3)}$ versus $P[C_2H_4]/P[C_2H_5SSC_2H_5]$ at 25, 60, 80, 120 and 145°C. $P(H_2) = 580 \pm 10$ Torr; photolysis time, 45 minutes.

TABLE XVIII

Slopes and Intercepts of the Plots in Figure 6^a

T, °C	Slope	Intercept	k ₅ /k ₁
25	0.1111±0.003	0.434±0.003	0.256±0.007
60	0.108±0.001	0.404±0.002	0.267±0.003
80	0.110±0.002	0.388±0.003	0.284±0.006
120	0.110±0.001	0.372±0.002	0.296±0.003
145	0.106±0.002	0.352±0.004	0.301±0.007

^aThe errors are standard deviations.

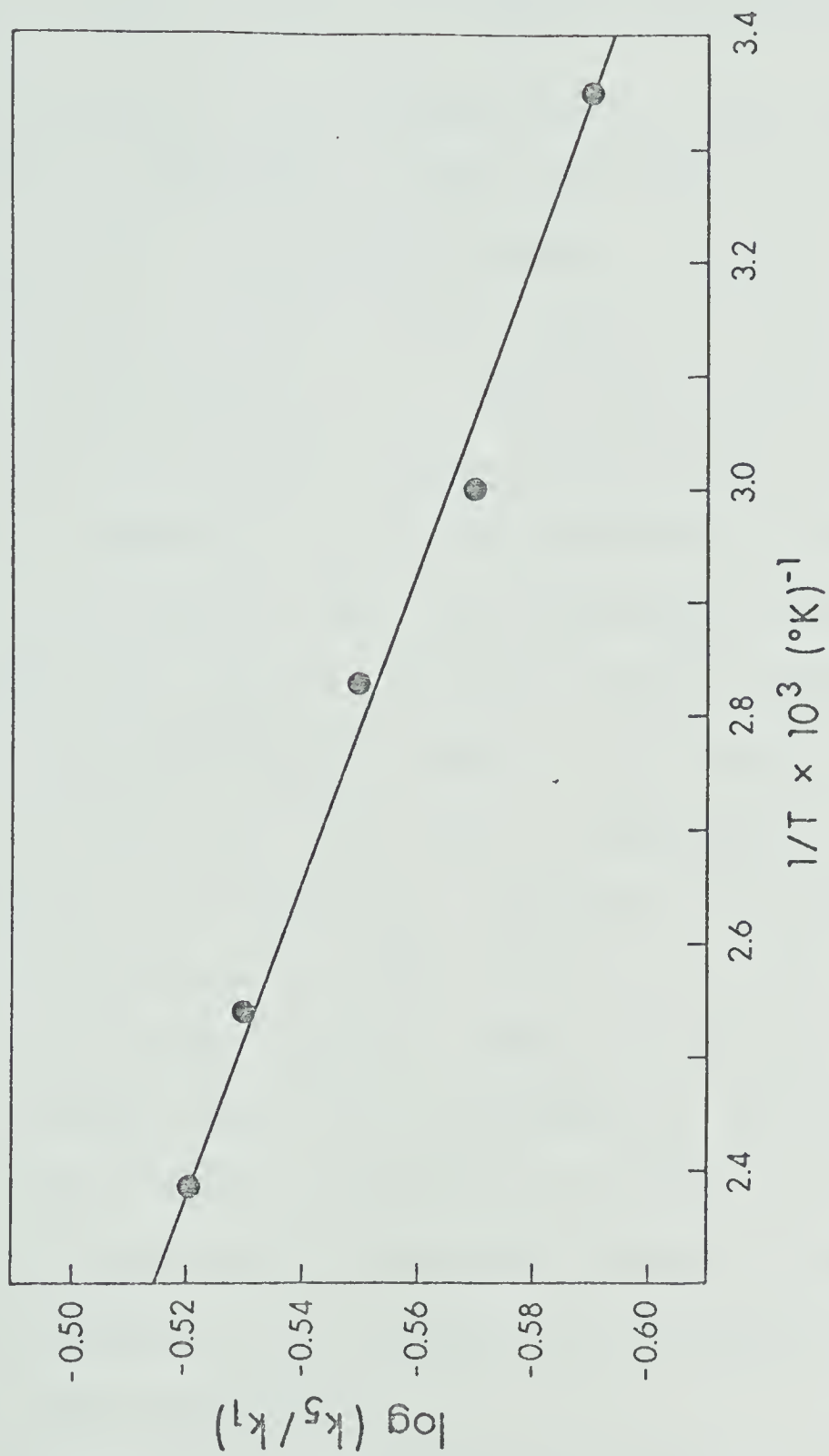


FIGURE 7. Arrhenius plot of k_5/k_1 versus $1/T$.

$$k_5 = (2.2 \pm 0.4) \times 10^{13} \exp[-(2066 \pm 83)/RT] \text{cm}^3 \text{mol}^{-1} \text{s}^{-1},$$

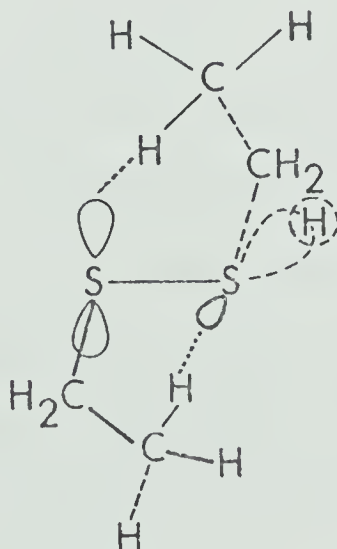
those for step (1) are

$$k_1 = (4.73 \pm 0.64) \times 10^{13} \exp[-(1710 \pm 69)/RT] \text{cm}^3 \text{mol}^{-1} \text{s}^{-1}.$$

The values of the preexponential factor and activation energy are, surprisingly, quite different for the $\text{H} + \text{CH}_3\text{SSCH}_3$ and $\text{H} + \text{C}_2\text{H}_5\text{SSC}_2\text{H}_5$ systems, in spite of the fact that the initial step in both reactions involves metathetical displacement of an alkyl thiyl radical. The relative reactivity of these two disulfides towards H atom attack is, however, clearly in line with the observed decrease in reaction rate with decreasing exothermicity in a homologous series. In this case the dimethyldisulfide reaction is considerably faster. From the data in Table II, $\Delta H = -19.7 \text{ kcal mol}^{-1}$ for the $\text{H} + \text{C}_2\text{H}_5\text{SSC}_2\text{H}_5$ reaction, compared to $-21.4 \text{ kcal mol}^{-1}$ for the $\text{H} + \text{CH}_3\text{SSCH}_3$ reaction and the difference, $1.7 \text{ kcal mol}^{-1}$, is in good agreement with the measured activation energy difference of 1.6 kcal . Interestingly, the exothermicity difference calculated on the basis of bond strength is $1.5 \text{ kcal mol}^{-1}$, indicating that the reactivity of disulfides toward H atom attack is governed mainly by the strengths of the bonds being broken and the new ones formed.

The experimental entropy of activation for the standard state of 1 atm., calculated from the A factor,

is -22.0 e.u., suggesting a somewhat looser transition state relative to that for the $\text{H} + \text{CH}_3\text{SSCH}_3$ reaction, where $\Delta S^\ddagger = -26.2$ e.u. ΔS^\ddagger can be estimated by Benson's method⁷⁷ since the gas phase structural parameters of $\text{C}_2\text{H}_5\text{SSC}_2\text{H}_5$ are known. Three rotamers of $\text{C}_2\text{H}_5\text{SSC}_2\text{H}_5$ exist in the gas phase, of which the gauche-gauche conformation is apparently the most stable.^{16,93} On the basis of the structural parameters and the spatial conformation of $\text{C}_2\text{H}_5\text{SSC}_2\text{H}_5$ we conclude that it is possible that one of the H atoms of a terminal methyl group can interact with the non-bonding electrons in the 3p orbital of the second sulfur atom leading to the formation of a five-membered hydrogen-bonded cyclic structure in which there is a barrier to rotation of the other C_2H_5 group about the C-S axis. Attack by the H atom on the 3p orbital of the second sulfur atom would result in cleavage of the weak hydrogen



bond, thus allowing free rotation of the ethyl group.

A freely rotating ethyl group contributes about 7.5 e.u.⁷⁷ at 300 K and in order to reproduce the experimental activation entropy, -22.0 e.u., the contribution required from the rotation of the ethyl group is:

$$\begin{aligned}
 \Delta S^\ddagger &= S^\ddagger(\text{H} \cdot \text{C}_2\text{H}_5\text{SSC}_2\text{H}_5) - S^\circ(\text{C}_2\text{H}_5\text{SSC}_2\text{H}_5) - S^\circ(\text{H}) \\
 &= S^\circ(\text{C}_2\text{H}_5\text{SSC}_2\text{H}_5) + R \ln 2 + x - S^\circ(\text{C}_2\text{H}_5\text{SSC}_2\text{H}_5) - S^\circ(\text{H}) \\
 &= R \ln 2 + x - S^\circ(\text{H}) \\
 &= 1.4 + x - 27.4 \\
 &= -26.0 + x \\
 &= -22.0 \text{ e.u.}
 \end{aligned}$$

Therefore, $x = 26.0 - 22.0$

$$= 4.0 \text{ e.u.}$$

This value, being lower than the full rotational contribution, is reasonable and seems to suggest that the ethyl group rotation is hindered but not fully frozen. This result is in agreement with the proposed gauche-gauche structure being the most stable conformer of $\text{C}_2\text{H}_5\text{SSC}_2\text{H}_5$,^{16,93} and with the larger activation energy associated with the $\text{H} + \text{C}_2\text{H}_5\text{SSC}_2\text{H}_5$ as compared to the $\text{H} + \text{CH}_3\text{SSCH}_3$ reaction.

CHAPTER V

THE REACTION OF HYDROGEN ATOMS WITH ETHYLMETHYLDISULFIDE

Results

1. Products of reaction.

In the gas phase and at room temperature H atoms react with ethylmethyldisulfide to yield CH_3SSCH_3 , $\text{C}_2\text{H}_5\text{SSC}_2\text{H}_5$, CH_3SH , $\text{C}_2\text{H}_5\text{SH}$ and, at longer illumination times, sulfur polymer. As will be seen, this system is much more complex than for the case of symmetrical disulfides. Control experiments with a reaction mixture consisting of 580 Torr H_2 and 2.5 Torr $\text{CH}_3\text{SSC}_2\text{H}_5$ showed that considerable amounts of CH_3SSCH_3 and $\text{C}_2\text{H}_5\text{SSC}_2\text{H}_5$ were formed by thermal exchange reactions. In subsequent sensitization experiments corrections were made for the thermally produced amounts of these products. It was estimated that less than 5% of the excited mercury atoms were quenched by $\text{C}_2\text{H}_5\text{SSC}_2\text{H}_5$.

2. Effects of exposure time, pressure, and temperature.

In the first series of experiments reaction mixtures consisting of 580 Torr H_2 and 2.50 Torr $\text{CH}_3\text{SSC}_2\text{H}_5$ were mercury sensitized and the quantum yields for the formation of the thiols and disulfides as a function of exposure time are listed in Table XIX. The quantum yields of formation for both symmetrical disulfides, which are

TABLE XIX

Time Dependence of the Quantum Yields of the Reaction Products^a

Time, min.	ϕ				$\phi(\text{CH}_3\text{SH})$
	CH_3SH	$\text{C}_2\text{H}_5\text{SH}$	CH_3SSCH_3	$\text{C}_2\text{H}_5\text{SSC}_2\text{H}_5$	$\phi(\text{C}_2\text{H}_5\text{SH})$
2	b	b	78.33	78.18	
5	b	b	58.46	58.25	
10	1.43	0.78	31.7	31.3	1.83
20	1.43	0.80	22.8	22.3	1.79
30	1.42	0.81	15.7	15.4	1.75
45	1.40	0.82	11.7	11.3	1.71
60	1.39	0.83	8.7	8.4	1.67
120	1.29	0.89	5.8	5.9	1.45

^a $(\text{C}_2\text{H}_5\text{SSCH}_3) = 250 \text{ Torr}$, $\text{P}(\text{H}_2) = 580 \text{ Torr}$; $\text{I}_a = 1.06 \times 10^{-8} \text{ einstein min}^{-1}$.

^b not measured.

essentially equal in the whole time range, are extremely high initially but decrease sharply with increasing time up to 120 minutes. The time dependence of $\phi(\text{CH}_3\text{SSCH}_3)$ and of $\phi(\text{C}_2\text{H}_5\text{SSC}_2\text{H}_5)$ are plotted in Figure 8; extrapolation to zero time gives the value $\phi(t = 0) = 92$. As seen from Table XIX the quantum yields of formation of CH_3SH and $\text{C}_2\text{H}_5\text{SH}$ show only moderate time dependence. The ratio $\phi(\text{CH}_3\text{SH})/\phi(\text{C}_2\text{H}_5\text{SH})$ is plotted as a function of time in Figure 9. Extrapolation to zero time gives the limiting value of 1.86 which is identical to the rate constant ratio for the $\text{H} + \text{CH}_3\text{SSCH}_3$ and $\text{H} + \text{C}_2\text{H}_5\text{SSC}_2\text{H}_5$ reactions.

Next, the quantum yields of the products were examined as a function of substrate pressure. On going from 2.5 Torr $\text{CH}_3\text{SSC}_2\text{H}_5$ to 5.0 Torr, the quantum yields of CH_3SH and $\text{C}_2\text{H}_5\text{SH}$ were unchanged while those for CH_3SSCH_3 and $\text{C}_2\text{H}_5\text{SSC}_2\text{H}_5$ increased from 31.7 and 31.3 to 63.5 and 62.8, respectively, i.e., in direct proportion to the pressure increase.

The effect of temperature on the quantum yields of the reaction products was not quantitatively determined because the system was exceedingly complex as a result of the occurrence of thermal exchange reactions. Qualitatively, however, the quantum yields of CH_3SSCH_3 and $\text{C}_2\text{H}_5\text{SSC}_2\text{H}_5$ increased significantly with increasing temperature, while the quantum yields of the thiols increased only moderately.

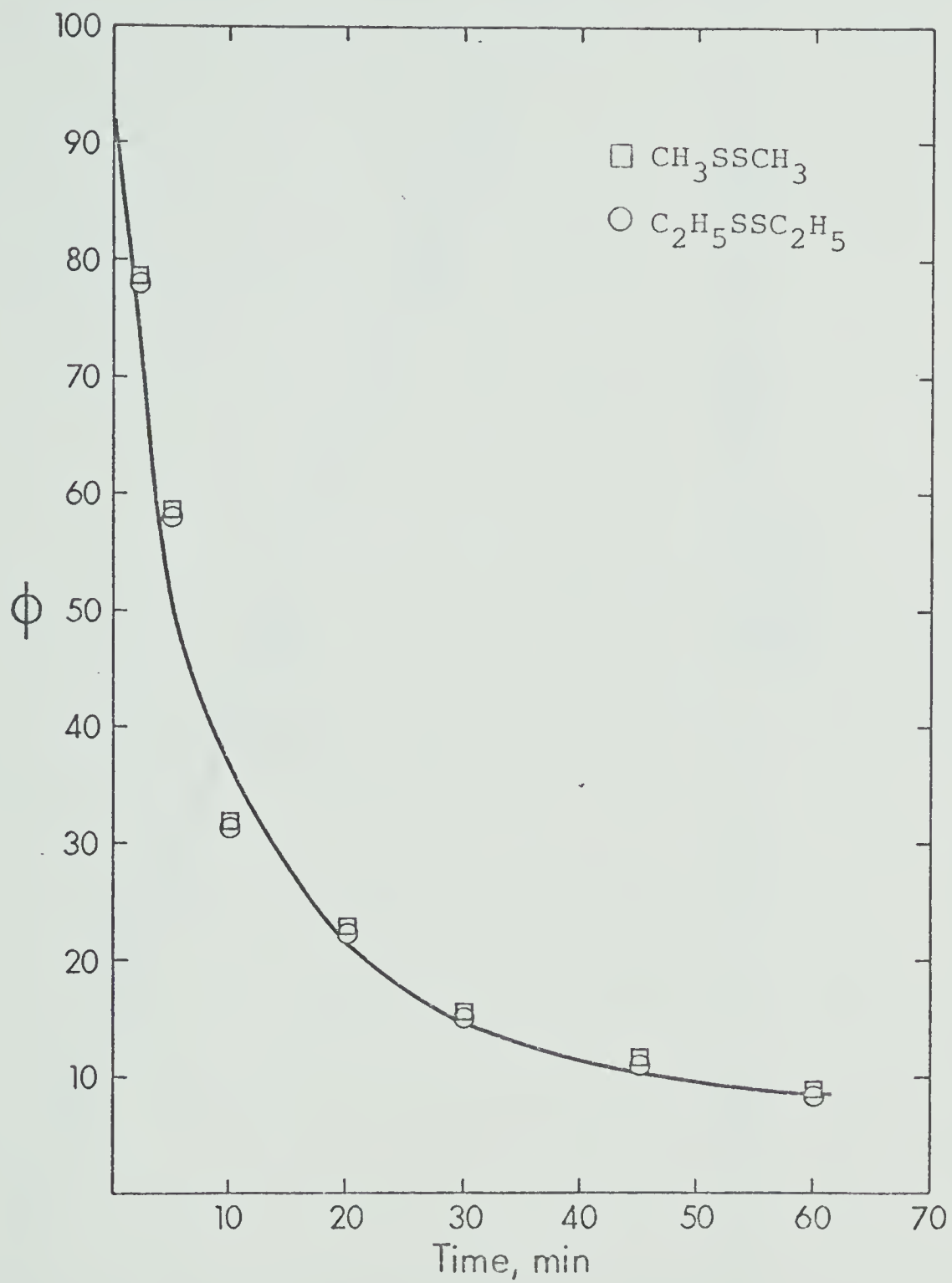


FIGURE 8. Average quantum yields for CH_3SSCH_3 and $\text{C}_2\text{H}_5\text{SSC}_2\text{H}_5$ formation as a function of irradiation time.

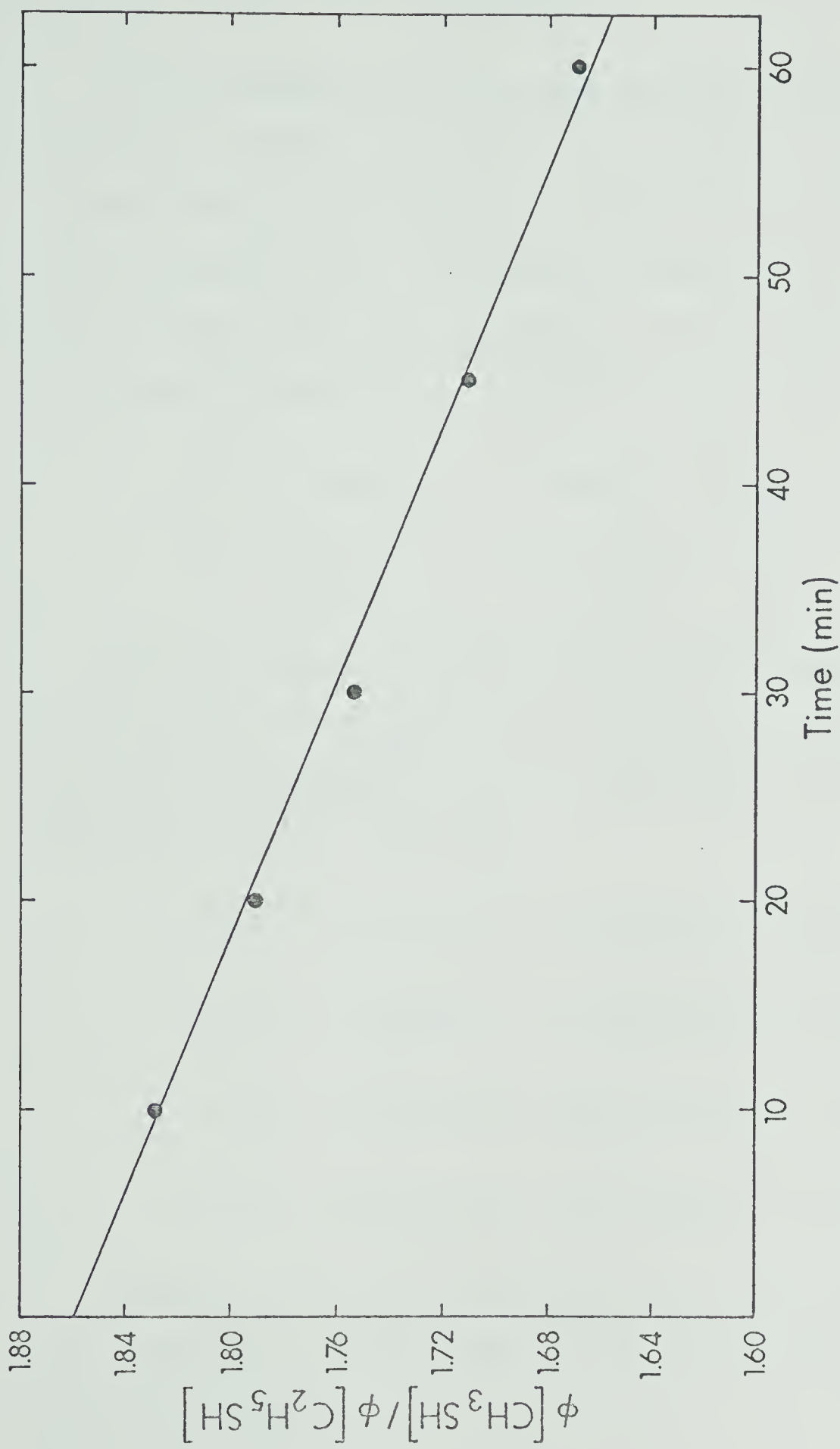
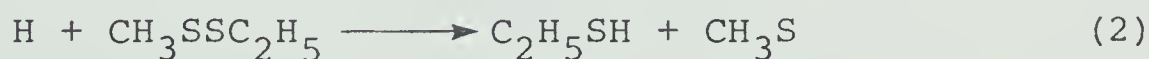


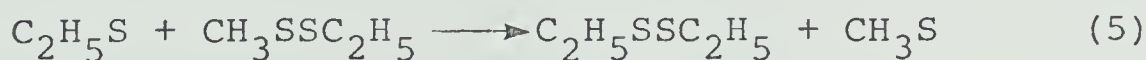
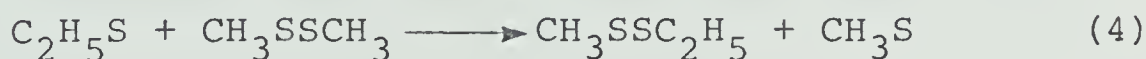
FIGURE 9. Dependence of $\phi(CH_3SH)/\phi(C_2H_5SH)$ on irradiation time.

Discussion

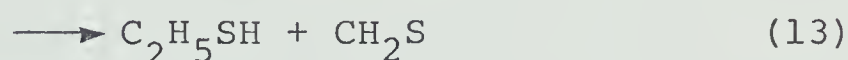
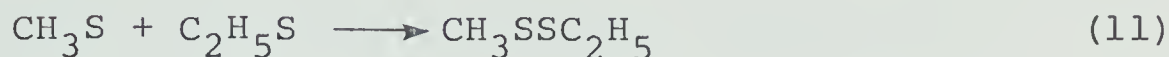
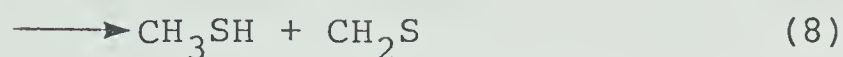
The invariance of the thiol quantum yields with $\text{CH}_3\text{SSC}_2\text{H}_5$ pressure suggests that scavenging of H atoms by the substrate is complete. Hence, and by analogy with the $\text{H} + \text{CH}_3\text{SSCH}_3$ and $\text{H} + \text{C}_2\text{H}_5\text{SSC}_2\text{H}_5$ reactions it is proposed that H atoms react with $\text{CH}_3\text{SSC}_2\text{H}_5$ *via* two parallel and competing metathetical steps (1) and (2):



The very high initial quantum yields obtained for the formation of CH_3SSCH_3 and $\text{C}_2\text{H}_5\text{SSC}_2\text{H}_5$ indicate that the thiyl radicals generated in reactions (1) and (2) propagate a chain sequence:



Termination of the chain and the final fate of the thiyl radicals is postulated to be combination and disproportionation:



The occurrence of disproportionation is clearly demonstrated by the fact that the sum of the quantum yields of the thiols is 2.2, whereas a value of 2.0 would be expected solely on the basis of reactions (1) and (2).

Because of the occurrence of this chain reaction, the symmetric disulfides accumulate rapidly in the system and their secondary reactions with H atoms also need to be considered in the overall mechanism:



The overall mechanism consisting of the elementary steps (1)-(15) has been tested by computer modeling. The objectives of the simulation were to see if the observed time dependence of the quantum yields can be

reproduced and also to estimate rate constant values for those individual reaction steps which have not been reported in the literature.

The set of differential equations corresponding to the above mechanism was solved numerically by using the algorithm DIFSUB developed by Gear⁷⁹ for the numerical integration of a set of stiff ordinary differential equations.

The rate constants k_1 and k_2 were assumed to be identical to those determined for the reactions of H atoms with the corresponding symmetric disulfides, CH_3SSCH_3 ⁹⁴⁻⁹⁶ and $\text{C}_2\text{H}_5\text{SSC}_2\text{H}_5$,⁹⁷ on the basis of the observation that the extrapolated value of $\phi(\text{CH}_3\text{SH})/\phi(\text{C}_2\text{H}_5\text{SH})$ at $t = 0$ is equal to k_{14}/k_{15} .

The rate constants for the reactions of thiyl radicals with disulfides are not known and values of k_3 - k_6 had to be established by fitting the calculated rate of formation for the symmetric disulfides to the measured quantum yields. The equilibrium constant for the disproportionation reaction



has been determined experimentally as being 5.5 at room temperature.²⁴ If we assume that reactions (3)-(6) approach a similar equilibrium then the corresponding rate constants must satisfy the following relationship:

$$k_4/k_3 \times k_6/k_5 = 5.5 \quad (17)$$

From the set of rate constants used in the simulation listed in Table XX, it is seen that the derived values of k_3 to k_6 conform to this relationship.

It was also considered that the conversion of symmetric disulfides to asymmetric ones should be faster, i.e., $k_3 < k_4$ and $k_5 < k_6$, because of the contribution to the entropy change from the loss of symmetry. The relative magnitudes of the rate constants $k_3 - k_6$ are also in line with the observation that substitution of the methyl group on the S atom by ethyl decreases the rate constant⁹⁷ for attack by H atoms.

The rate constant for the combination of CH_3S radicals has been reported to be:

$$k_7 = 2.4 \times 10^{13} \text{ cm}^3 \text{ mol}^{-1} \text{ s}^{-1}$$

and we assumed the same value for k_9 , the combination of $\text{C}_2\text{H}_5\text{S}$ radicals. The k_d/k_c ratios for CH_3S and $\text{C}_2\text{H}_5\text{S}$ radicals have been reported^{57a, 68} and the rate constants for the cross combination and disproportionation of CH_3S and $\text{C}_2\text{H}_5\text{S}$ (k_{12} and k_{13}) were taken to be twice as high as for the self reactions (k_8 and k_{10}), i.e.,

$$k_{12} = 2k_8 \text{ and } k_{13} = 2k_{10}$$

From Table XX $k_1/k_2 = 1.86$, $k_3/k_5 = 1.80$ and

TABLE XX

Rate Constants, ($\text{cm}^3 \text{ mol}^{-1} \text{ s}^{-1}$), Used in the Simulation

k_1	$4.90 \times 10^{12} \text{ a}$	k_6	$1.94 \times 10^{10} \text{ c}$	k_{11}	$4.80 \times 10^{13} \text{ a}$
k_2	$2.63 \times 10^{12} \text{ b}$	k_7	$2.40 \times 10^{13} \text{ d}$	k_{12}	$3.84 \times 10^{12} \text{ a}$
k_3	$1.40 \times 10^{10} \text{ c}$	k_8	$1.92 \times 10^{12} \text{ a}$	k_{13}	$1.10 \times 10^{13} \text{ b}$
k_4	$3.12 \times 10^{10} \text{ c}$	k_9	$2.40 \times 10^{13} \text{ e}$	k_{14}	$4.90 \times 10^{12} \text{ a}$
k_5	$7.78 \times 10^9 \text{ c}$	k_{10}	$5.04 \times 10^{12} \text{ b}$	k_{15}	$2.63 \times 10^{12} \text{ b}$

^aReference 96. ^bReference 97. ^cDerived from the simulation. ^dReference 69.

^eAssumed to be equal to k_7 .

$k_4/k_6 = 1.60$. The rate constant ratios for disproportionation and combination of thiyl radicals obtained from the simulation, $k_8/k_7 = 0.08$ for CH_3S and $k_{10}/k_9 = 0.21$ for $\text{C}_2\text{H}_5\text{S}$, are in good agreement with the experimentally derived values of 0.05^{57a} and 0.13^{68} respectively.

The simulated time dependence of $\phi(\text{CH}_3\text{SSCH}_3)$ calculated on the basis of the above mechanism is shown in Figure 10 along with the experimental values (in the whole time range, identical values were obtained for $\phi(\text{C}_2\text{H}_5\text{SSC}_2\text{H}_5)$). Curve A represents the change of the quantum yield with time, and curve B is the average quantum yield calculated from the amount of CH_3SSCH_3 formed at the given time. It is seen that curve B follows the experimental trend, reproducing the rapid decline of the quantum yield, and curve A rapidly approaches the value of zero. Both trends are manifestations that the system is approaching equilibrium. The concentrations of the symmetric and asymmetric disulfides calculated at $t = 20$ minutes correspond to an equilibrium constant of 5.5, in accordance with the assumed rate constants k_3 - k_6 .

For $\phi(\text{CH}_3\text{SH})$ and $\phi(\text{C}_2\text{H}_5\text{SH})$ the values of 1.41 and 0.79 were obtained, independently of exposure time, in good agreement with the experimental results.

$\phi(\text{CH}_3\text{SSCH}_3)$ calculated in the simulation (Curve B in Figure 10) reproduces satisfactorily the experimentally observed rapid decrease with increasing irradiation time

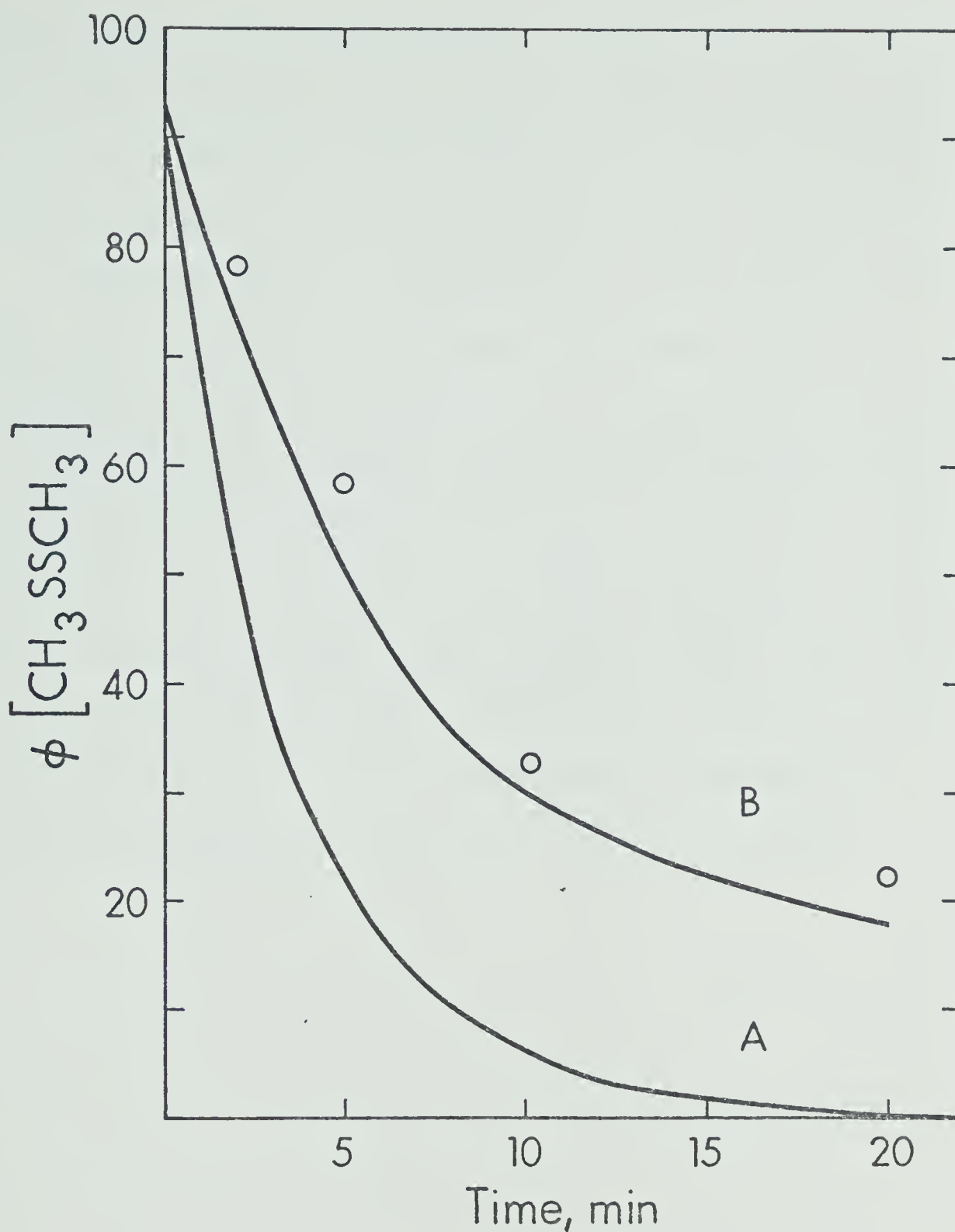


FIGURE 10. Dependence of $\phi(\text{CH}_3\text{SSCH}_3)$ on irradiation time

Curve A: instantaneous quantum yield calculated from the amount of CH_3SSCH_3 formed in one second;

Curve B: average quantum yield, calculated from the integrated amount of CH_3SSCH_3 ;

O: experimental data.

and together with the agreement between the observed and calculated $\phi(\text{CH}_3\text{SH})$ and $\phi(\text{C}_2\text{H}_5\text{SH})$ values supports the proposed mechanism. The agreement also shows that the assumed values of the rate constants are reasonable.

The derived rate constants for the reactions of thiyl radicals with disulfides are lower than the corresponding rate constants for H atoms and the difference is probably due to changes in both the preexponential factors and the activation energies. Thus for H atom reactions the gas kinetic collision frequency and the steric factor are both significantly higher than for thiyl radical reactions. Also, hydrogen atom reactions are about 15 kcal mol^{-1} more exothermic as compared to the nearly thermoneutral reactions of thiyl radicals.

CHAPTER VI

THE REACTIONS OF HYDROGEN ATOMS WITH BIS(TRIFLUOROMETHYL)- DISULFIDE

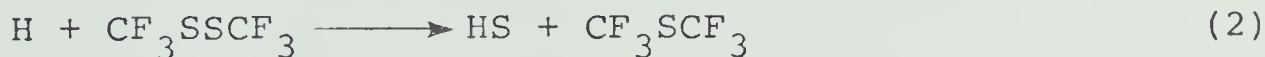
Results

1. Products of the Reaction

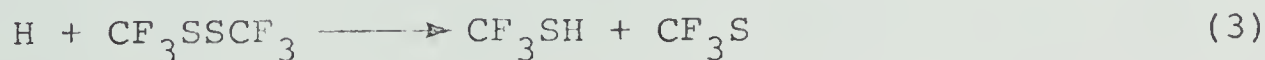
The Hg* photosensitization of a mixture of 600 Torr H₂ and 3.75 Torr CF₃SSCF₃ led to the formation of very small amounts of CF₃SCF₃ (typically, 0.07 μmoles for a 45 minute photolysis at 25°C) and extensive deposition of polymer. Subsequent blank experiments however showed that CF₃SCF₃ can be formed from a thermally induced exchange reaction:



The large amounts of polymer indicated that some reaction had taken place, but evidently the products must have been irretrievable. Two primary processes can be envisioned: direct S abstraction,



which would lead to the formation of H₂S *via* disproportionation of the HS radicals, and, by analogy with the alkyl disulfides, metathetical displacement:



The small yields of CF_3SCF_3 observed suggest that step (2), if it occurs, must be relatively inefficient since this sulfide is fairly stable⁹⁸ under the conditions employed here. Nevertheless, the possibility that H_2S undergoes a dark reaction with the substrate had to be explored. To this end, a mixture consisting of 3% H_2S in CF_3SSCF_3 was analyzed by gc on an 8 ft porapak N column at 59°C and only the CF_3SSCF_3 peak appeared on the chromatogram. As further confirmation, gc analysis of the reaction products formed from the Hg^* sensitization of 600 Torr H_2 in the presence of 3.75 Torr thiirane showed that the H_2S formed in the reaction could in fact be detected with the analytical techniques employed; yet when the experiment was carried out with 3.75 Torr added CF_3SSCF_3 , no H_2S was found.

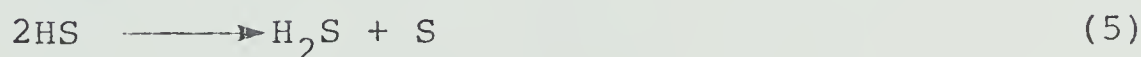
In the light of these results, it was suspected that CF_3SH might also engage in a dark reaction with CF_3SSCF_3 . Unfortunately, CF_3SH is not commercially available hence a mixture of CH_3SH (3%) in CF_3SSCF_3 was prepared and injected into the gc: as expected, CH_3SH was not eluted on the chromatogram.

In order to test for the intermediacy of thiyl radical in the $\text{H} + \text{CF}_3\text{SSCF}_3$ reaction a mixture consisting of 2 Torr C_2H_4 , 30 Torr CF_3SSCF_3 and 600 Torr H_2 was mercury photosensitized. In addition to CF_3SSCF_3 , C_4H_{10} , and C_2H_6 , $\text{CF}_3\text{SC}_2\text{H}_5$ was found to be a major product. The

mass spectrum of this compound is given in Appendix B. The formation of $\text{CF}_3\text{SC}_2\text{H}_5$ definitely shows that CF_3S radicals are intermediates in the $\text{H} + \text{CF}_3\text{SSCF}_3$ reaction.

2. Effect of added thiirane.

In order to determine the rate coefficient of the $\text{H} + \text{CF}_3\text{SSCF}_3$ reaction it was decided to carry out competitive studies with added thiirane. Firstly, the $\text{H} + \text{C}_2\text{H}_4\text{S}$ reaction was investigated as a function of exposure time for a mixture consisting of 600 Torr H_2 and 3.75 Torr $\text{C}_2\text{H}_4\text{S}$. The quantum yields of C_2H_4 and H_2S are listed in Table XXI. In this system C_2H_4 can be formed in two ways:³⁸ desulfurization by H atoms, and by S atoms:



From Table XXI, it is seen that $\phi(\text{C}_2\text{H}_4) = 2.47$ at 25° , independent of exposure time up to 60 minutes. Since $\phi(\text{H}) = 2.0$, it follows that $\phi(6) = 0.47$. The total quantum yield of ethylene is

$$\phi(\text{C}_2\text{H}_4) = \phi(4) + \phi(6)$$

and since $\phi(5) = \phi(6)$, the quantum yield of desulfurization

TABLE XXI

Effect of Exposure time on $\phi(\text{C}_2\text{H}_4)$ and $\phi(\text{H}_2\text{S})$ from the $\text{H} + \text{C}_2\text{H}_4\text{S}$ Reaction^a

Time, min	C_2H_4		H_2S		$\phi(\text{C}_2\text{H}_4)$	$\phi(\text{H}_2\text{S})$	γ^b
	Yield (μmoles)	Rate ($\mu\text{moles min}^{-1}$) $\times 10^2$	Yield (μmoles)	Rate ($\mu\text{moles min}^{-1}$) $\times 10^2$			
30	0.7861 ± 0.004	2.62 ± 0.01	0.1489 ± 0.002	0.496 ± 0.007	2.47 ± 0.01	0.468 ± 0.007	$2.00 \pm 0.01(2)^c$
45	1.179 ± 0.006	2.62 ± 0.01	0.2233 ± 0.002	0.496 ± 0.004	2.47 ± 0.01	0.468 ± 0.004	$2.00 \pm 0.01(2)$
60	1.568 ± 0.009	2.61 ± 0.01	0.2970 ± 0.002	0.496 ± 0.003	2.46 ± 0.01	0.467 ± 0.003	$1.99 \pm 0.01(2)$

^aT = 25°C; P(H_2) = 600 Torr; P($\text{C}_2\text{H}_4\text{S}$) = 3.75 Torr; $I_a = 1.06$ ($\mu\text{einstein min}^{-1}$) $\times 10^2$

^b $\gamma = \phi(\text{C}_2\text{H}_4) - \phi(\text{H}_2\text{S})$

^cnumber of experiments

by H atoms, γ , is then

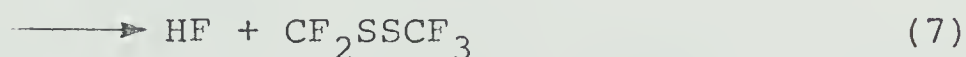
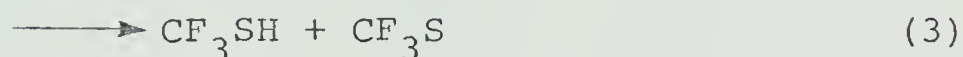
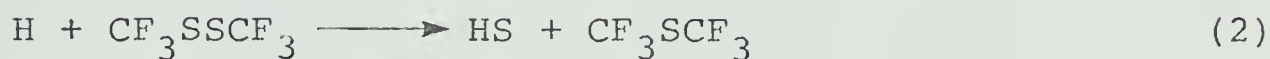
$$\gamma = \phi(4) = \phi(\text{C}_2\text{H}_4) - \phi(5) = 2.47 - 0.47 = 2.00$$

at 25°C. The results in Table XXI also show that γ is independent of temperature up to 152°C.

In the presence of 3.75 Torr CF_3SSCF_3 , $\phi(\text{C}_2\text{H}_4)$ decreases and H_2S is no longer detected. The values of $\phi(\text{C}_2\text{H}_4)$ and γ obtained at five different temperatures and $\text{C}_2\text{H}_4\text{S}$ concentrations are listed in Table XXII.

Discussion

H atom attack on CF_3SSCF_3 can take place *via* the following primary processes:



In the absence of measurable amounts of retrievable products it is not possible to make an unequivocal decision with regard to these possibilities, but the results from the $\text{H}_2/\text{CF}_3\text{SSCF}_3/\text{C}_2\text{H}_4$ system strongly point to the occurrence of step (3). Thus CF_3SCF_3 is formed in only trace amounts, and is most likely formed from the thermal exchange reaction (1). The occurrence of F abstraction, (7), can be ruled out since a prohibitively high activation

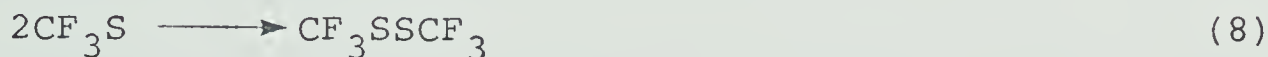
TABLE XXII

Effect of Temperature and C₂H₄S Pressure on γ^a

P(C ₂ H ₄ S) Torr	[CF ₃ SSCF ₃]/ [C ₂ H ₄ S]	ϕ (C ₂ H ₄)	γ	γ^{-1}
<u>25°C</u>				
3.75	0.00	2.47	2.00	0.500
7.50	0.50	2.22	1.75	0.571
3.75	1.00	2.02	1.55	0.645
2.50	1.50	1.85	1.38	0.725
1.88	2.00	1.66	1.19	0.840
1.50	2.50	1.59	1.12	0.893
<u>62°C</u>				
3.75	0.00	2.40	2.00	0.500
3.75	1.00	1.74	1.34	0.746
2.50	1.50	1.55	1.15	0.868
1.88	2.00	1.41	1.01	0.990
1.50	2.50	1.30	0.90	1.11
<u>84°C</u>				
3.75	0.00	2.37	2.00	0.500
7.50	0.50	1.89	1.52	0.660
3.75	1.00	1.63	1.26	0.794
2.50	1.50	1.41	1.04	0.962
1.88	2.00	1.25	0.880	1.14
1.50	2.50	1.12	0.750	1.33
<u>124°C</u>				
3.75	0.00	2.30	2.00	0.500
3.75	1.00	1.33	1.03	0.971
2.50	1.50	1.14	0.840	1.19
1.88	2.00	0.996	0.696	1.44
1.50	2.50	0.894	0.594	1.68
<u>152°C</u>				
3.75	0.00	2.20	2.00	0.500
7.50	0.50	1.47	1.27	0.787
3.75	1.00	1.13	0.930	1.08
2.50	1.50	0.919	0.719	1.39
1.88	2.00	0.792	0.592	1.69
1.50	2.50	0.700	0.500	2.00

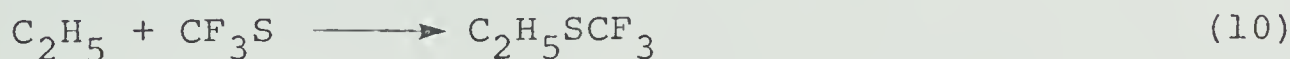
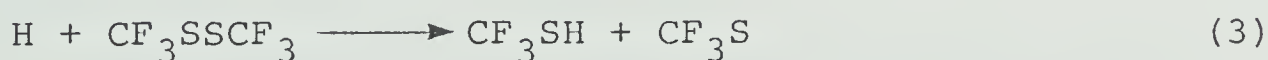
^a $\gamma = \phi(\text{C}_2\text{H}_4) - \phi(\text{H}_2\text{S})$; Photolysis time = 45 min; $I_a = 1.06 \times 10^{-8}$ einstein min⁻¹; P(H₂) = 600±10 Torr; P(CF₃SSCF₃) = 3.75 Torr.

energy⁹⁹ would be associated with this reaction. From these observations, and by analogy with the case of alkyl disulfides, it is therefore concluded that the sole primary process of importance is step (3). The only secondary reaction of importance is probably recombination,

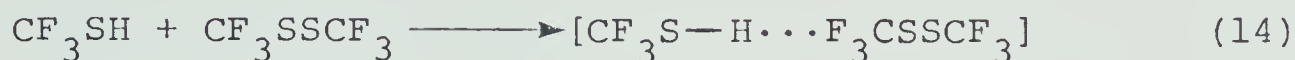


since, owing to the high C-F bond strength, disproportionation cannot take place at the temperatures used in this study.

Strong evidence for the intermediacy of thiyl radicals in this system, and hence in support of step (3), comes from the experiments carried out in the presence of ethylene, where $\text{C}_2\text{H}_5\text{SCF}_3$ is a major product. The following sequence of elementary reactions accounts for the formation of the observed products:



Since it has been shown that CF_3SH cannot be detected in the presence of large amounts of CF_3SSCF_3 , it is very likely that CF_3SH and CF_3SSCF_3 exist as a hydrogen bonded complex, e.g.,

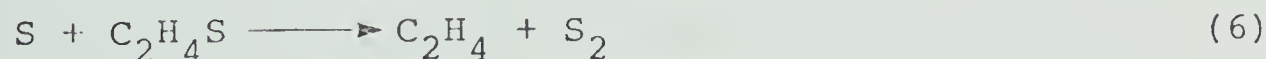
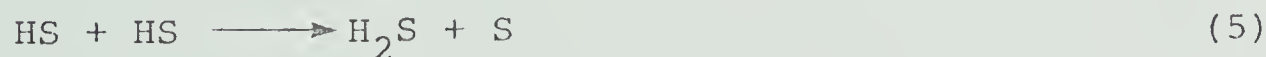
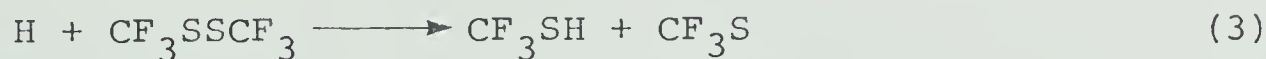


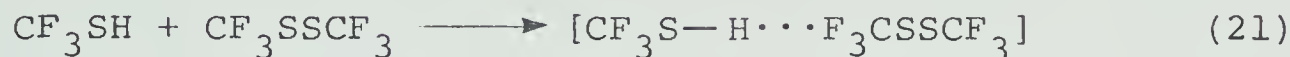
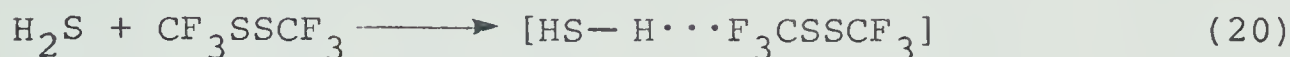
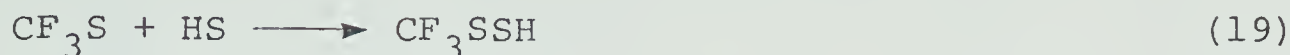
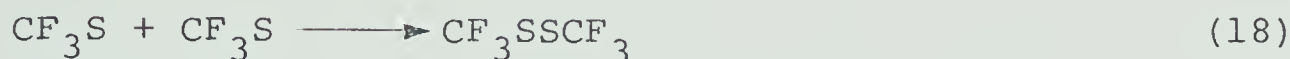
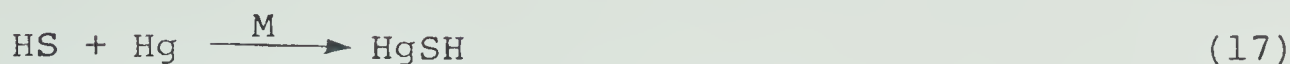
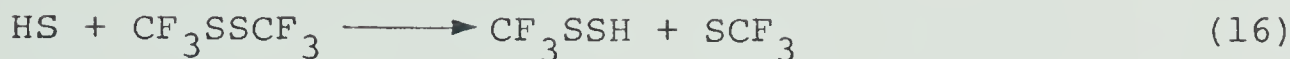
Evidence for the existence of a similar complex comes from the results of the photolysis of CF_3COCF_3 in the presence of H_2S .^{100,101} There was a mass balance deficiency of about 18% for the CF_3 radicals produced and this was ascribed to the following reaction:



Gc analysis for CF_3SH in the CF_3COCF_3 photolyzate however was difficult and the results were inconclusive.^{100,101} It is quite likely that in this system as well, CF_3SH forms a hydrogen bond with the substrate.

In the presence of thiirane, the following sequence of reaction steps explains the nature and the quantum yields of the observed products.





The possible occurrence of reaction (16) has to be considered since the following novel metathetical reaction has been shown to take place:⁴⁰



However, kinetic arguments (*vide infra*) indicate that reaction (16) is probably not important in the present system.

Steady state treatment of reactions (3)-(6), and (17) leads to the following kinetic expression:

$$\gamma^{-1} = 0.5 + \frac{k_3 [\text{CF}_3\text{SSCF}_3]}{2k_4 [\text{C}_2\text{H}_4\text{S}]} \quad \text{I}$$

where $\gamma = \phi(\text{C}_2\text{H}_4) - \phi(5) = \phi(4)$. The plots of γ^{-1} versus $[\text{CF}_3\text{SSCF}_3]/[\text{C}_2\text{H}_4\text{S}]$ at the five temperatures examined (Table XXII) shown in Figure 11, are linear and the slope and intercept values obtained by least mean square treatment of the data are given in Table XXIII. The plots

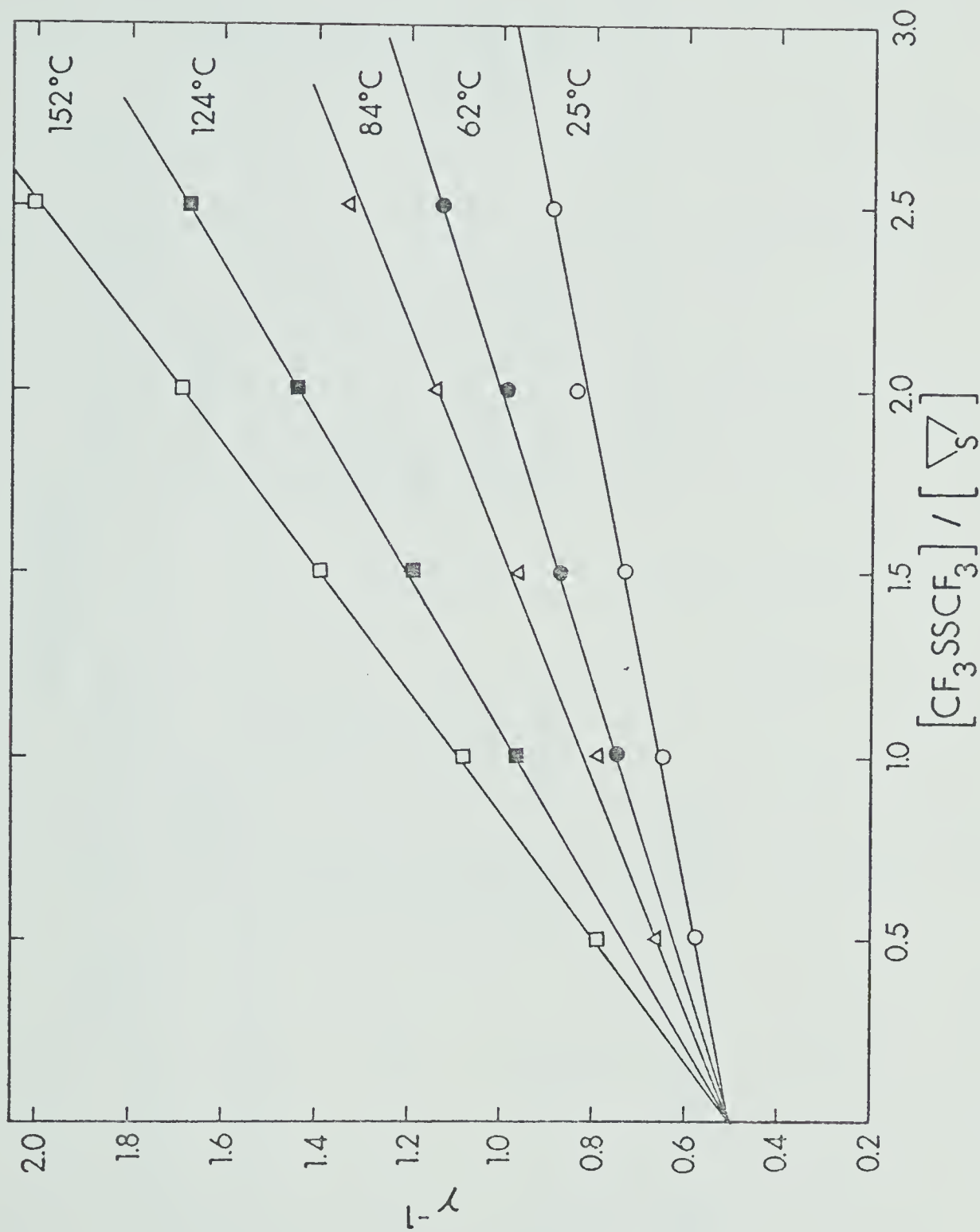


FIGURE 11. γ^{-1} versus $P[CF_3SSCF_3]/[C_2H_4S]$ at 25, 62, 84, 124 and 152°C. $P(H_2) = 580 \pm 10$ Torr; photolysis time, 45 minutes.

TABLE XXIII

Slopes and Intercepts of the Plots in Figure 11^a

T, °C	Slope	Intercept	k_3/k_4
25	0.163 ± 0.007	0.492 ± 0.0011	0.326 ± 0.014
62	0.245 ± 0.001	0.501 ± 0.001	0.489 ± 0.002
84	0.330 ± 0.010	0.485 ± 0.015	0.659 ± 0.020
124	0.472 ± 0.005	0.496 ± 0.008	0.943 ± 0.010
152	0.601 ± 0.005	0.489 ± 0.007	1.20 ± 0.010

^aThe errors are standard deviations

feature a common intercept close to the value of 0.5 predicted by Equation I, and therefore reaction (16) is probably not important in the overall scheme. The values of k_3/k_4 , also listed in Table XXIII, are plotted in the Arrhenius form in Figure 12, from which

$$\log(k_3/k_4) = (1.41 \pm 0.06) - (2604 \pm 53)/2.3RT$$

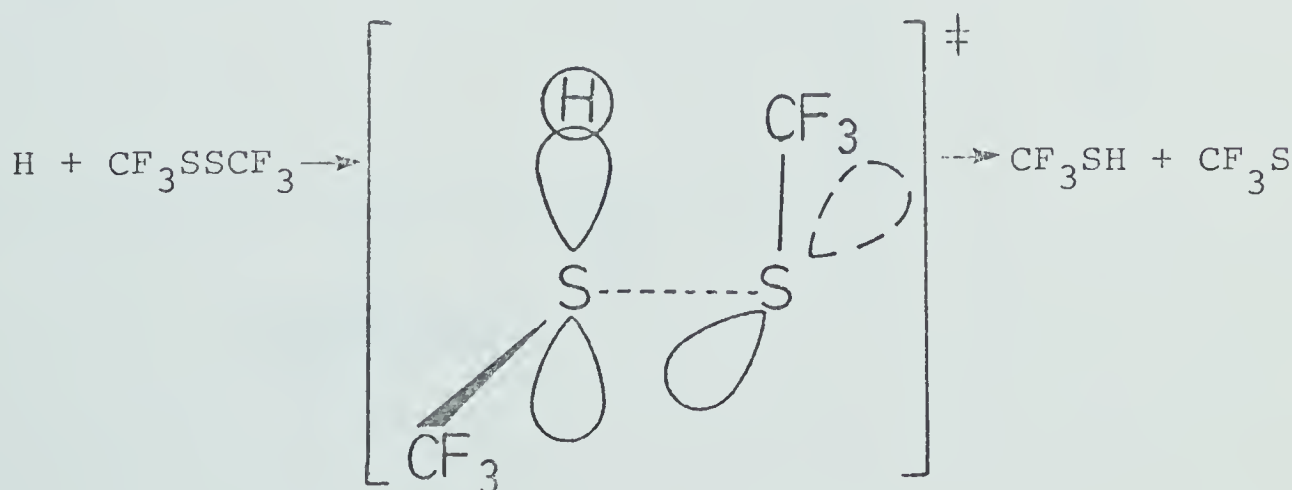
Taking the absolute rate parameters for reaction (4)¹⁰² as

$$k_4 = (1.73 \pm 0.07) \times 10^{13} \exp[-(1880 \pm 24)/RT] \text{ cm}^3 \text{ mol}^{-1} \text{ s}^{-1},$$

those for reaction (3) are:

$$k_3 = (4.45 \pm 0.20) \times 10^{14} \exp[-(4484 \pm 44)/RT] \text{ cm}^3 \text{ mol}^{-1} \text{ s}^{-1}.$$

By analogy with the other H + disulfide systems described above it is proposed that H atom attack takes place exclusively at the sulfur atom, and the complex subsequently decomposes to give trifluoromethanethiol and a trifluoromethylthiyl radical:



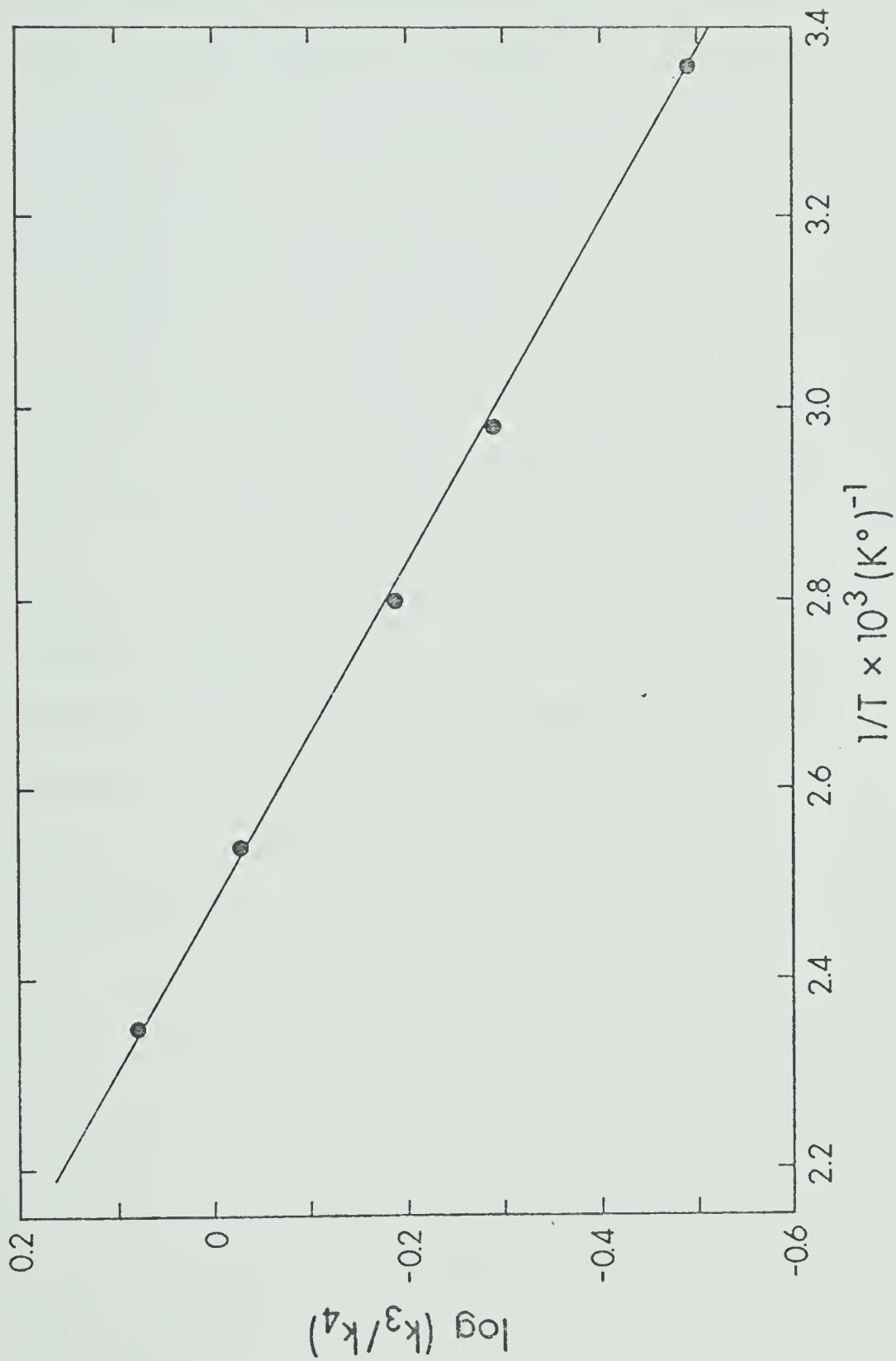


FIGURE 12. Arrhenius plot of k_3/k_4 versus $1/T$.

The higher activation energy for the $\text{H} + \text{CF}_3\text{SSCF}_3$ reaction, $4.5 \text{ kcal mol}^{-1}$, as compared to the $\text{H} + \text{CH}_3\text{SSCH}_3$ reaction, $0.1 \text{ kcal mol}^{-1}$, is a clear indication that the strongly electronegative fluorine atoms promote delocalization of the sulfur 3p orbitals. Because of this delocalization it is anticipated that CF_3SSCF_3 would not be readily amenable to attack by atoms or radicals less reactive than H atoms.

The experimental entropy of activation for the standard state of 1 atm. calculated from the A factor is -17.6 e.u. This value, as compared to $\Delta S^\ddagger = -26.2 \text{ e.u.}$ for the $\text{H} + \text{CH}_3\text{SSCH}_3$ reaction, suggests a looser transition state. This can result from steric hindrance at the sulfur atom by the CF_3 group, or, more likely, from the contributions of internal modes arising from hindered internal rotations brought about by interactions of lone pairs of electrons of fluorine atoms with the lone pair of the S atom.

CHAPTER VII

THE REACTION OF HYDROGEN ATOMS WITH DIETHYLSULFIDE

Results

When H atoms are generated by the Hg (3P_1) sensitized decomposition of H_2 in the presence of $C_2H_5SC_2H_5$, the observed products are C_2H_5SH , C_2H_6 , C_4H_{10} , C_2H_4 , $C_2H_5SCH(C_2H_5)$ (4-methyl-3-thiahexane, MTH), $C_2H_5SCH(CH_3)CH(CH_3)SC_2H_5$ (4,5-dimethyl-3,6-dithiaoctane, DMDTO), and some polymer at longer illumination times.

The sulfur-containing products were identified by comparison of the mass spectra with those of authentic materials, with the exception of DMDTO, the spectrum of which has not been reported. The mass spectrum of this compound is given in Appendix B, along with the major peak assignments. Although DMDTO was relatively volatile, its elution time was very long and consequently the peak was extremely broad and featured considerable tailing. Attempts to quantify the peak areas proved to be quite difficult and inconclusive and hence quantitative measurements were not carried out for this compound.

Control experiments at each temperature in the range 25-188°C showed that $C_2H_5SC_2H_5$ was thermally stable. The amount of quenching of the excited mercury atoms by

$C_2H_5SC_2H_5$ was estimated to be less than 5% in all the experiments.

1. Effects of exposure time and $C_2H_5SC_2H_5$ concentration.

In the first set of runs 580 Torr hydrogen was mercury photosensitized in the presence of 20 Torr $C_2H_5SC_2H_5$ for various time intervals at 25°C. The results, listed in Table XXIV, show that $\phi(C_2H_5SH) = 1.53$, independent of the time of irradiation.

In the next series of experiments the pressure of $C_2H_5SC_2H_5$ was varied between 1.0 and 30 Torr while keeping the irradiation time constant at 45 minutes. The quantum yields of C_2H_5SH , C_2H_6 , C_4H_{10} , and C_2H_4 are tabulated in Table XXV, where it is seen that they increase with increasing substrate pressure then level off above 10 Torr $C_2H_5SC_2H_5$. In this region H atoms are completely scavenged in the overall reaction. $\phi(MTH)$ was not measured because its yield at room temperature was negligibly small.

2. Effect of temperature.

The mercury sensitization of 580 Torr hydrogen in the presence of various amounts of $C_2H_5SC_2H_5$ was carried out at 25, 110, 130, 150, 167, and 170°C at a constant exposure time of 45 minutes. The results, tabulated in Table XXVI, show that the yield of ethane increases with increasing temperature, while that of butane decreases, and the ethylene yield shows only moderate temperature

TABLE XXIV

Effect of Exposure Time on $\phi(\text{C}_2\text{H}_5\text{SH})^a$

Time, min	$\text{C}_2\text{H}_5\text{SH}$		$\phi(\text{C}_2\text{H}_5\text{SH})$
	Yield (μmoles)	Rate ($\mu\text{moles min}^{-1}$) $\times 10^2$	
25	0.402 ± 0.005	0.0161 ± 0.0002	$1.53 \pm 0.02(2)^b$
35	0.566 ± 0.007	0.0162 ± 0.0002	$1.54 \pm 0.02(2)$
45	0.730 ± 0.005	0.0161 ± 0.0001	$1.53 \pm 0.01(2)$
55	0.884 ± 0.005	0.0161 ± 0.0001	$1.53 \pm 0.01(2)$
			Ave. 1.53 ± 0.03^c

^aTemperature = 25-25°C; P(H₂) = 580±10 Torr; P(C₂H₅SC₂H₅) = 20.00±0.02 Torr;

I_a ($\mu\text{einstein min}^{-1}$) $\times 10^2 = 1.06$

^bNumber of experiments

^cStandard error

TABLE XXV

Effect of P(C₂H₅SC₂H₅) on the Product Quantum Yields^a

P(C ₂ H ₅ SC ₂ H ₅) Torr	φ(C ₂ H ₆)	φ(C ₂ H ₄)	φ(C ₄ H ₁₀)	φ(C ₂ H ₅ SH)
1.00	0.421 ± 0.005	0.0625 ± 0.0030	0.276 ± 0.006	0.987 ± 0.03(2) ^b
10.00	0.630 ± 0.004	0.0982 ± 0.0025	0.407 ± 0.004	1.53 ± 0.01(2)
30.00	0.630 ± 0.005	0.0980 ± 0.0021	0.408 ± 0.005	1.53 ± 0.02(2)

^aTemperature = 25-26°C; P(H₂) = 580±10 Torr; Photolysis time = 45 min; I_a (μeinstein min⁻¹)
X 10² = 1.06.

^bNumber of experiments

TABLE XXVI

Effect of Temperature and Substrate Pressure on the Yields of Products^a

Temperature °C	P(C ₂ H ₅ SC ₂ H ₅) Torr	Yields (μmoles)			
		C ₂ H ₆	C ₂ H ₄	C ₄ H ₁₀	C ₂ H ₅ SH
170	31.6	0.721	0.054	0.094	trace
170	20.0	0.710	0.051	0.094	trace
167	10.0	0.690	0.047	0.113	trace
150	20.0	0.568	0.053	0.139	0.065
130	20.0	0.470	0.051	0.153	0.130
110	20.0	0.311	0.050	0.173	0.251
25	20.0	0.301	0.047	0.194	trace

^aP(H₂) = 580±10 Torr; I_a (μeinstein min⁻¹) x 10² = 1.06; Photolysis time = 45 min

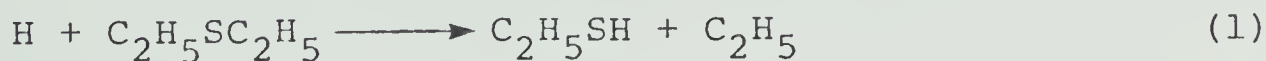
dependence. It is also seen from Table XXVI that the yield of ethanethiol increased from 0.73 to 0.96 μ moles between 25 and 110°C, after which it remained constant. The yield of MTH becomes measurable at 110°C, then decreases with increasing temperature and finally becomes negligibly small above 167°C.

3. Effect of added ethylene.

In the presence of C_2H_4 no additional products were detected but polymer formation was greatly reduced. The quantum yields of C_2H_5SH from the mercury photosensitization of 10 Torr $C_2H_5SC_2H_5$ in the presence of increasing amounts of ethylene, at 25, 96, 132, 170, and 188°C, are listed in Table XXVII. $\phi(C_2H_5SH)$ decreases with increasing ethylene pressure, owing to the competitive scavenging of H atoms by C_2H_4 .

Discussion

Since the yield of C_2H_5SH is directly proportional to exposure time, as seen in Table XXIV, this product appears to be of primary origin. By analogy with the $H + CH_3SCH_3$ reactions then, the initial step is postulated to be



followed by combination and disproportionation of C_2H_5

TABLE XXVII

Effect of C_2H_4 Pressure and Temperature on $\phi(C_2H_5SH)^a$

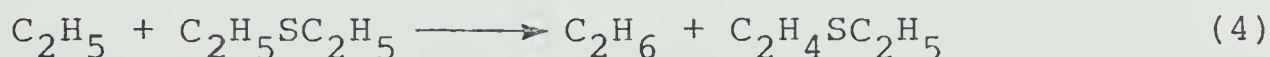
$P(C_2H_4)$ Torr	$[C_2H_4]/$ $[C_2H_5SC_2H_5]$	$\phi(C_2H_5SH)$	$1/\phi(C_2H_5SH)$
<u>25°C</u>			
0.000	0.000	1.53	0.654
0.500	0.0500	1.15	0.371
1.00	0.100	0.917	1.09
1.50	0.150	0.769	1.30
2.00	0.200	0.658	1.52
<u>96°C</u>			
0.000	0.000	2.00	0.500
0.500	0.0500	1.49	0.671
1.00	0.100	1.32	0.758
1.50	0.150	1.11	0.901
2.00	0.200	1.00	1.00
<u>132°C</u>			
0.000	0.000	2.03	0.493
0.500	0.0500	1.63	0.614
1.00	0.100	1.39	0.719
1.50	0.150	1.26	0.794
2.00	0.200	1.07	0.935
2.00	0.200	1.12	0.893
<u>170°C</u>			
0.000	0.000	2.00	0.500
0.500	0.0500	1.72	0.581
1.00	0.100	1.51	0.662
1.20	0.120	1.44	0.694
1.50	0.150	1.36	0.735
2.00	0.200	1.22	0.820
<u>188°C</u>			
0.000	0.000	2.01	0.498
1.00	0.100	1.62	0.618
2.00	0.200	1.24	0.806
3.00	0.300	1.04	0.962

^a $P(H_2) = 580$ Torr; $P(C_2H_5SC_2H_5) = 10.0$ Torr; $I_a = 1.06 \times 10^{-8}$
Einstein min^{-1} ; exposure time = 45 min.

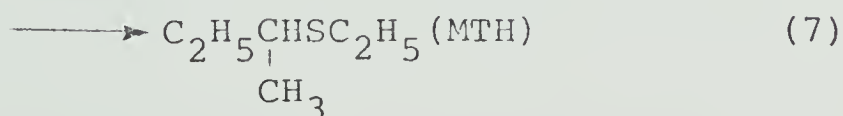
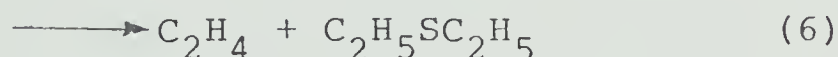
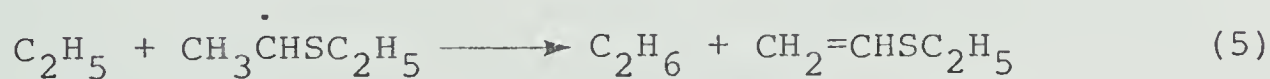
radicals:

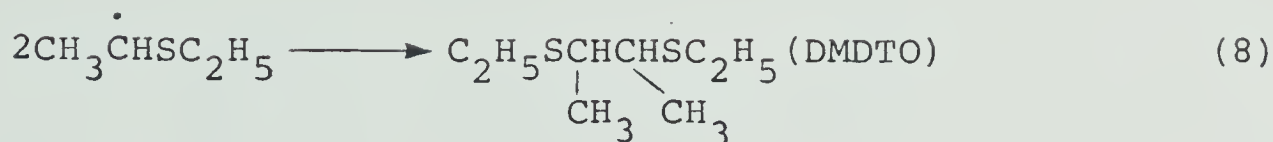


for which k_d/k_c ratios of 0.1,¹⁰³ 0.14,¹⁰⁴ and 0.2¹⁰⁵ have been reported (the latter value is almost certainly too high). If C_2H_6 is formed exclusively from step (2), our results (Table XXVI) indicate that $k_2/k_3 \sim 0.24$ at 25° and increases to 0.58 at 170°. The room temperature value is much too high and moreover, the reported temperature dependence of k_d/k_c for ethyl radicals is very small.⁹⁰ Therefore, an additional C_2H_6 -producing reaction must be occurring, i.e., abstraction from the substrate:



The site of abstraction is probably at the methylene moiety since the C-H bond here is weaker ($\sim 92 \text{ kcal mol}^{-1}$) than in the methyl group (98 kcal mol^{-1}) and moreover, MTH and DMDTO were identified among the products. A complete reaction sequence would then consist of steps (1)-(4) and (5)-(8)

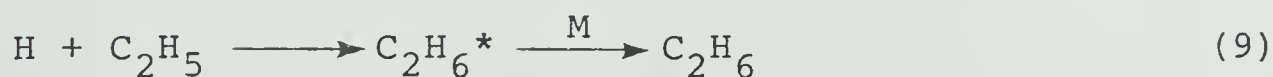




where it is seen that all the products, with the exception of $\text{C}_2\text{H}_5\text{SH}$, arise from ethyl radical reactions.

Ethylvinylthioether was not identified as a product. This may be because step (5) is relatively slow, but even if it were formed, gc analysis for ethylvinylthioether in a mixture containing large quantities of $\text{C}_2\text{H}_5\text{SC}_2\text{H}_5$ would be difficult since both compounds would probably have similar elution times. The disproportionation reactions (5) and (6) are probably inefficient but are included for the sake of completeness.

The only other reaction of ethyl radicals which might be of importance under the conditions employed is:



Although H atoms are completely scavenged in the system above 10 Torr $\text{C}_2\text{H}_5\text{SC}_2\text{H}_5$ at 25° , the results in Table XXVIII show that scavenging by $\text{C}_2\text{H}_5\text{SC}_2\text{H}_5$ itself is only complete at $\geq 110^\circ\text{C}$. Hence at room temperature an additional H-scavenging reaction, step (9), must be included in the mechanism. Kinetic considerations (*vide infra*) lend support to this conclusion.

The excess energy of C_2H_6^* is about $97.5 \text{ kcal mol}^{-1}$ ¹⁰⁶ and unless collisional stabilization takes place it will

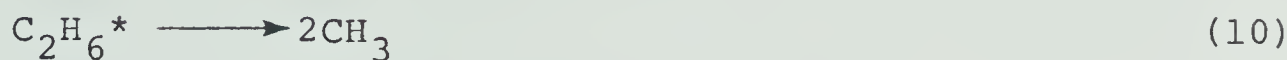
TABLE XXVIII

Effect of Temperature and Substrate Pressure on the Quantum Yields of Products^a

Temperature		ϕ				
P(C ₂ H ₅ SC ₂ H ₅)						
°C	Torr	C ₂ H ₆	C ₂ H ₄	C ₄ H ₁₀	MTH	C ₂ H ₅ SH
170	31.6	1.51	0.114	0.197	~0	2.01
170	20.0	1.49	0.107	0.197	~0	2.00
167	10.0	1.45	0.0982	0.236	~0	2.01
150	20.0	1.19	0.110	0.291	0.136	2.01
130	20.0	0.984	0.107	0.321	0.272	2.01
110	20.0	0.652	0.104	0.363	0.527	2.01
25	20.0	0.630	0.0982	0.407	~0	1.53

^aP(H₂) = 580±10 Torr; I_a (μeinstein min⁻¹) x 10² = 1.06; Photolysis time = 45 min

decompose *via* C-C cleavage,



for which $A = 1 \times 10^{17} \text{ s}^{-1}$ and $E_a = 87.4 \text{ kcal mol}^{-1}$.

From the RRK equation,

$$k_{10} = A \left(\frac{E - E_a}{E} \right)^{s-1}$$

with $s = 9$, where E is the total excess energy, E_a the critical energy required for decomposition, A the high pressure A factor, and s is usually taken to be half the normal modes in the molecule, i.e., 9 for C_2H_6 . The decomposition rate constant k_{10} is calculated to be $\sim 10^9 \text{ s}^{-1}$. However, at 580 Torr H_2 $\text{d}_{\text{C}_2\text{H}_6-\text{H}_2}$ can be estimated to be 6.3°A and since the collisional efficiency of hydrogen is about 0.2¹⁰⁶ the rate constant for collisional stabilization,

$$k_9 = d_{\text{C}_2\text{H}_6-\text{H}}^2 \times 10^{-19} N \left(\frac{8\pi kT}{\mu} \right)^{1/2} [M]$$

where k is the Boltzmann constant, N Avogadro's number, μ the reduced mass and M the concentrations of the deactivating species in moles ℓ^{-1} , is calculated to be 10^{10} s^{-1} . Therefore 91% stabilization will be achieved in the present system. The absence of CH_4 as a product constitutes additional evidence to the effect that the decomposition

of $C_2H_6^*$ is probably not significant; moreover, $\phi(C_2H_6)$ from step (9), $\phi(9)$, can be calculated from the relation

$$\phi(9) = \phi_{\text{total}}(C_2H_6) - \phi(C_2H_4) - \phi(4) \quad \text{I}$$

and from the results in Table XXVIII it is seen that

$$\phi(9) + \phi(C_2H_5SH) \sim 2.0 \quad \text{II}$$

at 25°C, as required by the mechanism, neglecting step (10).

Of all the ethyl radical reactions taking place, reaction (4), H-abstraction from the substrate, is of greatest interest. On the basis of the above mechanism the total rate of ethane formation can be expressed as:

$$R_{C_2H_6} = R_2 + R_4 + R_5 + R_9 \quad \text{III}$$

Similarly, the total initial rate of ethylene formation is

$$R_{C_2H_4} = R_2 + R_6 \quad \text{IV}$$

and assuming that $R_5 \sim R_6$, then

$$R_{C_2H_6} = R_4 + R_{C_2H_4} + R_9 \quad \text{V}$$

Since $R_9 = 0$ for $T \geq 110^\circ\text{C}$, the values of R_4 can be calculated directly from the C_2H_6 and C_2H_4 yields listed in Table XXVI. For the experiments at 25° R_9 can be calculated using equations (I) and (V). The observed and derived values of R_3 and R_4 , respectively, over the

temperature range examined are listed in Table XXIX along with those of $R_4/R_3^{1/2}$.

The Arrhenius plot of $R_4/R_3^{1/2}$, shown in Figure 13, is linear between 25° and 170°C and from the slope, $E_3/2 - E_4 = -6.9 \pm 0.1 \text{ kcal mol}^{-1}$. If E_3 is assumed to be zero, then $E_4 = 6.9 \pm 0.1 \text{ kcal mol}^{-1}$. This value seems reasonable when compared to those determined for other similar reactions, listed in Table XXX. Hydrogen abstraction from the methylene group of $C_2H_5SC_2H_5$ by ethyl radicals could be facilitated by the presence of the α -heteroatom and the rate enhancement as compared to alkane substrates can be explained in terms of stabilization of the incipient radical as a result of electron-releasing conjugative effects of the α -heteroatom, as shown below:



Comparison between the $C_2H_5 + C_2H_5SC_2H_5$ and the $C_2H_5 + C_2H_5OC_2H_5$ ¹⁰⁷ reactions shows that E_a for the former is considerably less than that for the latter. This is probably due to the greater electron releasing conjugative effects of sulfur, as a consequence of the greater physical size of sulfur and greater availability of the 3p orbital electrons. Similar considerations apply to the $C_2H_5 + C_2H_5NNC_2H_5$ ¹⁰⁸ and $C_2H_5 + C_2H_5COC_2H_5$ ¹⁰³ reactions.

TABLE XXIX

Effect of Temperature on $R_{C_2H_6/R_{C_4H_{10}}}^{1/2}$ ^a

Temperature °C	Rates, $\mu\text{moles min}^{-1}$		$R_2/R_4^{1/2}$
	$C_2H_6(R_2)$	$C_4H_{10}(R_4) \times 10^3$	
25	0.000463	4.32	0.00705
110	0.00598	3.85	0.0964
130	0.00930	3.40	0.159
150	0.0115	3.08	0.207
167	0.0143	2.50	0.286
170	0.0146	2.09	0.319
170	0.0148	2.09	0.324

^a $P(H_2) = 580 \pm 10$ Torr; $I_a (\mu\text{einstein min}^{-1}) \times 10^2$; Photolysis time = 45 min.

$[C_2H_5SC_2H_5] = 9.48 \times 10^{-4} \text{ mol}^{-1}$.

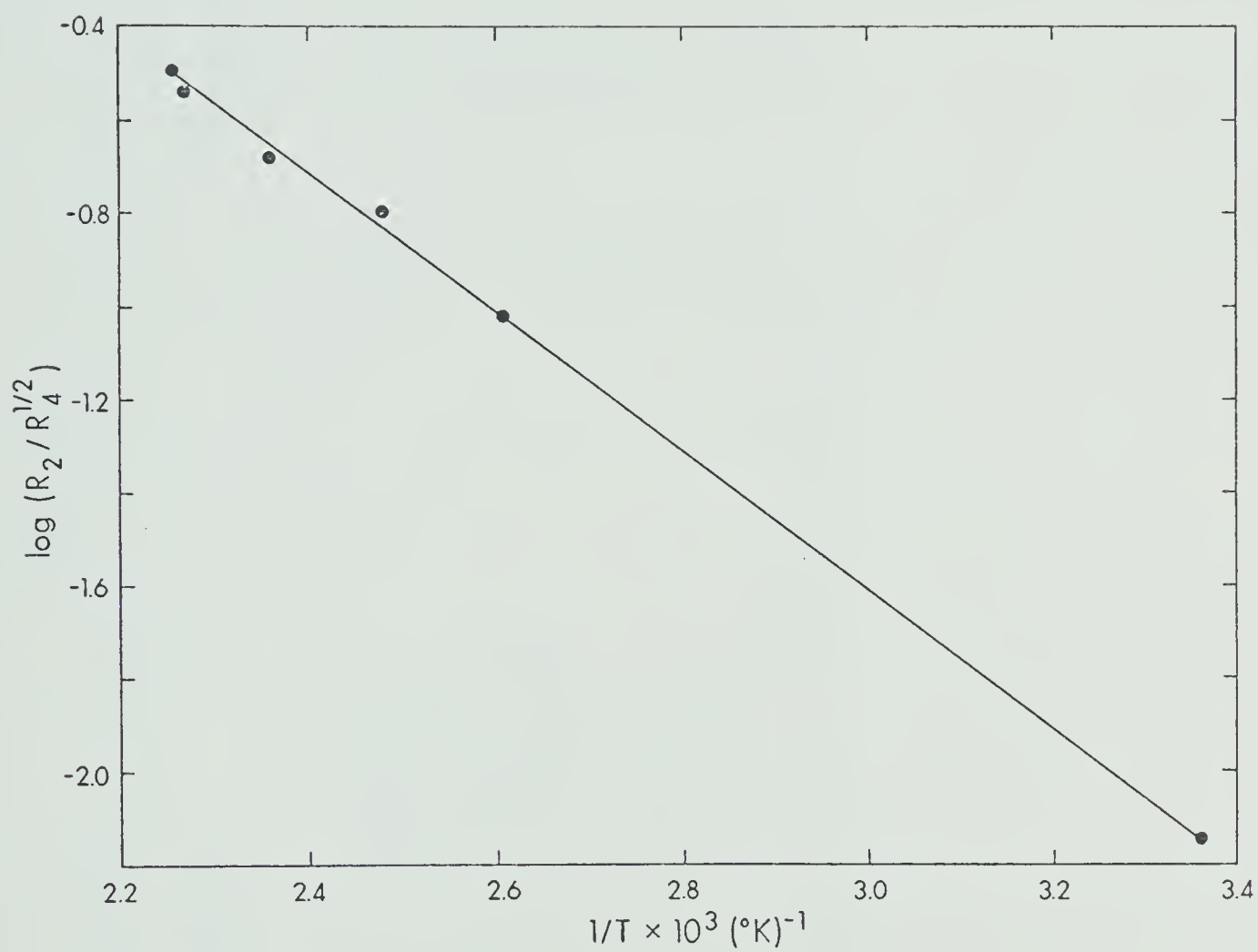


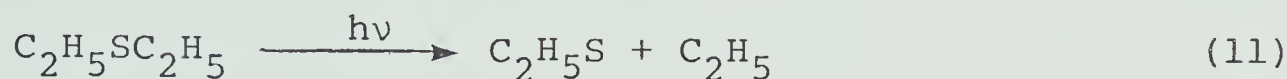
FIGURE 13. Arrhenius plot of $R_2/R_4^{1/2}$ versus $1/T$.

TABLE XXX

Activation Energies for Methylene Hydrogen Abstraction by C₂H₅ Radicals

Reaction	E _a (kcal mol ⁻¹)	Temperature Range (°C)	Method	Ref.
C ₂ H ₅ + C ₂ H ₅ OC ₂ H ₅ → C ₂ H ₆ + CH ₃ $\dot{\text{C}}\text{HOC}_2\text{H}_5$	9.0	87-218	γradiolysis	107
C ₂ H ₅ + C ₂ H ₅ COC ₂ H ₅ → C ₂ H ₆ + CH ₃ $\dot{\text{C}}\text{HCOC}_2\text{H}_5$	7.3	25-225	Photolysis	103
C ₂ H ₅ + C ₂ H ₅ NNC ₂ H ₅ → C ₂ H ₆ + CH ₃ $\dot{\text{C}}\text{HNNC}_2\text{H}_5$	7.5	30-171	Photolysis	108
C ₂ H ₅ + C ₂ H ₅ SC ₂ H ₅ → C ₂ H ₆ + CH ₃ $\dot{\text{C}}\text{HSC}_2\text{H}_5$	3.4	30-90	Photolysis	109
C ₂ H ₅ + C ₂ H ₅ SC ₂ H ₅ → C ₂ H ₆ + CH ₃ $\dot{\text{C}}\text{HSC}_2\text{H}_5$	6.9	25-170	Hg* sensitization	This work
C ₂ H ₅ + CH ₃ CH ₂ CH ₂ CH ₂ CH ₃ → C ₂ H ₆ + CH ₃ $\dot{\text{C}}\text{H}(\text{CH}_2)_3\text{CH}_3$	10.1	87-252	Photolysis	110

Our measured value of the activation energy for the $\text{C}_2\text{H}_5 + \text{C}_2\text{H}_5\text{SC}_2\text{H}_5$ reaction is twice as high as that reported by Knight and Smith¹⁰⁹ from the photolysis of ethylsulfide vapor at 2537°A ;



However, since the S-C bond strength in $\text{C}_2\text{H}_5\text{SC}_2\text{H}_5$ is 71 kcal mol^{-1} ^{32c} then at 2537°A , the reaction is exothermic by 41 kcal mol^{-1} . If the distribution of this excess energy is proportional to the number of oscillations, then $E_{\text{C}_2\text{H}_5} = 28$ and $E_{\text{C}_2\text{H}_5\text{S}} = 13 \text{ kcal mol}^{-1}$ if the energy is localized on the S-C bond and thus the low activation energy determined by them is probably due to the involvement of "hot" ethyl radicals.

ΔH values for the reactions listed in Table XXXI can be estimated from the methylene C-H bond strengths in $\text{C}_2\text{H}_5\text{SC}_2\text{H}_5$ ($\sim 92 \text{ kcal mol}^{-1}$), $\text{C}_2\text{H}_5\text{OC}_2\text{H}_5$ ($\sim 94.5 \text{ kcal mol}^{-1}$) and C_6H_{14} ($\sim 95 \text{ kcal mol}^{-1}$), and $D(\text{C-H}) = 97.5 \text{ kcal mol}^{-1}$ in C_2H_6 . These are listed in Table XXXI, along with the calculated activation energies for the reverse reactions. The latter appear to be of the right order of magnitude and exhibit a slight downward trend with increasing electrophilicity.

In the presence of ethylene, a complete reaction sequence would then include the competing reaction:

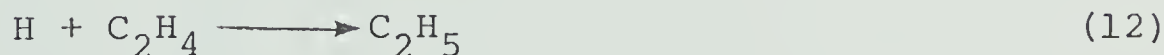
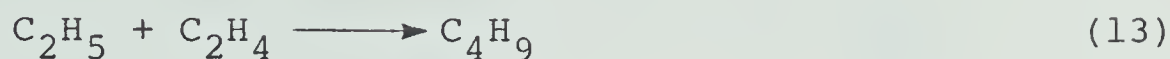


TABLE XXXI

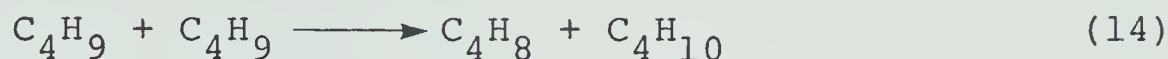
Heats of Reaction and Activation Energies for Some Metathetical Reactions
Involving C₂H₅ Radicals

Reaction	ΔH kcal mol ⁻¹	E _f kcal mol ⁻¹	E _r kcal mol ⁻¹
$\text{C}_2\text{H}_5 + \text{C}_2\text{H}_5(\text{CH}_2)_2\text{C}_2\text{H}_5 \xrightleftharpoons[\text{r}]{\text{f}} \text{C}_2\text{H}_6 + \text{CH}_3\dot{\text{C}}\text{H}(\text{CH}_2)_2\text{C}_2\text{H}_5$	-2.5	10.1	12.6
$\text{C}_2\text{H}_5 + \text{C}_2\text{H}_5\text{SC}_2\text{H}_5 \xrightleftharpoons[\text{r}]{\text{f}} \text{C}_2\text{H}_6 + \text{CH}_3\dot{\text{C}}\text{HSC}_2\text{H}_5$	-5.5	6.9	12.3
$\text{C}_2\text{H}_5 + \text{C}_2\text{H}_5\text{OC}_2\text{H}_5 \xrightleftharpoons[\text{r}]{\text{f}} \text{C}_2\text{H}_6 + \text{CH}_3\dot{\text{C}}\text{HOC}_2\text{H}_5$	-3.0	9.0	12.0

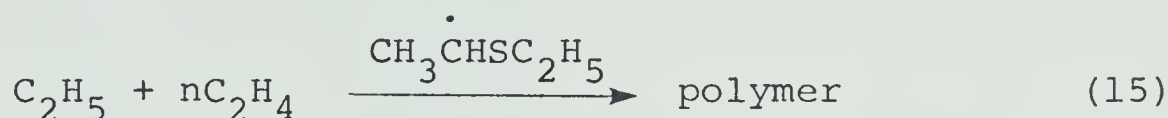
Addition of C_2H_5 to C_2H_4 , step (13),



is a relatively slow process compared with the other radical-radical reactions involving C_2H_5 , i.e., steps (2)-(7), and moreover, butene, the expected disproportionation product of C_4H_9 radicals,



was demonstrably absent. The only remaining possible reaction,



did not seem to be important since polymer formation was greatly reduced in the presence of ethylene. Steady state treatment of steps (1)-(7), (9) and (12) leads to the following rate expression:

$$\phi(C_2H_5SH)^{-1} = \frac{1}{2} \left(1 + \alpha + \frac{k_{12}[C_2H_4]}{k_1[C_2H_5SC_2H_5]} \right) \quad \text{VI}$$

where $\alpha = R_9/R_1$ and for $T \geq 110$, α is equal to zero. From the data in Table XXVII, equation VI is plotted in Figure 14. The plots are linear within the temperature range examined and feature a common intercept of 0.5 in the range 96-188°C, Table XXXII. These results substantiate our earlier suggestion that reaction (9) is important

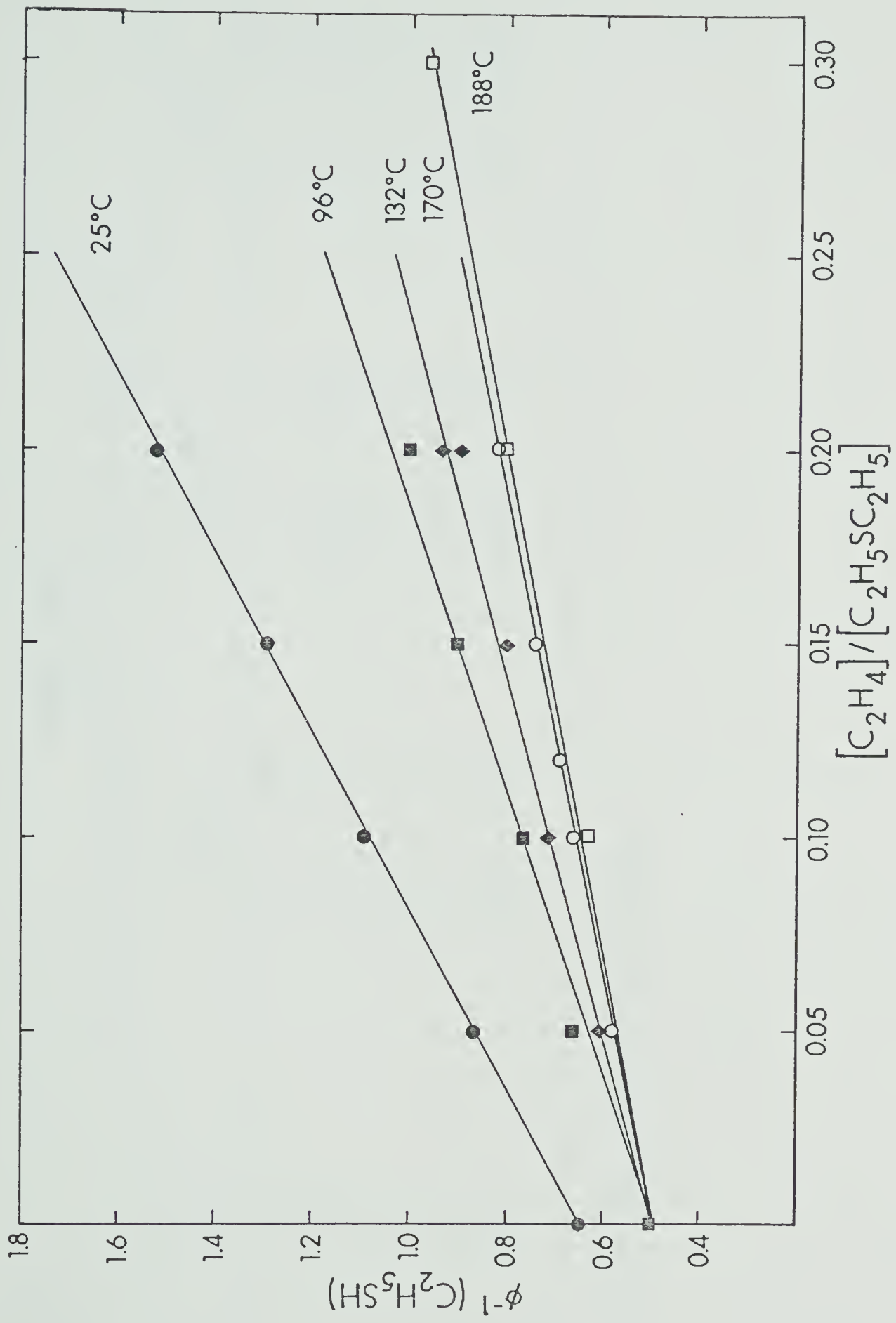


FIGURE 14. $\phi(\text{C}_2\text{H}_5\text{SH})^{-1}$ versus $\text{P}[\text{C}_2\text{H}_4]/\text{P}[\text{C}_2\text{H}_5\text{SC}_2\text{H}_5]$ at 25, 96, 132 and 170 and 188°C.

TABLE XXXII

Slopes and Intercepts of the Plots in Figure 14^a

T, °C	slope	Intercept	k_{16}/k_1
25	4.31 ± 0.01	0.655 ± 0.001	8.61 ± 0.01
96	2.46 ± 0.10	0.502 ± 0.002	4.92 ± 0.07
132	2.05 ± 0.10	0.502 ± 0.010	4.10 ± 0.07
170	1.59 ± 0.02	0.501 ± 0.002	3.18 ± 0.01
188	1.51 ± 0.10	0.501 ± 0.003	3.02 ± 0.07

^aThe errors are standard deviations.

only at room temperature. At 25°C however the intercept is 0.66 and therefore $\alpha = 0.32$, in agreement with the calculated ratio $\phi(9)/\phi(1) = 0.47/1.53 = 0.31$ using equation I.

The slopes of the plots, listed in Table XXXII, are plotted in the Arrhenius form in Figure 15 from which the value of the rate coefficient ratio is

$$\log(k_{12}/k_1) = -(0.357 \pm 0.035) + (1.768 \pm 60)/2.30 \text{ RT}$$

Accepting Michael and coworkers' value for the limiting high pressure rate parameter for step (12)⁸⁹ as

$$k_{12} = (2.2 \pm 0.4) \times 10^{13} \exp[-(2066 \pm 83)/RT] \text{ cm}^3 \text{ mol}^{-1} \text{ s}^{-1}$$

those for step(1) are

$$k_1 = (2.28 \pm 0.4) \times 10^{13} \exp[-(3834 \pm 41)/RT] \text{ cm}^3 \text{ mol}^{-1} \text{ s}^{-1}$$

Of all the substrates examined in the present investigation, $\text{C}_2\text{H}_5\text{SC}_2\text{H}_5$ would have been the most amenable to abstractive attack, but such does not seem to be the case. Instead, attack appears to take place exclusively at the sulfur atom, and the complex subsequently decomposes to give ethanethiol and an ethyl radical.

The experimental entropy of activation for the standard state of 1 atm, calculated from the A factor, is -23.5 e.u. This value, as compared to $\Delta S^\ddagger = -24.1$ e.u.

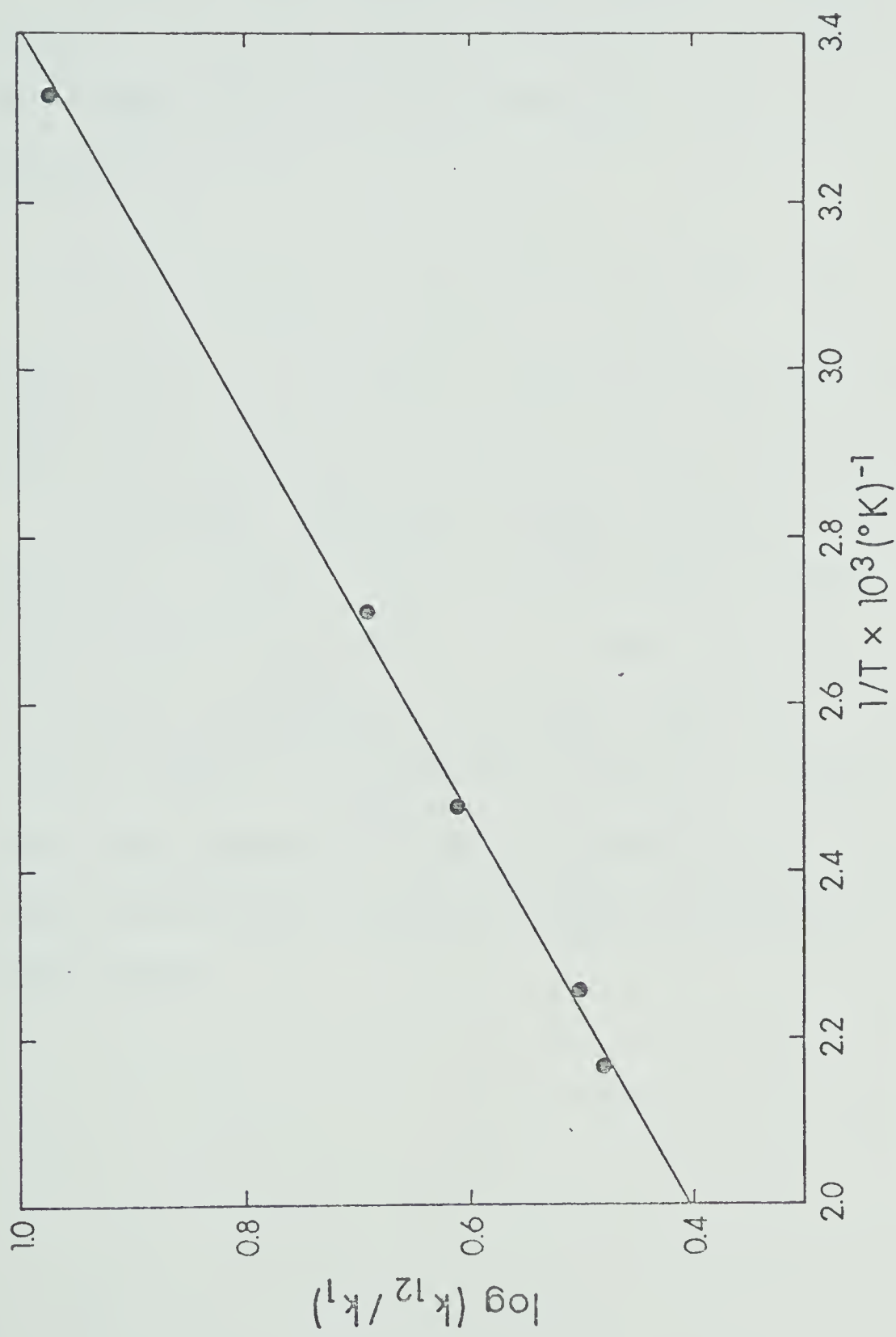


FIGURE 15. Arrhenius plot of k_{12}/k_1 versus $1/T$.

for the $\text{H} + \text{CH}_3\text{SCH}_3$ reaction, suggests that the transition state for the $\text{H} + \text{C}_2\text{H}_5\text{SC}_2\text{H}_5$ reaction is similar to that of the $\text{H} + \text{CH}_3\text{SCH}_3$ reaction.

Indeed, the value of the A factor for the $\text{H} + \text{C}_2\text{H}_5\text{SC}_2\text{H}_5$ reaction can be reproduced by assuming a transition state similar to that proposed for the $\text{H} + \text{CH}_3\text{SCH}_3$ system,⁴⁰



which involves an initial interaction between the H atom and the non-bonding 3p orbital of the sulfur atom.

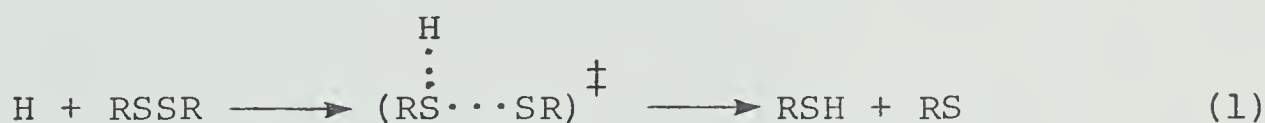
The higher activation energy for the $\text{H} + \text{C}_2\text{H}_5\text{SC}_2\text{H}_5$ reaction, $3.8 \text{ kcal mol}^{-1}$, as compared to the $\text{H} + \text{CH}_3\text{SCH}_3$ reaction, $2.6 \text{ kcal mol}^{-1}$, is a clear indication that the C-S bond in $\text{C}_2\text{H}_5\text{SC}_2\text{H}_5$ is stronger than that in the CH_3SCH_3 : indeed, values of 71 and 70 kcal mol^{-1} , respectively, have been reported.^{32c} This is probably due to the greater hyperconjugative effects of methylene hydrogens in the ethyl group.

CHAPTER VIII

SUMMARY AND CONCLUSIONS

The gas phase reactions of hydrogen atoms, generated by the $\text{Hg}(^3\text{P}_1)$ sensitization of hydrogen, with dimethyldisulfide, diethyldisulfide, ethylmethyldisulfide, bis(trifluoromethyl)disulfide and diethylsulfide have been examined at room and moderately elevated temperatures.

With dialkyldisulfides, thiols are the only retrievable products and solid polymer formation was observed. From the effects of exposure time, light intensity and concentration, it is concluded that H atoms attack disulfides exclusively at one of the sulfur atoms, thereby displacing a thiyl radical:



Hydrogen abstraction, even from the relatively weak methylenic C-H of $\text{C}_2\text{H}_5\text{SSC}_2\text{H}_5$ appears to be an unimportant process. In the presence of ethylene, compounds of the type, $\text{CH}_3\text{SC}_2\text{H}_5$ and $\text{C}_2\text{H}_5\text{SC}_2\text{H}_5$ were found to be major products, a clear indication of the intermediacy of thiyl radicals in these systems.

With the unsymmetrical disulfide, $\text{CH}_3\text{SSC}_2\text{H}_5$, formation of CH_3SSCH_3 and $\text{C}_2\text{H}_5\text{SSC}_2\text{H}_5$ were observed in high yields along with CH_3SH and $\text{C}_2\text{H}_5\text{SH}$. These are formed in a chain

reaction involving metathetical $\text{C}_2\text{H}_5\text{S}$ and CH_3S displacement reactions. The initial ratio of the quantum yields $\phi(\text{CH}_5\text{SH})/\phi(\text{C}_2\text{H}_5\text{SH})$ is 1.86, identical to the rate constant for the $\text{H} + \text{CH}_3\text{SSCH}_3$ and $\text{H} + \text{C}_2\text{H}_5\text{SSC}_2\text{H}_5$ reactions.

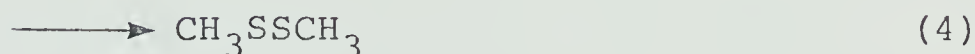
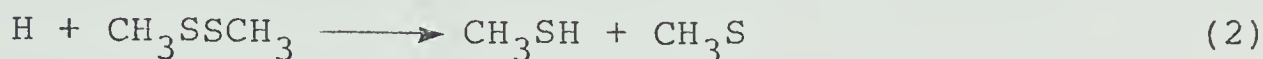
Polymerization is the only observable result of the $\text{H} + \text{CF}_3\text{SSCF}_3$ reaction. However, it was shown that CF_3SH , the expected primary product, cannot be detected in the presence of CF_3SSCF_3 , possibly because of strong hydrogen bonding associations. That reaction had taken place was deduced from the following observations:

1. polymer formation was apparent.
2. in competitive experiments with $\text{C}_2\text{H}_4\text{S}$, the C_2H_4 yields from the $\text{H} + \text{C}_2\text{H}_4\text{S}$ reaction decreased with increasing CF_3SSCF_3 concentration.
3. in the presence of C_2H_4 , $\text{CF}_3\text{SC}_2\text{H}_5$ was found to be a major product, pointing to the intermediacy of CF_3S radicals.

By analogy with the other $\text{H} +$ disulfide reactions studied here, and since F abstraction requires a very high activation energy, it is concluded that the primary process in the $\text{H} + \text{CF}_3\text{SSCF}_3$ reaction is also a metathetical displacement reaction, i.e., (1).

Although the $\text{H} + \text{RSSR}$ reactions ($\text{R} = \text{CH}_3, \text{C}_2\text{H}_5, \text{CF}_3$) feature a common primary process, some differences are apparent in the ensuing secondary reactions.

For the $\text{H} + \text{CH}_3\text{SSCH}_3$ reaction $\phi(\text{CH}_3\text{SH}) = 2.1$, independent of temperature up to 120° . Thus, the following simple mechanism applies



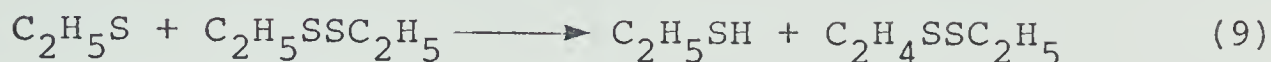
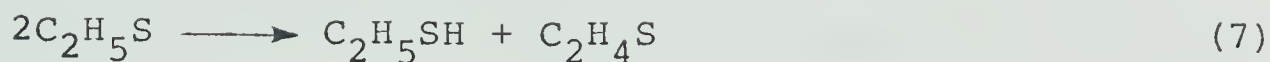
and abstraction from the substrate,



is apparently not important. On the basis of thermochemical considerations it can be estimated that $E_5 \sim 8.6 \text{ kcal mol}^{-1}$ and hence this reaction cannot compete with disproportionation and combination, both of which proceed with very little or no activation energy. From the reported value of $k_3/k_4 \sim 0.05$, $\phi(2) \sim 2.0$, as required by the mechanism.

With diethyldisulfide however, $\phi(\text{C}_2\text{H}_5\text{SH})$ varies from 2.32 at 25° to 2.84 at 145°C . Since, by analogy with CH_3S radicals, the rate of disproportionation of $\text{C}_2\text{H}_5\text{S}$ radicals should be temperature independent, this can only mean that the abstractive route to thiol formation is operative. The major reactions occurring are then





From the reported value of $k_7/k_8 = 0.13$, the quantum yield for reaction (9) could be calculated at each temperature and from kinetic analysis of the results, $E_9 \sim 3.6 \text{ kcal mol}^{-1}$. This is substantially lower than that estimated for abstraction from CH_3SSCH_3 by CH_3S radicals and hence in this system reaction (9) can compete with reactions (7) and (8).

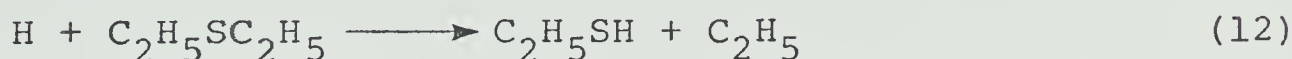
The $\text{H} + \text{C}_2\text{H}_5\text{SSCH}_3$ reaction proved to be more complex since, in addition to disproportionation, combination and hydrogen abstraction, the CH_3S and $\text{C}_2\text{H}_5\text{S}$ radicals generated in the primary process undergo thiyl radical displacement reactions with the substrate, thus generating a long chain:



Chain termination was assumed to take place *via* radical-radical combination and disproportionation. The quantum yields of the symmetrical disulfides were equal and time dependent, the extrapolated value at zero exposure time being 92. Those for CH_3SH and $\text{C}_2\text{H}_5\text{SH}$ changed only

moderately with time and $\phi(\text{CH}_3\text{SH})/\phi(\text{C}_2\text{H}_5\text{SH})$ at $t = 0$ was 1.86. A mechanism consisting of 15 elementary steps was tested by computer modeling using the algorithm DIFSUB.¹¹¹ Although rate constants for the reactions of thiyl radicals with alkyldisulfides are not known, reasonable estimates could be arrived at such that the simulated variation in $\phi(\text{CH}_3\text{SSCH}_3)$ was in good agreement with the experimentally observed trend.

The $\text{H} + \text{C}_2\text{H}_5\text{SC}_2\text{H}_5$ system was also investigated, not only in order to complement the $\text{H} + \text{CH}_3\text{SCH}_3$ reaction examined recently, but to ascertain whether higher alkyl substituents might render hydrogen abstraction more competitive. No evidence, however could be adduced for the occurrence of this reaction and the only primary process of significance is ethyl radical displacement.



The various ensuing reactions of C_2H_5 radicals confer some complexity on this system. Thus, in addition to combination and disproportionation, C_2H_5 abstracts from the substrate, probably at the methylenic site:



and a complete mechanism featuring disproportionation and combination of C_2H_5 and $\text{C}_2\text{H}_4\text{SC}_2\text{H}_5$ radicals was

considered. It was also observed that the $\text{H} + \text{C}_2\text{H}_5$ combination reaction is important at room temperature. From kinetic analysis of the results E_{13} was found to have the value $6.9 \pm 0.1 \text{ kcal mol}^{-1}$. This value is quite low compared to abstraction from other methylenic sites by C_2H_5 radicals and is believed to be a consequence of enhanced stabilization of the incipient radical due to the superior conjugation properties of sulfur.

Arrhenius parameters for the $\text{H} + \text{CH}_3\text{SSCH}_3$, $\text{C}_2\text{H}_5\text{SSCH}_3$ and $\text{C}_2\text{H}_5\text{SC}_2\text{H}_5$ reactions were determined in competitive experiments employing C_2H_4 , since the rate parameters for the competing reaction:



have been well established. For the $\text{H} + \text{CF}_3\text{SSCF}_3$ system the reference was the $\text{H} + \text{thiirane}$ reaction:

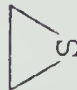


The resulting activation energies and A factors are summarized in Table XXXIII, along with the exothermicities for the overall reactions, calculated from the data in Table II. Corresponding values for the $\text{H} + \text{COS}$, $\text{C}_2\text{H}_4\text{S}$ and CH_3SCH_3 reactions are also included for the sake of comparison.

Many years ago, Evans and Polanyi¹¹² noted that, for exothermic reactions of Na atoms and CH_3 radicals

TABLE XXXIII

Arrhenius Parameters and Heats of Reaction for H Atom Reactions with Organosulfur Compounds

Reaction	A cm ³ mol ⁻¹ s ⁻¹	E _a kcal mol ⁻¹	ΔH _f ^o kcal mol ⁻¹	ΔS [‡] e.u.		Reference
				expt.	calc	
H + CH ₃ SSCH ₃	5.7x10 ¹²	0.1	-21.0	-26.2	-26.0	This work
H + C ₂ H ₅ SSC ₂ H ₅	4.7x10 ¹³	1.7	-19.5	-22.0	-26.0	This work
H + CH ₃ SCH ₃	1.7x10 ¹³	2.6	-18.0	-24.1	-24.6	40
H + C ₂ H ₅ SC ₂ H ₅	2.3x10 ¹³	3.8	-17.5	-23.5	-24.6	This work
H + CF ₃ SSCF ₃	4.4x10 ¹⁴	4.5	-16.5 ^a	-17.6	-26.0	This work
H + 	5.7x10 ¹³	1.9	-24.3	-19.7	-24.6	37
H + O=C=S	9.1x10 ¹²	3.9	-10.3	-23.4	-25.4	38
H + CH ₃ SSC ₂ H ₅	-	-	-20.2 ^b	-	-	This work

^aExtrapolated from Figure 16.

^bAverage value estimated from ΔH_f^o values for H + CH₃SSCH₃ and C₂H₅SSC₂H₅.

with a homologous series of molecules, an empirical relationship of the form

$$E_a = A + \alpha \Delta H$$

was often obeyed. Semenov¹¹³ showed that the reactions of H, D and OH with selected classes of compounds also follow this trend. Typically, values of α range between 0.2 and 0.4, and the A values only differed by a small amount, 10-15 kcal, among the various atoms and radicals examined. Hence, for the cases examined, the predominant factor governing the magnitude of E_a is ΔH .

The plot of E_a versus ΔH for the H + COS, C₂H₄S, CH₃SCH₃, C₂H₅SC₂H₅, CH₃SSCH₃ and C₂H₅SSC₂H₅ reactions, is illustrated in Figure 16. The alkyl sulfides and disulfides follow a linear relationship of the form

$$E_a = 0.9 \Delta H + 19.36 \text{ kcal mol}^{-1}$$

from which E_a for the H + C₂H₅SSCH₃ reaction is predicted to be 0.9-1.4 kcal mol⁻¹. This is a reasonable value, being intermediate between those for the corresponding symmetrical disulfides. COS and C₂H₄S do not follow the above trend, as expected, since desulfurization takes place with these substrates. For H + CF₃SSCF₃ reaction with $E_a = 4.5 \text{ kcal mol}^{-1}$, if H atom is assumed to attack S atom, then $\Delta H \sim 16.5 \text{ kcal mol}^{-1}$.

The experimental entropies of activation, calculated from the A factors, also listed in Table XXXIII, are

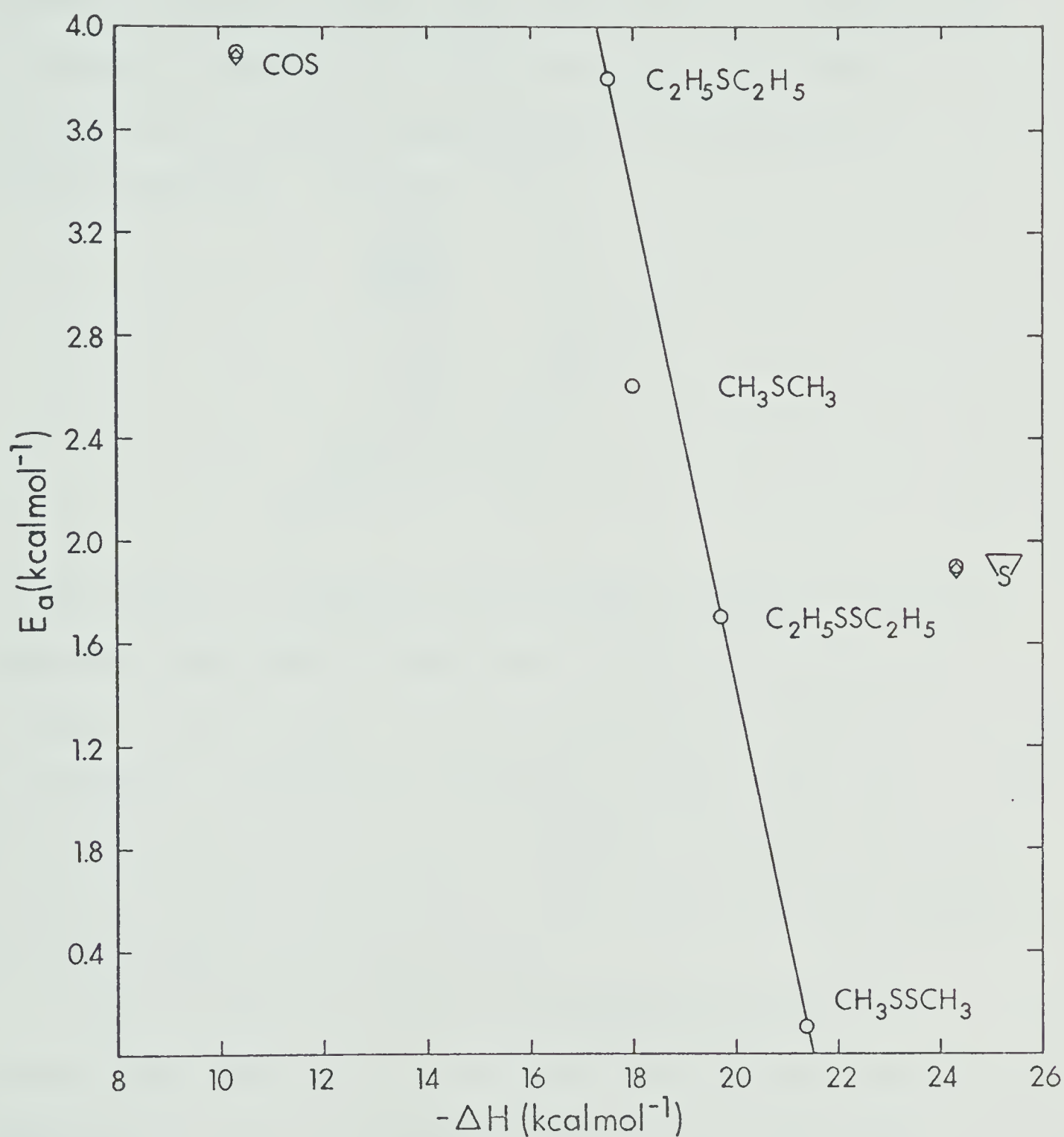
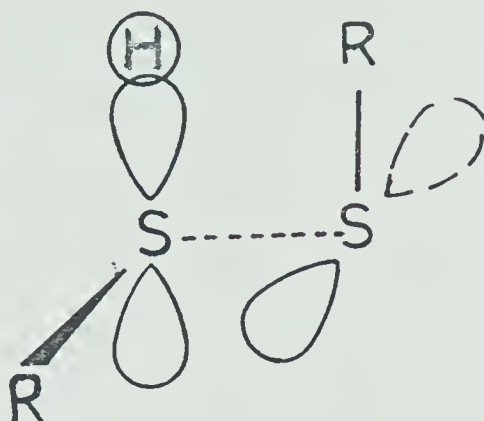


FIGURE 16. Plot of an empirical relationship for activation energies: $E_a = 0.9\Delta H + 19.36$ for the reaction series $\text{H} + \text{CH}_3\text{SSCH}_3$, $\text{C}_2\text{H}_5\text{SSC}_2\text{H}_5$, CH_3SCH_3 and $\text{C}_2\text{H}_5\text{SC}_2\text{H}_5$.

consistently high and negative, suggesting a "tight" transition state. It was shown that good agreement could be obtained between the experimental and calculated entropies of activation if the transition state was assumed to be a rigid complex wherein H attacks the sulfur lone pair orbital, e.g.,



For the case of $\text{C}_2\text{H}_5\text{SSC}_2\text{H}_5$ and CF_3SSCF_3 hindered internal rotations give rise to additional contributions to the entropy; in the former, this is probably due to the possibility of hydrogen bonding with one of the S 3p orbitals in the *gauche-gauche* conformation and in the latter, to interactions between the lone pairs of electrons on the fluorine and sulfur atoms.

The activation energies associated with the H + alkylsulfide reactions are somewhat higher than those required by the H + alkyldisulfide reactions and this is entirely due to the difference between the C-S and S-S bond strengths. On the other hand, E_a for the CF_3SSCF_3 reaction is substantially higher and this is

undoubtedly due to delocalization of the 3p sulfur orbitals by the electron-withdrawing fluorine atoms.

The room temperature rate constants for the reactions of H, O, S, OH, CH₃, CF₃, CH₃S and C₂H₅ with sulfides and disulfides are summarized in Table XXXIV and the Arrhenius parameters, where available, in Table XXXV. Although the data available to date are rather limited, some interesting features are worthy of note.

Firstly, OH radicals appear to be the most reactive of the species examined. This is not unusual however since the primary process is electron transfer, which is known to be rapid.

Oxygen and sulfur atoms appear to be more reactive than hydrogen atoms and the low and, for oxygen, occasionally negative activation energies associated with attack on C₂H₄S and CH₃SCH₃, Table XXXV, point to the electrophilic nature of the interaction. The values for CH₃S and C₂H₅S radicals, derived from the simulations, are approximately two orders of magnitude lower than those for hydrogen atoms and this may be due to delocalization of the unpaired orbital. The data available to date indicate that CH₃ radical attack at the sulfur atom of organosulfur molecules is very slow: The most reasonable explanation for this is a thermochemical one, i.e., the new C-S bond formed in the CH₃ + CH₃SSCH₃ reaction

TABLE XXXIV

Rate Constants for Atom or Radical Attack on the Sulfur Atom of Sulfides and Disulfides^a

No.	Compound	H	O	S	OH	CH ₃ ^b	CH ₃ S	C ₂ H ₅ S
1	COS	1.25x10 ^{10b}	6.69x10 ^{9f}	7.2x10 ^{11h}		1.80x10 ^{3k}		
2	C ₂ H ₄ S	2.30x10 ^{12c}	7.61x10 ^{12g}	1.4x10 ¹³ⁱ		8.41x10 ^{5k}		
3	CH ₃ SCH ₃	2.11x10 ^{11d}	2.92x10 ^{13g}					
4	C ₂ H ₅ SC ₂ H ₅	3.76x10 ^{10e}			1.7x10 ^{13j}	~3x10 ^{7m}		3.12x10 ^{10e}
5	CH ₃ SSCH ₃	4.90x10 ^{12e}			1.4x10 ^{13j}		1.94x10 ^{10e}	
6	C ₂ H ₅ SSC ₂ H ₅	2.63x10 ^{12e}					1.40x10 ^{10e}	7.78x10 ^{9e}
7	CH ₃ SSC ₂ H ₅	4.90x10 ^{12e}						
8	CF ₃ SSCF ₃	2.29x10 ^{11e}						
9	(<i>i</i> -C ₃ H ₇) ₂ S ₂				2.0x10 ^{13j}			
10	(<i>t</i> -C ₄ H ₉) ₂ S ₂				6.5x10 ^{12j}			

^aIn cm³ mol⁻¹ s⁻¹ units at 25°; ^bRef. 37; ^cRef. 38; ^dRef. 40; ^eThis work; ^fRef. 114;

^gRef. 48; ^hRef. 45; ⁱRef. 52; ^jRef. 60; ^kRef. 54; ^lRef. 54; ^mRef. 59.

TABLE XXXV

Arrhenius Parameters for Atom or Radical Reactions with Sulfides and Disulfides^a

No.	Compound	H		O		S		CH ₃ ^b	
		A	E _a	A	E _a	A	E _a	A	E _a
1	COS	9.1x10 ^{12b}	3.9 ^b	1.2x10 ^{14f}	5.80 ^f			3.80x10 ¹¹ⁱ	11.4 ⁱ
2	C ₂ H ₄ S	5.7x10 ^{13c}	1.9 ^c	8.1x10 ^{12g}	0.04 ^g	2.2x10 ^{13h}	~0 ^h	2.25x10 ¹¹ⁱ	6.7 ⁱ
3	CH ₃ SCH ₃	1.7x10 ^{13d}	2.6 ^d	8.6x10 ^{12g}	-0.7 ^g				
4	C ₂ H ₅ SC ₂ H ₅	2.3x10 ^{13e}	3.8 ^e						
5	CH ₃ SSCH ₃	5.7x10 ^{12e}	0.1 ^e						
6	C ₂ H ₅ SSC ₂ H ₅	4.7x10 ^{13e}	1.7 ^e						
7	CF ₃ SSCF ₃	4.5x10 ^{14e}	4.5 ^e						

^aFor attack on sulfur; A in cm³ mol⁻¹ s⁻¹ and E_a in kcal mol⁻¹; ^bRef. 37; ^cRef. 38; ^dRef. 40; ^eThis work; ^fRef.115; ^gRef. 48; ^hRef. 53; ⁱRef. 54.

is considerably weaker than the S-H bond formed in the $\text{H} + \text{CH}_3\text{SSCH}_3$ reaction, thus lowering the exothermicity.

The present results provide a rationale for the well documented observation that hydrodesulfurization of petroleums produces large quantities of volatile, sulfur-containing material. It is hoped that future studies will be directed towards the elucidation of the reactions of hydrogen atoms with thiophenic substrates in order to set up a suitable data base for computer simulation of this vital yet little understood process.

BIBLIOGRAPHY

1. T.Y. Liu in "The Proteins", H. Neurath, Editor, Vol III, 3rd ed., Academic Press, New York, 1975, pp 240-382.
2. A. Meister in "The Enzymes", P.D. Boyer, Editor, Vol X, 3rd ed., Academic Press, New York, 1970, pp 671-695.
3. R.A. Dean and E.V. Whitehead, "Status of Work in Separation and Identification of Sulfur Compounds in Petroleum and Shale Oil", 7th World Petrol. Cong.: Panel Discussion 23, Paper 7, 1967.
4. H.T. Rall, C.J. Thompson, H.J. Coleman, and R.L. Hopkins, "Sulfur Compounds in Crude Oil", U.S. Bureau of Mines Bull. 659, 1972.
5. W.L. Orr in "Oil Sand and Oil Shale Chemistry", O.P. Strausz and E.M. Lown, Editors, Verlag Chemie, New York, 1978, pp. 224-231; Y. Kawaguchi, I.G. Dalla Lana and F.D. Otto, Can. J. Chem. Eng., 56, 65 (1978).
6. W.A. Pryor, "Mechanism of Sulfur Reactions", McGraw-Hill, New York, 1962, pp. 16-70.
7. L. Field in "Organic Chemistry of Sulfur", S. Oae, Editor, Plenum Press, New York, 1977, pp. 303-382.
8. E.C. Kooymann, Pure Appl. Chem., 15, 81 (1967).
9. (a) W.A. Pryor and H. Guard, J. Am. Chem. Soc., 86, 1150 (1964); (b) W.A. Pryor and P.K. Platt, J. Am. Chem. Soc., 85, 1496 (1963).
10. B. Beagley u.K.T. McAloon, Trans. Faraday Soc., 67, 3216 (1971).

11. D. Sutter, H. Dreizler, and H.D. Rudolph, Z. Naturforsch., 20a, 1676 (1965).
12. R. Steudel, Angew. Chem. Internat. Edit., 14, 655 (1975); A. Yokozeki and S.H. Bauer, J. Phys. Chem., 88, 618 (1975).
13. Reference 6, pp. 16-27.
14. O. Foss in "Organic Sulfur Compounds", N. Kharasch, Editor, Vol. 1, Pergamon Press, New York, 1961, pp. 75-82.
15. M.E. Van Wart, L.L. Shipman, and H.A. Scheraga, J. Phys. Chem., 78, 1848 (1974); D.B. Boyd, J. Phys. Chem., 78, 1554 (1974).
16. H.E. Van Wart, F. Cardinaux and H.A. Scheraga, J. Phys. Chem., 80, 625 (1975).
17. G. Bergson, G. Claeson and L. Schotte, Acta Chem. Scand., 16, 1159 (1962); see also Reference 15.
18. G. Wagner and H. Bock, Chem. Ber., 107, 68 (1974); R.J. Colton and J.W. Rabalais, J. Electron Spectrosc. Relat. Phenom., 3, 345 (1974); A.D. Baker, M. Brisk, and M. Gellender, J. Electron Spectrosc. Relat. Phenom., 3, 227 (1974).
19. W.G. Penny and G.M. Sutherland, J. Chem. Phys., 2, 492 (1934); L. Pauling, Proc. Nat. Acad. Sci., 35, 495 (1949); L.S. Levitt and C. Párkányi, Int. J. Sulfur Chem., 8, (1973).
20. Reference 7, pp. 345-370.

21. E.E. Reid, "Organic Chemistry of Bivalent Sulfur", Vol. III, Chemical Publishing Co., New York, 1960, pp. 362-462.
22. W.E. Savige and J.A. Maclaren in "Organic Sulfur Compounds", N. Kharasch, Editor, Vol. 2, Pergamon Press, New York, 1966, pp. 367-402.
23. O. Foss in Reference 14, pp.83-96; E. Block, Quart. Rep. Sulfur Chem., 4, 237 (1969).
24. L. Haraldson, C.J. Olander, S. Sunner and E. Varde, Acta Chem. Scand., 14, 1509 (1960) and references therein.
25. J.D. Coyle, Chem. Soc. Rev., 4, 523 (1975).
26. W. Tagaki in "Organic Chemistry of Sulfur", S. Oae, Editor, Plenum Press, New York, 1977, pp. 231-302.
27. S.D. Thompson, D.G. Carroll, F. Watson, M. O'Donnell, and S.P. McGlynn, J. Chem. Phys., 45, 1367 (1966).
28. (a) Y. Shiro, M. Ohsaku, M. Hayashi and H. Murata, Bull. Chem. Soc. Jpn., 43, 609 (1970); M. Ohsaku, Y. Shiro and H. Murata, *ibid*, 45, 113, 956 (1972);
(b) D.W. Scott and J.P. MacGullough, J. Am. Chem. Soc., 80, 3554 (1958); D.W. Scott and M.Z. El-Sabban, J. Mol. Spectrosc., 30, 317 (1969).
29. T. Matsushita, Y. Osamura, N. Misawa, K. Nishimoto, and Y. Tsuno, Bull. Chem. Soc. Jpn., 52, 2521 (1979).
30. F.G. Bordwell, H.M. Anderson and B. Pitt, J. Am. Chem. Soc., 76, 1082 (1954).

31. J. Deganin and R. Fochi, Boll. Sci. Fac. chim. Ind. Bologna, 22, 7 (1964).
32. (a) H. Mackle, and P.A.G. O'Hare, Tetrahedron, 19, 961 (1963); (b) S.W. Benson, "The Foundations of Chemical Kinetics", McGraw-Hill, Toronto, 1960; (c) H. Mackle, Tetrahedron, 19, 1159 (1963).
33. D.E. Nagel, R.S. Julian, and J.R. Zacharias, Phys. Rev., 72, 971 (1947); K.R. Jennings and J.W. Linnett, Nature (London), 182, 597 (1959).
34. H.W. Melville and J.C. Robb, Proc. Roy Soc. Ser. A, 196, 445, 466, 479, 494 (1949); K.R. Jennings and R.J. Cvetanovic, J. Chem. Phys., 35, 1233 (1961); R.J. Cvetanovic, and L.C. Doyle, J. Chem. Phys., 50, 4705 (1969).
35. B. de B. Darwent and R. Roberts, Disc. Faraday Soc., 14, 55 (1953).
36. B.G. Dzantiev, A.V. Shishkov, and M.S. Unukovich, Khim. Vys. Energ., 3, 111 (1969); Chem. Abstr., 71, 2772t (1969).
37. S. Tsunashima, T. Yokota, I. Safarik, H.E. Gunning, and O.P. Strausz, J. Phys. Chem., 79, 775 (1975).
38. T. Yokota, M.G. Ahmed, I. Safarik, O.P. Strausz, and H.E. Gunning, J. Phys. Chem., 79, 1758 (1975).
39. W.R. Trost, B. de B. Darwent, and E.W.R. Steacie, J. Chem. Phys., 16, 353 (1948).

40. T. Yokota and O.P. Strausz, J. Phys. Chem., 83, 3196 (1979).
41. O. Horie, K. Onuki, and A. Amano, J. Phys. Chem., 81, 1706 (1977).
42. O. Horie, N.H. Hanh and A. Amano, Chem. Lett., 1015 (1975).
43. N.H. Hanh, J. Nishino, M. Yamada, O. Horie and A. Amano, J. Org. Chem., 44, 3321 (1979).
44. L.I. Avramenko and R.V. Kolesnikova, Akad. Nauk. SSSR, Moscow, 1955, pp. 7-17. Natural Research Council of Canada Technical Translation 789, Ottawa, 1959.
45. I.R. Slagle, R.E. Graham, and D. Gutman, Int. J. Chem. Kinet., 8, 451 (1976).
46. J.G. Calvert and J.N. Pitts, Jr., "Photochemistry", John Wiley and Sons, Inc., New York, 1966, pp. 782-783.
47. R.J. Cvetanovic, J. Chem. Phys., 23, 1203 (1955).
48. J.H. Lee and R.B. Timmons, J. Chem. Phys., 64, 300 (1976).
49. H.F. LeFevre, J.F. Meagher, and R.B. Timmons, Int. J. Chem. Kinet., 4, 103 (1972).
50. D.J. Bogan, Ph.D. Thesis, Carnegie Mellon Univ., 1973.
51. R.J. Cvetanovic, private communication. We thank Dr. Cvetanovic for providing us with his results prior to publication.

52. A. van Roodselaar, Ph.D. Thesis, University of Alberta, 1976; J. Connor, A. van Roodselaar, R.W. Fair, and O.P. Strausz, J. Am. Chem. Soc., 93, 560 (1971).
53. R.B. Klemm and D.D. Davis, Int. J. Chem. Kinet., 5, 149 (1973).
54. E. Jakubowski, M.G. Ahmed, E.M. Lown, H.S. Sandhu, R.K. Gosavi, and O.P. Strausz, J. Am. Chem. Soc., 94, 4094 (1972).
55. M.G. Ahmed. M.Sc. Thesis, University of Alberta, 1974.
56. R. Gomer and W.A. Noyes, Jr., J. Am. Chem. Soc., 72, 101 (1950); M.K. Phibbs and B. de B. Darwent, Can. J. Res. Sect. B, 28, 395 (1950).
57. (a) P.M. Rao and A.R. Knight, Can. J. Chem., 50, 844 (1972); (b) N.L. Arthur and M.S. Lee, Aust. J. Chem., 29, 1483 (1976).
58. N.L. Arthur and K.S. Yeo, Aust. J. Chem., 25, 803 (1972); N.L. Arthur and K.S. Yeo, Aust. J. Chem., 32, 2077 (1979).
59. M. Suama and Y. Takezaki, Bull. Inst. Chem. Res. Kyoto Univ. (Japan), 40, 229 (1962).
60. M. Bonifáčić , K. Schäfer, H. Möckel and K.-D. Asmus, J. Phys. Chem., 79, 1496 (1975).
61. B.C. Gilbert, C.M. Kirk, R.O.C. Norman, and H.A.H. Laue, J. Chem. Soc. Perkin II, 497 (1977).
62. Reference 7, pp. 365-367.

63. P.S.H. Bolman, I. Safarik, D.A. Stiles, W.J.R. Tyerman, and O.P. Strausz, *Can. J. Chem.*, 48, 3872 (1970).
64. (a) K.J. Rosengren, *Acta Chem. Scand.*, 16, 1401, 1418 (1962);
(b) J.K.S. Klan, *Chem. Commun.*, 429 (1967).
65. P. Goldberg, *J. Chem. Phys.*, 40, 427 (1964).
66. V. Schmidt, A. Muller, and K. Markau, *Chem. Ber.*, 97, 405 (1964); V. Schmidt, A. Muller, and K. Markau, *Tetrahedron Lett.*, 1091 (1963).
67. A.B. Callear, J. Connor and D.R. Dickson, *Nature* 221, 1238 (1969).
68. C.S. Smith and A.R. Knight, *Can. J. Chem.*, 54, 1290 (1976).
69. D.M. Graham, R.L. Mieville and C. Sivertz, *Can. J. Chem.*, 42, 2239 (1964); D.M. Graham, R.L. Mieville, R.N. Pallen and C. Sivertz, *Can. J. Chem.*, 42, 2250 (1964).
70. H.E. Van den Berg, A.B. Callear and R.J. Norstrom, *Chem. Phys. Lett.*, 4, 101 (1969).
71. D.R. Tycholiz and A.R. Knight, *J. Am. Chem. Soc.*, 95, 1726 (1973); P.M. Rao, J.A. Copeck, and A.R. Knight, *Can. J. Chem.*, 45, 1369 (1967).
72. J.A.R. Coope and W.A. Bryce, *Can. J. Chem.*, 32, 768 (1954); W.N. Patrick, M.Sc. Thesis, University of British Columbia, Vancouver, 1951.

73. (a) C. Walling and R. Rabinowitz, J. Am. Chem. Soc., 81, 1137 (1959); C. Walling and W. Helmreich, J. Am. Chem. Soc., 81, 1144 (1959); (b) B.N. Geers, G.J. Gleicher, and D.F. Church, Tetrahedron, 36, 997 (1980).
74. A.F. Trotman-Dickenson and G.S. Milne, "Tables of Bimolecular Gas Reactions" Report NSRDS-NBS9. U.S. Government Printing Office, Washington, D.C., 1967.
75. P.M. Rao and A.R. Knight, Can. J. Chem., 46, 2462 (1968).
76. C.J. Olander and S. Sunner, Pure Appl. Chem., 2, 117 (1961).
77. S.W. Benson, D.M. Golden and J.R. Barker, Eds., "Proceeding of the Symposium on Chemical Kinetics Data for the Upper and Lower Atmosphere," Wiley, New York, 1975, p. 359. S.W. Benson, "Thermochemical Kinetics", Wiley, New York, 1968.
78. C.W. Gear, "Applications and Algorithms in Science and Engineering", Science Research Associates, U.S.A. 1978.
79. C.W. Gear, "Numerical Initial Value Problems in Ordinary Differential Equations", Prentice-Hall, Englewood-Cliffs, N.J., 1971.
80. (a) J.W. Bottenheim and O.P. Strausz, Alberta Oil Sand Environmental Research Program, Report No. 25, 1977; (b) J.W. Bottenheim and O.P. Strausz, Alberta Environmental Research Secretariat, Report No. 5, 1978.

81. T.L. Pollock, Ph.D. Thesis, University of Alberta, 1971; R.J. Cvetanovic in "Progress in Reaction Kinetics", Vol. II. G. Porter, Ed., Pergamon Press, New York, N.Y., 1963.
82. R.A. Back, Can. J. Chem., 37, 1854 (1959).
83. A.B. Callear and J.C. McGurk, J. Chem. Soc., Far. Trans. II, 68, 289 (1972); A.B. Callear and P.M. Wood, *ibid*, 68, 302 (1972).
84. A.C. Vikis and D.J. LeRoy, Can. J. Chem., 51, 8207 (1973).
85. A.C. Vikis and D.J. LeRoy, *ibid*, 50, 595 (1972).
86. T.L. Pollock, E.J. Jakubowski, H.E. Gunning and O.P. Strausz, Can. J. Chem., 47, 3474 (1969).
87. A. Jones, S. Yamashita and F.P. Lossing, Can. J. Chem., 46, 833 (1969).
88. H. Böhme in "Methoden der Organischen Chemie" E. Muller, Editor, Vol. IX, 4th Ed., Georg. Thieme Verlag, Stuttgart, 1955, pp. 49-54.
89. J.H. Lee, J.V. Michael, W.A. Payne and L.J. Stief, J. Chem. Phys., 88, 1817 (1978).
90. J.A. Kerr in "Free Radicals" J.K. Kochi, Editor, Vol. 1, John Wiley and Sons, New York, 1973, pp. 14-22.
91. J. Heicklen and H.S. Johnston, J. Am. Chem. Soc., 84, 4030, 4394 (1962).
92. K.W. Watkins and L.A. O'Deen, J. Phys. Chem., 73, 4094 (1969).

93. H. Sugeta, A. Go and T. Miyazawa, Bull. Chem. Soc., Jpn, 46, 3407 (1973).
94. M.M. Ekwenchi and O.P. Strausz, paper presented at the 33rd Northwest American Chemical Society Regional Meeting, Seattle, 1978.
95. M.M. Ekwenchi, A. Jodhan and O.P. Strausz, paper presented at the 62nd Canadian Chemical Conference, Vancouver, 1979.
96. M.M. Ekwenchi, A. Jodhan and O.P. Strausz, Int. J. Chem. Kinet., 12, 431 (1980).
97. M.M. Ekwenchi and O.P. Strausz, Int. J. Chem. Kinet., in press.
98. R.N. Haszeldine and J.M. Kidd, J. Chem. Soc., 3219 (1953).
99. V.F. Kochubei and F.B. Moin, Kinet. Kataliz, 10, 405 (1969).
100. N.L. Arthur and T.N. Bell, Can. J. Chem., 44, 1445 (1966).
101. J.D. Kale and R.B. Timmons, J. Phys. Chem., 36, 4239 (1968).
102. J.H. Lee, L.J. Stief and R.B. Timmons, J. Chem. Phys., 67, 1705 (1977).
103. K.O. Kutschke, M.H.J. Wijen, and E.W.R. Steacie, J. Am. Chem. Soc., 74, 714 (1952).
104. K.J. Ivin and E.W.R. Steacie, Proc. Roy. Soc. A., 208, 25 (1951).

105. D.G.L. James and G.E. Troughton, Trans. Faraday Soc., 65, 763 (1969); A.C.R. Brown and D.G.L. James, Can. J. Chem., 43, 660 (1965).
106. B.S. Rabinovitch and D.W. Setser in "Advances in Photochemistry", Vol. 3, Interscience Publishers, N.Y., 1964; p. 1.
107. K.M. Basal and G.R. Freeman, J. Am. Chem. Soc., 88, 4326 (1966).
108. P. Ausloos and E.W.R. Steacie, Bull. Soc. Chim. Belg., 63, 87 (1954).
109. C.S. Smith and A.R. Knight, Can. J. Chem., 51, 780 (1973).
110. P.J. Boddy and E.W.R. Steacie, Can. J. Chem., 39, 13 (1961).
111. M.M. Ekwenchi, I. Safarik and O.P. Strausz, paper presented at the 63rd Canadian Chemical Conference, Ottawa, 1980.
112. M.G. Evan and M. Polanyi, Trans. Faraday Soc., 34, 11 (1938).
113. N.N. Semenov, "Some Problems of Chemical Kinetics and Reactivity", Vol. 1 (translated by J.E.S. Bradley), Pergamon Press, London, 1958.
114. J.O. Sullivan and P. Warneck, Ber. Bunsenges. Phys. Chem., 69, 7 (1965).
115. K. Hoyer mann, H. Gg. Wagner and J. Wolfrum, Ber. Bunsenges. Phys. Chem., 71, 599 (1967).

116. R.B. Cundall and A. Gilbert, "Photochemistry", Nelson Press, London, 1970.
117. B. de B. Darwent, M.K. Phibbs, and F.G. Hurtubise, J. Chem. Phys., 22, 859 (1954).

APPENDIX A

Competitive Quenching Correction

When mercury photosensitization experiments are carried out in the presence of more than one substrate, the amount of quenching by each substrate can be readily calculated, as shown in the following example for the $H_2-C_2H_4$ case.

From simple collision theory, the quenching rate constants for the quenching of H_2 and C_2H_4 are:

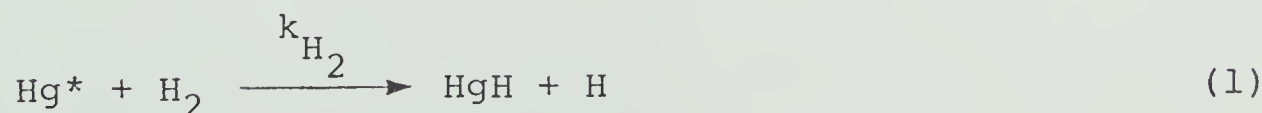
$$k_{H_2} = \sigma_{H_2}^2 \left[8\pi RT \left(\frac{M_{Hg} + M_{H_2}}{M_{Hg} M_{H_2}} \right) \right]^{1/2} \quad \text{I}$$

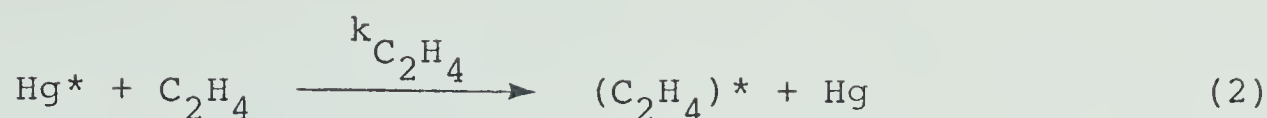
$$\text{and } k_{C_2H_4} = \sigma_{C_2H_4}^2 \left[8\pi RT \left(\frac{M_{Hg} + M_{C_2H_4}}{M_{Hg} M_{C_2H_4}} \right) \right]^{1/2} \quad \text{II}$$

where σ^2 is the collision cross-section, M the molecular weight, and the other terms have their usual significance. Dividing equation I by II, we have

$$\frac{k_{H_2}}{k_{C_2H_4}} = \frac{\sigma_{H_2}^2}{\sigma_{C_2H_4}^2} \left[\frac{M_{C_2H_4}}{M_{H_2}} \left(\frac{M_{Hg} + M_{H_2}}{M_{Hg} + M_{C_2H_4}} \right) \right]^{1/2} \quad \text{III}$$

Consider the following reactions:





The rate expressions for reactions (1) and (2) are:

$$\text{Rate}_{\text{Hg}+\text{H}_2} = k_{\text{H}_2} [\text{Hg}^*] [\text{H}_2] \quad \text{IV}$$

$$\text{Rate}_{\text{Hg}+\text{C}_2\text{H}_4} = k_{\text{C}_2\text{H}_4} [\text{Hg}^*] [\text{C}_2\text{H}_4] \quad \text{V}$$

Dividing IV by V, we have

$$\frac{\text{Rate}_{\text{Hg}+\text{H}_2}}{\text{Rate}_{\text{Hg}+\text{C}_2\text{H}_4}} = \frac{k_{\text{H}_2} [\text{H}_2]}{k_{\text{C}_2\text{H}_4} [\text{C}_2\text{H}_4]} \quad \text{VI}$$

Hence,

$$\frac{k_{\text{H}_2} [\text{H}_2]}{k_{\text{C}_2\text{H}_4} [\text{C}_2\text{H}_4]} = \frac{\sigma_{\text{H}_2}^2}{\sigma_{\text{C}_2\text{H}_4}^2} \left[\frac{M_{\text{C}_2\text{H}_4} \left(\frac{M_{\text{Hg}} + M_{\text{H}_2}}{M_{\text{Hg}} + M_{\text{C}_2\text{H}_4}} \right)}{M_{\text{H}_2}} \right]^{1/2} \cdot \frac{[\text{H}_2]}{[\text{C}_2\text{H}_4]} \quad \text{VII}$$

In the present study $[\text{H}_2] = 580$ Torr, $[\text{C}_2\text{H}_4] = 30$ Torr;

and since $\sigma_{\text{H}_2}^2 = 10 \text{ \AA}^2$, $\sigma_{\text{C}_2\text{H}_4}^2 = 26 \text{ \AA}^2$, $M_{\text{H}_2} = 2$ and

$M_{\text{C}_2\text{H}_4} = 28$, equation VII becomes

$$\frac{10}{26} \left[\frac{28}{2} \left(\frac{202}{228} \right) \right]^{1/2} \times \frac{580}{30} = 26$$

Therefore the percentage quenching by H_2 is

$$\frac{k_{H_2} [H_2] [Hg^*]}{k_{H_2} [H_2] [Hg^*] + k_{C_2H_4} [C_2H_4] [Hg^*]} \times 100$$

$$= \left(\frac{k_{H_2} [H_2]}{k_{H_2} [H_2] + k_{C_2H_4} [C_2H_4]} \right) \times 100 = \frac{1}{1.038} \times 100 = 96.3\%$$

For all the systems examined in the present study, the maximum total pressures of sulfide or sulfide + ethylene were 30 Torr and the hydrogen pressure was always 580 Torr. For CH_3SCH_3 $\sigma^2 = 49.3 \text{ Å}^2$ ⁸⁷ and the σ^2 values for $C_2H_5SC_2H_5$, CH_3SSCH_3 and $C_2H_5SSC_2H_5$ are probably not too different. Hence it is concluded that $\geq 95\%$ of the excited mercury atoms are quenched by H_2 .

APPENDIX B

Mass Spectral Data

Ethyltrifluoromethylsulfide

m/e	Relative Intensity	Tentative Assignment
28	15.9	C_2H_4^+
29	74.3	C_2H_5^+
41	2.8	C_3H_5^+
42	8.2	C_3H_6^+
43	<u>100</u>	$\text{CH}_2\text{CH}_2\text{CH}_3^+$
44	4.5	CS^+
45	18.5	CHS^+
57	4.3	C_4H_9^+
58	28.3	$\text{C}_4\text{H}_{10}^+$
59	13.4	$\text{C}_2\text{H}_3\text{S}^+$
60	13.2	CH_3CHS^+
61	6.3	$\text{CH}_3\text{CH}_2\text{S}^+$
69	13.6	CF_3^+
115	8.2	$\text{CH}_2\text{SCF}_3^+$
130	17.9	$\text{CH}_3\text{CH}_2\text{SCF}_3^+$

4,5-dimethyl-3,6-dithia-octane (DMDTO)

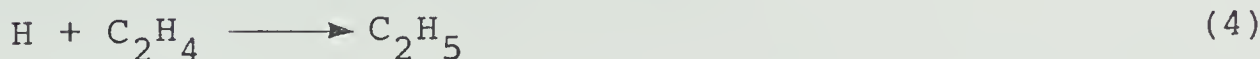
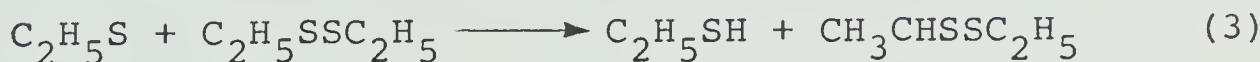
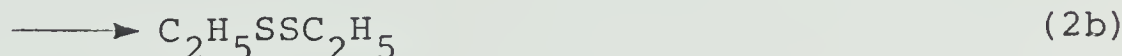
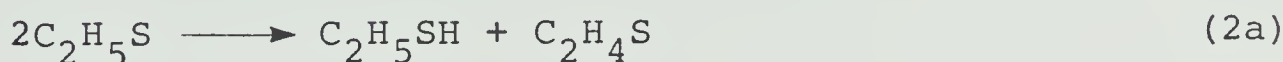
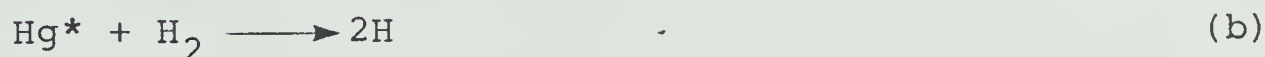
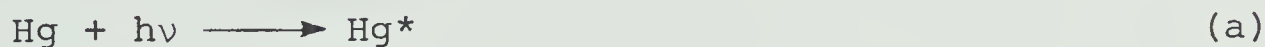
m/e	Relative Intensity	Tentative Assignment
29	27.2	$C_2H_5^+$
41	14.2	$C_3H_5^+$
45	10.4	CHS^+
57	13.4	C_2HS^+
59	18.8	$C_2H_3S^+$
60	14.4	$C_2H_4S^+$
61	50.7	$C_2H_5S^+$
75	38.7	$CH_2SC_2H_5^+$
89	<u>100</u>	$CH_3CHSC_2H_5^+$
117	37.2	$CH_3CHC(CH_3)HSC_2H_5^+$
178	21.0	$C_2H_5SCH(CH_3)-CH(CH_3)SC_2H_5^+$

APPENDIX C

Kinetic Treatment of the $\text{H} + \text{C}_2\text{H}_4 + \text{C}_2\text{H}_5\text{SSC}_2\text{H}_5$ System

The mercury photosensitized decomposition of 580 Torr hydrogen in the presence of 5 Torr $\text{C}_2\text{H}_5\text{SSC}_2\text{H}_5$ yields $\text{C}_2\text{H}_5\text{SH}$ as the only retrievable reaction product. In the presence of increasing amounts of ethylene at any given temperature, it has been shown that $\phi(\text{C}_2\text{H}_5\text{SH})$ decreases with increasing pressure of C_2H_4 , owing to the competitive scavenging of H atoms by C_2H_4 .

The following kinetic scheme was used to analyze the data:



In the unscavenged system, $\text{C}_2\text{H}_5\text{SH}$ is assumed to be formed exclusively *via* steps (1), (2a) and (3), hence the following steady state equations apply:

$$\phi^\circ(\text{H}) = \phi^\circ(\text{C}_2\text{H}_5\text{S}) = 2\phi^\circ(2\text{a}) + 2\phi^\circ(2\text{b}) + \phi^\circ(3) = 2.0 \quad \text{I}$$

$$\phi^\circ(1) + \phi^\circ(2\text{a}) + \phi^\circ(3) = \phi^\circ(\text{C}_2\text{H}_5\text{SH})_{\text{total}} \quad \text{II}$$

The rate expressions in the absence and presence of C_2H_4 are:

$$R_1^\circ = k_1 [\text{H}]^\circ [\text{C}_2\text{H}_5\text{SSC}_2\text{H}_5] \quad \text{III}$$

$$R_{2\text{a}}^\circ = 2k_{2\text{a}} [\text{C}_2\text{H}_5\text{S}]^\circ{}^2 \quad \text{IV}$$

$$R_3^\circ = k_3 [\text{C}_2\text{H}_5\text{S}]^\circ [\text{C}_2\text{H}_5\text{SSC}_2\text{H}_5] \quad \text{V}$$

$$R_1 = k_1 [\text{H}] [\text{C}_2\text{H}_5\text{SSC}_2\text{H}_5] \quad \text{VI}$$

$$R_{2\text{a}} = 2k_{2\text{a}} [\text{C}_2\text{H}_5\text{S}]^2 \quad \text{VII}$$

$$R_3 = k_3 [\text{C}_2\text{H}_5\text{S}] [\text{C}_2\text{H}_5\text{SSC}_2\text{H}_5] \quad \text{VIII}$$

$$2\text{I}_\text{a} = k_1 [\text{H}]^\circ [\text{C}_2\text{H}_5\text{SSC}_2\text{H}_5] \quad \text{IX}$$

$$2\text{I}_\text{a} = k_1 [\text{H}] [\text{C}_2\text{H}_5\text{SSC}_2\text{H}_5] + k_4 [\text{H}] [\text{C}_2\text{H}_4] \quad \text{X}$$

where R° and R are the rates in the absence and presence of C_2H_4 respectively. Dividing R° by the corresponding R and assuming that $[\text{H}] = [\text{C}_2\text{H}_5\text{S}]$ and $[\text{H}]^\circ = [\text{C}_2\text{H}_5\text{S}]^\circ$, we obtain the following expressions:

$$\frac{R_1^\circ}{R_1} = \frac{[\text{H}]^\circ}{[\text{H}]} \quad \text{XI}$$

$$\frac{R_{2\text{a}}^\circ}{R_{2\text{a}}} = \frac{[\text{H}]^\circ{}^2}{[\text{H}]^2} \quad \text{XII}$$

$$\frac{R_3^{\circ}}{R_3} = \frac{[H]^{\circ}}{[H]} \quad \text{XIII}$$

Substituting for the values of $[H]^{\circ}$ and $[H]$ from Equations IX and X,

$$\frac{\phi^{\circ}(1)}{\phi(1)} = 1 + \frac{k_4 [C_2H_4]}{k_1 [C_2H_5SSC_2H_5]} \quad \text{XIV}$$

$$\frac{\phi^{\circ}(2a)}{\phi(2a)} = \left\{ 1 + \frac{k_4 [C_2H_4]}{k_1 [C_2H_5SSC_2H_5]} \right\}^2 \quad \text{XV}$$

$$\text{and } \frac{\phi^{\circ}(3)}{\phi(3)} = 1 + \frac{k_4 [C_2H_4]}{k_1 [C_2H_5SSC_2H_5]} \quad \text{XVI}$$

where ϕ° and ϕ are the quantum yields in the absence and presence of C_2H_4 . Assuming that Equation II also applies in the presence of C_2H_4 , i.e.,

$$\phi(1) + \phi(2a) + \phi(3a) = \phi(C_2H_5SH)_{\text{total}} \quad \text{XVII}$$

and substituting for the values of $\phi(1)$, $\phi(2a)$ and $\phi(3)$, derived from Equations XIV, XV, and XVI respectively, in Equation XVII, we have

$$\frac{\phi^{\circ}(1)}{f} + \frac{\phi^{\circ}(2a)}{f^2} + \frac{\phi^{\circ}(3)}{f} = \phi(C_2H_5SH)_{\text{total}} \quad \text{XVIII}$$

where $f = 1 + k_4 [C_2H_4]/k_1 [C_2H_5SSC_2H_5]$, i.e., f is the suppressing effect of added C_2H_4 on the quantum yields.

By using Equation XVIII, f can be determined by iteration, and therefore, the values of $\phi(1)$, $\phi(2a)$ and $\phi(3)$, listed in Table XVII, can be calculated.

B30291